Università
Ca'Foscari
Venezia

Graduate School

PhD Programme in
Science and Management of Climate Change

Cycle XXVIII
Year 2016

Climatic variability and human impact during the Holocene from an Alpine peat bog

PhD Student
Michela Segnana

Student ID number: 955996
Scientific Disciplinar Sector: CHIM/01

Supervisor:
Dr. Jacopo Gabrieli

PhD Coordinator:
Prof. Carlo Barbante

Co-Supervisors:
Prof. Carlo Barbante
Dr. Luisa Poto

Delle strade inesplorate non si può dire granchè. Si può solo provare a percorrerle, sbagliando e correggendosi in continuazione.

Maurizio Pallante

Abstract

It is scientifically well-established that the air temperature at the Earth's surface has been significantly increasing during the past 150 years, with a noticeably rapid temperature rise at the end of the 20th century. In this framework of current global warming, mountain environments are particularly sensitive and vulnerable areas. European Alps registered in the last 150 years an exceptionally mean temperature increase of about 2°C, more than twice the average increase that characterized the warming of the Northern Hemisphere. The rapid climate change and the necessity of future projections require a deep understanding of the climatic system, which is ruled by natural forcings and affected by anthropogenic impacts. Therefore, insights into past climate variations, aiming at a better understanding of this complex system, are fundamental. Climatic information may be directly or indirectly registered in natural archives, e.g., ice cores, marine sediments, lake sediments, tree rings and peatlands. Among peatlands, ombrotrophic peat bogs, receiving water and nutrients exclusively from dry and wet atmospheric depositions, are among the most suitable matrices for climate reconstruction, as they register solely atmospheric conditions.

The Coltrondo peat bog (46° 39' 28.37"N, 12° 26' 59.17"E), located in the Eastern sector of the Italian Alps (Dolomitic area) is the object of this research project. The selection of a multi-proxy approach that combines physical, chemical and biological analyses, provides independent evidence about past climate changes and human activities, allowing us to obtain new insights into variability in the Eastern Italian Alps over the last 7900 years cal BP, adding important information about this area, given the scarcity and fragmentation of records investigated.

A robust and reliable chronology was obtained by combining ^{210}Pb and ^{14}C dating techniques that allowed the interpretation of the data in an accurate chronological framework. The physical properties of the peat (bulk density and ash content), the pore water pH and Ca/Mg ratio, together with the profile of Ca and Sr in peat were determined to assess the trophic status of the peat bog: ombrotrophic conditions are suggested down to ca. 180

cm of the core (6300 cal BP). Below this depth, the atmospheric dust input is integrated with the upward migration of chemical elements from the underlying bedrock, characterizing the chemical composition of the basal peat layers.

Information about geochemical processes occurring in the peat bog were obtained by determining the concentration of major, trace and rare earth elements by means of Inductively Coupled Plasma Mass Spectrometry (ICP-MS). Enrichment factors (EFs) of trace elements related to human activities, such as Pb, Zn, As, Ag, Cd and Cu, were calculated to infer the human impact in the area marked by a first slight increase of Pb EF during Roman Times, possibly related to mining activities carried out by the Romans. Subsequently, mining activities carried out in the area during the Middle Ages mostly under the domination of the Republic of Venice are recorded, with an increase of Pb, Ag and Cu EFs. The advent of the industrialization in the 20th century is also registered by the highest EFs values for all the elements considered.

To help and support the interpretation of geochemical data, lead isotopes ratios were measured using ICP-MS with the main aim to discriminate between natural and anthropogenic sources of lead. The $^{206}Pb/^{207}Pb$ ratio clearly records a pre-anthropogenic period from 7800 to 2500 cal BP, followed by a period in which humans had an impact on the environment. During the Middle Ages the $^{206}Pb/^{207}Pb$ ratio values suggest both local and regional mining activities that prospered at that time in that specific area and throughout in Europe. The drop of $^{206}Pb/^{207}Pb$ ratio during the 20th century is linked with the introduction of leaded gasoline in Italy. The subsequent phasing out of leaded gasoline in the 1980s is also registered by the peat bog with an increase in the $^{206}Pb/^{207}Pb$ ratio values.

The analysis of pollen, non-pollen palynomorphs (NPPs) and micro-charcoal particles was also performed along the core, obtaining fundamental information about the climatic and human history of the Coltrondo area. The main climatic events of the Middle and Late Holocene, on both regional and more global scales, were indeed registered by the bog before humans started having an impact on the area, ca. 2500 cal BP. The major Eastern Alpine cold events (e.g., Frosnitz event, Rotmoos I and Rotmoos II events, Löbben event) are registered by the climax vegetation of the area, which shows a considerable decrease during these colder periods. The Roman Warm Period, the Medieval Climate Anomaly and the Little Ice Age are also registered by the vegetation. However, human pressure on the environment at that time makes it difficult to clearly distinguish Holocene climate natural variability from human-related changes. Land-use changes from ca. 2500 cal BP are indeed well evidenced by the presence of human-related pollen and non-pollen

palynomorphs (NPPs), as well as by the increase in micro-charcoal particles, mainly attributable to forest clearance, pasture and agricultural activities. Periods of increased human impact are registered at the end of the Middle Ages and later, at the end of the 19th century. With the advent of industrialization, a general abandonment of the area is registered both by pollen and geochemical analyses.

The multi-proxy approach selected for this study, combining the results of physical, geochemical and pollen analyses, allowed us to reconstruct the development of the peat bog since its initiation, unravelling different aspects of the past history recorded by the peat bog and achieving new insights into Holocene climate variability in the Eastern Italian Alps and into human pressure on the environment. This work may be considered as a fundamental step for the study of a strategic sector that is still scarcely investigated. It adds valuable information and gives new insights into the climate variability and the human presence in the area.

Acknowledgements

Gli studi paleoclimatici e paleoambientali hanno sempre suscitato in me una grande curiosità ed interesse. La possibilità di fare un Dottorato proprio in quest'area scientifica è stata per me una grande opportunità, che ho voluto cogliere. Tre anni sono passati e il mio Dottorato volge al termine, tre anni nei quali ho iniziato a scoprire e capire il mondo della ricerca, durante i quali ho iniziato a fare ricerca. Ci sono stati momenti facili e momenti difficili, momenti di sorpresa ed entusiasmo alternati ad altri di sfiducia e scoramento. Tre anni in cui indubbiamente sono cresciuta dal punto di vista scientifico, ma anche dal punto di vista personale. Se sono arrivata qui, a scrivere queste righe, lo devo a tante persone che ho avuto attorno in questo periodo, che mi hanno aiutato, guidato, sostenuto, anche criticato, come è giusto che sia.

Ringrazio inanzitutto il mio tutor, Dr. Jacopo Gabrieli e i miei co-tutors, Dr. Luisa Poto e Prof. Carlo Barbante. Se ho potuto affacciarmi al mondo della paleoclimatologia e portare a termine questo lavoro di Dottorato, è stato grazie a voi. Un ringraziamento in particolare va a Luisa: non sei stata solo co-tutor e collega di lavoro, ma anche e soprattutto amica e confidente.

Ringrazio poi il Prof. Klaus Oeggl, che mi ha accolto nel suo gruppo di palinologia all'Università di Innsbruck. Mi ha permesso di affacciarmi al bellissimo mondo della palinologia ed è sempre stato disponibilissimo nei miei confronti.

Un sentito grazie a Piergiorgio Cesco Frare per la disponibilità e le preziose informazioni e documentazione sulla storia del Comelico e del Cadore. Allo stesso modo ringrazio Dino Preloran per la pazienza, la disponibilità e il materiale fornitomi sulle principali attività minerarie della zona del Comelico. Entrambi mi hanno trasmesso l'entusiasmo che deriva dalla passione di studiare la storia e le tradizioni del proprio paese, dei propri posti.

Un ringraziamento particolare va alla persona con cui ho condiviso tutti i momenti di questo Dottorato, dal colloquio di ammissione all'upload finale, Fabio. Dal giorno in cui ci siamo conosciuti, nervosi in attesa di fare il nostro colloquio, come sempre gli ultimi in lista date le iniziali dei nostri cognomi, abbiamo percorso questo "viaggio" insieme, confrontandoci, consigliandoci,

lamentandoci, supportandoci (e sopportandoci) a vicenda. Durante questo percorso ho sempre potuto contare su di te, in qualsiasi momento, per qualsiasi cosa. Ti ringrazio per la tua capacità di sdrammatizzare e farmi ridere, anche quando non mi pareva che ci fosse proprio nulla da ridere! Ti ringazio perchè siamo stati degli ottimi colleghi di Dottorato, ma soprattutto ottimi amici.

Un grande ringraziamento va a tutta la "classe" del primo anno di Dottorato: i due Fabio, Giuliano, Angela, Federica, Barbara, Shouro e Azizul. Insieme siamo riusciti ad affrontare lezioni, compiti a casa, presentazioni ed esami. Non c'è mai stata competizione tra noi, ma una sana collaborazione che ci ha portato ad affrontare tutto al meglio, sempre con una battuta pronta per ridere insieme.

Ringrazio poi un altro grande gruppo, quello di "Santa Marta" (ora "Via Torino"). In particolare Torben, Piero, Patrizia, Andrea, Daniela, Alice, Michele, Federico, Maria, Giulio, Clara e Warren. Grazie per l'aiuto, l'ascolto e il confronto. Ciò che più ho apprezzato in questi anni a Venezia è stato trovare nel gruppo di ricerca non solo dei ricercatori ma anche degli amici.

Un ringraziamento di cuore va al gruppo di Innsbruck, in particolare a Daniela, Benji, Werner, Burgi, Edith e Fabio (Fritolin). Mi avete fatto sentire tutti subito a casa, mi sono trovata a mio agio e ho potuto imparare veramente molto. E' stato un periodo sereno e molto costruttivo, dove ho potuto portare avanti il mio lavoro di ricerca sentendomi sempre seguita e aiutata e dove non è mai mancata la possibilità di fare quattro chiacchiere e quattro risate insieme.

Sicuramente non sarei arrivata alla fine di questo Dottorato senza il supporto di molti amici, vecchi e nuovi. Spesso vedere la propria situazione da un punto diverso dal proprio aiuta a capirsi meglio e a fare le scelte giuste. Un ringraziamento particolare va ad Elga, Maddalena, Cristina, Alice e Marta, le amiche di casa. Anche se le strade che percorriamo sono tanto diverse, questo non ci impedisce di capirci e renderci vicendevolmente partecipi delle nostre vite. Un ringraziamento a Chiara, Matteo (Tambu), Francesco, Daniele, Sara, Bruno e Isabella, gli amici dell'università. Il legame che ho ancora con ciascuno di voi dopo tanti anni penso sia una cosa grande. Un ringraziamento ad Andrea, Alice e Antonio che a Padova sono i miei punti saldi, di riferimento. Un grazie anche ad Alessia, conosciuta grazie a Piero, con cui ho legato subito e che ha reso la mia vita veneziana un po' più pepata!

E voglio ringraziare tante altre persone che ho incontrato sulla mia strada in questi tre anni, soprattutto ballerini e ballerine folk, che con il loro modo di fare, con le loro opinioni e idee, con le loro vite mi hanno ispirato, dato nuovi spunti di riflessione e mi hanno aiutato a conoscere meglio me stessa.

L'ultimo ringraziamento va alla mia famiglia. Ai miei genitori, Carla ed

Enrico, a mia sorella Chiara, mio cognato Andrea e ai miei splendidi nipoti Niccolò e Jacopo. Da brava trentina non sempre riesco ad esprimere quanto siete importanti per me e quanto vi voglio bene. In particolare ti ringrazio mamma, perchè mi sostieni sempre, mi ascolti, mi capisci, mi consigli e sopporti il mio carattere non sempre facile! E ringrazio te papà, pap, perchè per me ci sei sempre e non c'è una volta che tu mi dica di no. E infine ringrazio te Chiara e tutta la tua bella famiglia. Essere zia è la cosa più bella in assoluto che mi sia capitata: tornare a casa sapendo di poter stare con voi e giocare con Niccolò e Jacopo mi riempie sempre di una grande gioia. A loro due dedico questo lavoro, sperando crescano persone interessate ed interessanti, curiose e rispettose della vita.

Contents

List of Figures

List of Tables

Part I

Introduction

Chapter 1

The Holocene

The Holocene epoch covers the interval of time from the very end of the last glacial period, approximately 11,700 years before present up to present days (Wanner et al., 2011). Holocene climate is relatively stable compared to the major shift that marks the transition from glacial to interglacial throughout the entire Pleistocene. However, variations in temperature and rate of precipitation occur also during the Holocene (Mayewski et al., 2004; Wanner et al., 2008).

At the turn of the 19th and 20th century, the study of several Scandinavian peat bogs led to the first subdivision of the Holocene, the so-called Blytt-Sernander classification (Blytt, 1876; Sernander, 1908). Four periods were recognized, based on visually distinguishable layers in bogs. Dark, more humified, wood-containing layers characterized the Boreal and Subboreal periods, while lighter, less humified layers and the absence of wood characterized the Atlantic and Subatlantic periods. Later, the earliest postglacial period was added by Deevey and Flint (1957). It was named the Preboreal period (Table 1.1).

Today the Holocene climate subdivision is based on climate reconstructions derived not only from peat bog records, but also from other natural archives, such as Greenland ice cores, North Atlantic ocean sediments, Alpine glaciers and lake sediments (e.g., O'Brien et al., 1995; Bond et al., 2001; Holzhauser et al., 2005; Ivy-Ochs et al., 2009; Solomina et al., 2015). All climate proxies in these studies provide evidence for a similar division of the Holocene, from Preboreal to Subatlantic, although for each climatic subdivisions there are regional variations and additional climatic shifts.

The Holocene climatic oscillations are triggered by different drivers, such as orbital, solar and volcanic forcings. On a multi-millennial time scale, the main factors that affect Holocene climate changes are related to variations in the Earth's orbit and axis (Milanković theory; Milanković, 1969).

Table 1.1: The Holocene subdivision following the Blytt-Sernander classification. The ages in years cal BP represent the boundaries between the different climatic phases (Stuiver et al., 1998; Ravazzi, 2003).

Climatic subdivision	**Climatic conditions**	**Age** (cal BP)
Subatlantic	wet, cool	2728 – 2476
Subboreal	dry, warm	5728
Atlantic	wet, warm	8776 – 9004
Boreal	dry, warm	10189 (9944 – 10004)
Preboreal	warming	11268 – 11553

The variation of the precession of the equinoxes, the obliquity of the ecliptic and the eccentricity of the orbit, each presenting its own periodicity, affect the amount of solar radiation that reaches the Earth's surface, thereby inducing major climatic changes. Climatic variations occurring over shorter frequencies, however, cannot be explained by astronomical forcing (Lowe et al., 2013). Changes in solar activity and ocean circulations may trigger these centennial-scale climatic shifts (e.g., Bond cycles; Bond et al., 2001), while volcanic eruptions generally lead to short-term cooling effects (Robock, 2000).

The climatic variability observed in the Holocene cannot be entirely ascribed to forcing factors, as other factors and a chain of feedback mechanisms that constitute the global environmental system also play an important role. Understanding the complexity of these mechanisms is indeed a difficult challenge (Lowe et al., 2013). Among such mechanisms, during the Holocene human activities started impacting on the environment as well as on the climate system, mainly through land use changes, such as deforestation and burning of fossil fuel, with consequent greenhouse gas (mainly CO_2 and CH_4) and aerosol emissions. These activities started changing the environment thousands of years ago (Zennaro et al., 2015), with a dramatic increase in the rate of changes in the last few decades, switching the scale of the impacts from local to global.

1.1 Ongoing climate change

The Intergovernmental Panel on Climate Change (IPCC) states that "warming of the climate system is unequivocal, and since the 1950s, many of the observed changes are unprecedented over decades to millennia" (IPCC, 2013). It is scientifically well established that the Earth's surface air temperature has significantly increased over the past 150 years, and an upward trend with a remarkably rapid temperature rise is registered at the end of the 20th century (Fig. 1.1a). The IPCC states that anthropogenic factors, like massive deforestation and burning of fossil fuels, presently push the climate system into a warming direction at a remarkably high speed.

This ongoing global warming is changing the Earth's system, shrinking the vast majority of mountain glaciers (e.g., Diolaiuti et al., 2011; Gobiet et al., 2014), warming oceans (e.g., Abraham et al., 2013), shrinking Arctic sea ice (e.g., Laxon et al., 2013; Parkinson and Comiso, 2013), and modifying the behaviour of plants and animals (e.g., Theurillat and Guisan, 2001; Walther et al., 2002).

In 2013, the IPCC reported a warming between 0.65°C and 1.06°C over the period 1901 to 2012, with almost the entire globe experiencing surface warming (Fig. 1.1b). Different scenarios (Representative Concentration Pathways, RCPs) with different assumptions on the future amount of radiative forcing are considered to project future climatic trends (van Vuuren et al., 2011). Projections about global surface temperature change for the end of the 21st century (2081 – 2100) relative to 1986 – 2005 are of an increase in the range of 0.3°C to 1.7°C in the best scenario (RCP2.6, radiative forcing max ca. 3 W/m^2 with a decreasing trend to 2.6 W/m^2 by 2100) and in the range of 2.6°C to 4.8°C in the worst scenario (RCP8.5, radiative forcing leading to 8.5 W/m^2 by the end of the 21st century) IPCC (2013, Fig. 1.2a).

Furthermore, precipitations over the Northern Hemisphere have increased since the 1901. In Europe, winters in the next century are expected to see increased amounts of precipitations, whereas summer drought and heat waves are expected to occur more frequently (Fig. 1.2b).

1.2 European Alps and climate change

In the framework of the current global warming, mountain environments are particularly sensitive and vulnerable areas. In the last 150 years, the European Alps registered an exceptional mean temperature increase of about

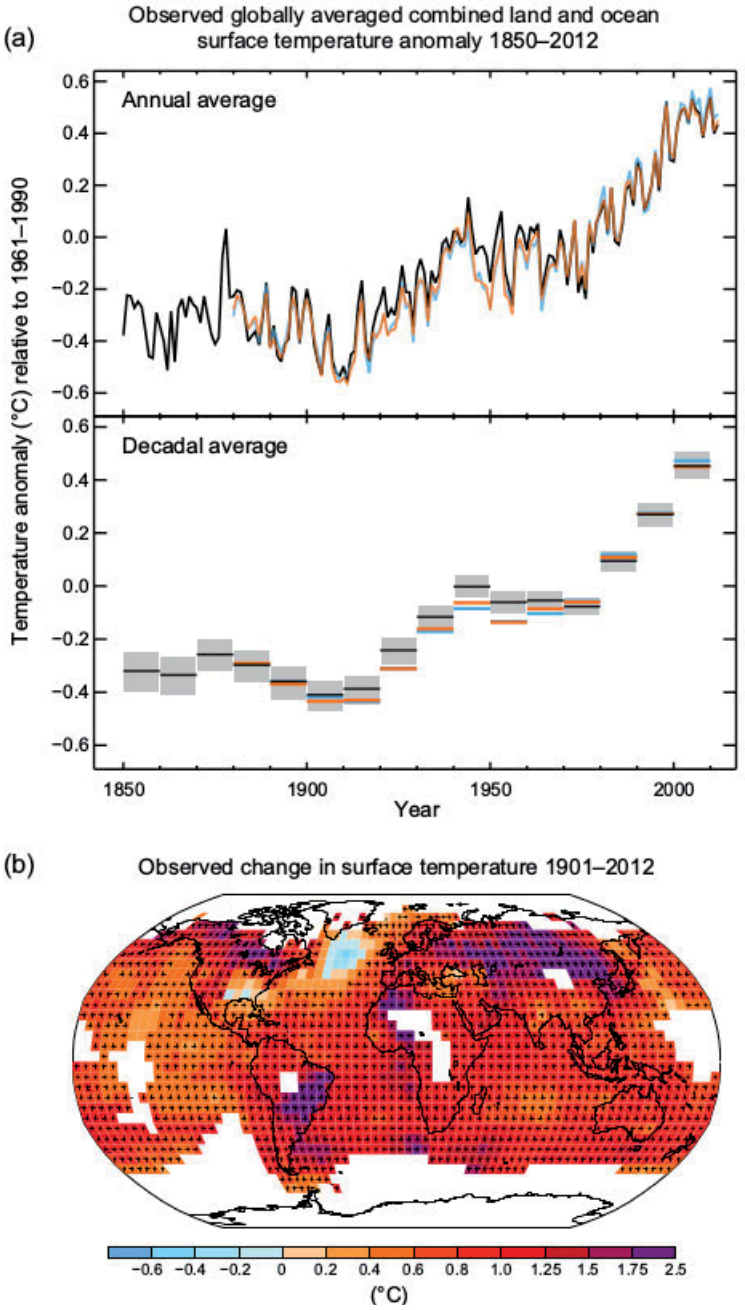

Figure 1.1: (a) Observed global mean surface temperature anomalies, from 1850 to 2012 (IPCC, 2013); (b) Map of the observed surface temperature change from 1901 to 2012 (IPCC, 2013).

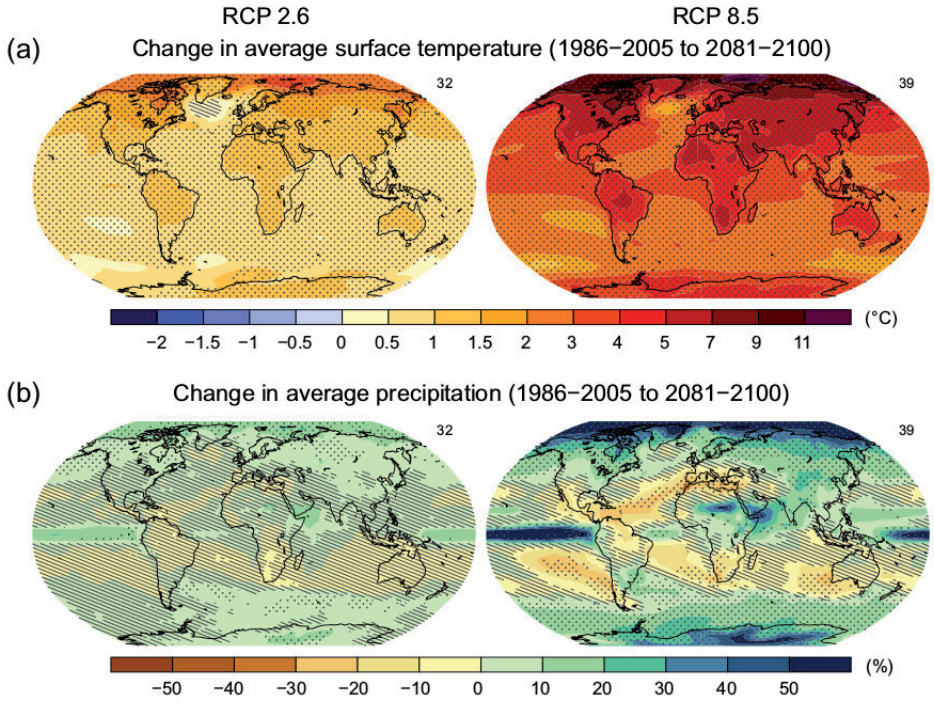

Figure 1.2: (a) Annual mean surface temperature change in 2081–2100 for the scenarios RCP2.6 and RCP8.5 (IPCC, 2013); (b) Average percent change in annual mean precipitation in 2081–2100 for the scenarios RCP2.6 and RCP8.5 (IPCC, 2013).

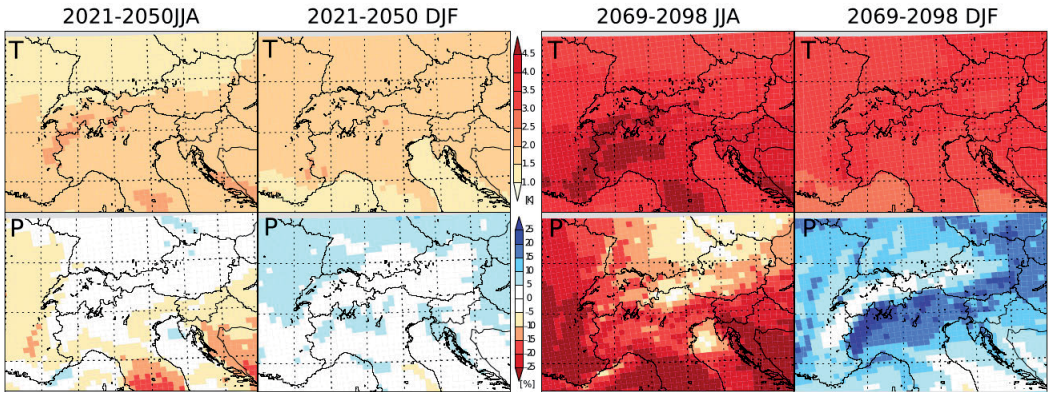

Figure 1.3: Seasonal mean change in the Alpine region for temperature (T) and precipitation (P). Map taken from Gobiet et al. (2014)

2°C, more than twice the average temperature increase of the Northern Hemisphere (Auer et al., 2007).

Climatic scenarios for the Alps predict a general warming trend in the range of 1.6 °C until the mid of the 21st century and 3.8°C until the end of the 21st century. Models indicate less precipitation in the summer (–20.4%), particularly for the Southern Alps, and more precipitations in the winter (+10.4%) until the end of the 21st century (Fig. 1.3) (Gobiet et al., 2014).

A robust and reliable estimation of future climate changes in the Alps is of relevant importance, due to various factors, such as the high population density, the importance of the Alpine region for water resources employed in energy production and the high economic importance of both winter and summer tourism (Gobiet et al., 2014). Alpine region is particular challenging for climate modellers, as the regional climate is the result of the interaction of large-scale dynamics with orography and physical proprieties that characterize the environment at regional and local scales. Therefore, to understand the future climate changes in the Alpine region, past climate reconstruction at a regional scale is more than necessary.

Several studies attempted to reconstruct the environmental and climatic evolution of the European Alps, mainly focusing on the Western and Central Alps (e.g., Wick and Tinner, 1997; Nicolussi and Patzelt, 2000b; Pini, 2002; Tinner and Theurillat, 2003; Heiss et al., 2005; Holzhauser et al., 2005; Mangini et al., 2005; Orombelli et al., 2005; Magny, 2013) while only fragmentary data exist for the Eastern Italian Alps (Fairchild et al., 2001; Frisia et al., 2003; Baroni et al., 2006; Scholz et al., 2012; Poto et al., 2013). The lack of climate data in the latter area is due to scarcity of well-preserved deposits at high altitudes and of high-resolution records with adequate chronological control.

1.3 Palaeoclimate relevance

The Earth's climate is an interactive system involving the atmosphere, the hydrosphere, the cryosphere, the land surface and the biosphere (Ruddiman, 2008). As mentioned above, the climate is forced and influenced by various external forcing mechanisms and internal feedback mechanisms. The rapid climate change and the necessity of future projections require a deep understanding of this complex system. Therefore, insights in past climate variations, aimed at a better understanding of the climate system and its driving mechanisms, are fundamental.

Instrumental records of climate go back no further than decades or centuries, and we therefore need natural archives to reconstruct climate changes

that date back millennia or more (Table 1.2).

Table 1.2: Main palaeoclimatic natural archives. T = temperature, P = precipitation, humidity; B = biomass and vegetation patterns; V = volcanic eruptions; M = geomagnetic field variations; L = sea level; S = solar activity; C = chemical composition. Modified from Bradley (1999).

Palaeoclimatic Archive	**Max temporal resolution**	**Temporal range (years)**	**Information obtained**
Historical records	day/hour	ca. 10^3	T, P, B, V, M, L, S
Tree rings	year/season	ca. 10^4	T, P, B, V, M, S
Peat bogs	year/decade	ca. 10^4	T, P, C, B, V, S
Corals	year	ca. 10^4	C, L, T, P
Lake sediments	year/ decade	ca. 10^4 - 10^6	T, B, M, P, V, C
Ice cores	year	ca. 5 x 10^5	T, P, C, B, V, M, S
Speleothems	100 years	ca. 5 x 10^5	C, T, P
Marine sediments	500 years	ca. 10^7	T, C, B, M, L, P

From those natural archives, physical, chemical and biological proxies can be selected and investigated to acquire indirect information on environmental and climate conditions. The combination of information from different types of proxies, using a multi-proxy approach, is the best way to obtain independent evidence about past climatic changes, leading to a more reliable reconstruction. Palaeoclimatic records can document transitions between different climate states, including abrupt events, which occurred on time scales of years, decades to a few centuries. They inform us about multi-centennial to millennial baseline variability, against which the recent changes can be compared (IPCC, 2013).

Palaeoclimatic records therefore provide the backdrop against which our understanding of the climate system can be calibrated. They are essential for the creation of confident climate models, i.e. the tools we use to project future changes: climate scenarios, predicting the amplitude of future climate change, become more robust if they can be validated against data from past climate changes, although current changes that force anthropogenic climate change are unprecedented (Schneider and Mastrandrea, 2013).

Chapter 2

Peatlands

A peatland is an area with naturally accumulated layers of peat formed under waterlogged conditions (Charman, 2002). Peat is an organic deposit formed by partly decomposed plants and contains at least 65% of organic matter and less than 35% mineral content (Clymo, 1983; Charman, 2002). Peatlands generally comprise two parts: 1. a near-surface aerobic layer composed by a matrix of living plants and recently deposited dead material, known as the acrotelm and 2. a deeper anaerobic layer that is permanently waterlogged, where decomposition is much slower, known as the catotelm (Ingram et al., 1978; Clymo, 1984).

The main requisite for the formation of any peatland is that the rate of biomass production must exceed the rate of decomposition (Charman, 2002). These conditions are initially driven by external factors such as climate, geology, geomorphology and biogeography. In temperate areas, for example, low temperatures and a high rate of precipitation permit limited evapotranspiration and the waterlogging of the substrate, when the underlying geology ensures sufficient water retention and impermeability. Moreover, topography plays a role, creating spaces where water is naturally collected. The type of vegetation, with plants more suitable to peat formation and development (i.e., Bryophytes), also has an important role in facilitating the initial creation of peat over time (Charman, 2002).

Two main processes lead to the initiation of a peatland: terrestrialization and paludification (Gore, 1983). Terrestrialization is the process by which a shallow lake is slowly infilled with accumulated organic and inorganic matter. Paludification consists in the formation of peat directly over a mineral substrate, with the absence of a previous limnic phase. Only the initiation stage differs in the formation of peatlands, while the other developmental steps are similar.

There are different types of peatlands and their classification varies among

authors and countries, following different criteria, such as vegetation, morphology, hydrology, chemistry or trophic status (Charman, 2002). Depending on their trophic status, two main categories are distinguishable:

- minerotrophic peatlands that receive inputs from the atmosphere, but they are also supplied by groundwater and surface water, resulting in a more nutrient-rich and alkaline environment (Shotyk, 1996).

  Different types of minerotrophic peatlands exist: marshes, swamps and fens. Marshes are wetlands and peatlands often associated with bodies of open waters. Periodic or regular inundations characterize these environments, supplying detrital mineral material that provides abundant plant nutrients. Therefore marshes may present a luxuriant growth of sedges, grasses, rushes, reeds and floating aquatic plants in the zones of open water (Shotyk, 1996).

  Swamps are treed peatlands and wetlands. Similarly to marshes, they are subjected to periodic or regular inundations. Most of the water percolates through the surrounding mineral soils, therefore it may be rich in dissolved solids. The vegetation in swamps is characterized by a cover of deciduous or coniferous trees, shrubs, herbs and mosses (Shotyk, 1996).

  Fens are meadow-like peatlands dominated by sedges, grasses, reeds, brown mosses and shrubs. They are fed by solutions that have percolated through mineral soils (Shotyk, 1996).

- ombrotrophic peatlands, also called bogs, receive water and nutrients solely through wet and dry atmospheric depositions (rain, snow, fog, dust, ash) and are therefore acid and low in plant nutrients (Damman, 1986).

  The higher acidity registered in ombrotrophic peat bogs is principally due to the different source of water and nutrients. There are also internal processes involved, including the release of organic acids through decay and cation exchange in the pore water (Gorham et al., 1984). The low supply of mineral particles deriving only from atmospheric deposition hinders the neutralization of acids produced via the decomposition of the organic matter (Shotyk, 1988). Moreover the specialized vegetation that characterizes these environments, constituted predominantly by *Sphagnum* mosses along with ericaceous shrubs, has a role in increasing the acidity. *Sphagnum* mosses, due to their high cation exchange capacity, efficiently remove cations from the solution and replaces them with hydrogen ions, resulting in a lowering of the pH (Rydin et al., 2013).

High acidity, low oxygen availability and scarcity of nutrients are key factors in regulating the decomposition of organic matter, which is slowed down in these environments, with the consequent accumulation of dead plant material as peat beneath the living vegetation. Ombrotrophic peatlands are generally less decomposed than minerotrophic ones (Clymo, 1983; Damman, 1995).

Because of the features listed above, ombrotrophic peatlands are more suitable for palaeoenvironmental studies and should be preferred over minerotrophic ones.

2.1 Peat bogs and environmental reconstructions

Peat bogs are valuable archives for environmental and climatic reconstructions, presenting several advantages compared to other natural archives (e.g., ice cores, lake sediments) (Chambers et al., 2012):

- a widespread global distribution that ensures better accessibility and easier sampling;
- an easy application of dating techniques, using radionuclide and radiocarbon methods. Peats are almost exclusively constituted by organic matter, leading to high-resolution and low-uncertainty chronologies;
- they are isolated from groundwater, registering only the atmospheric – and therefore climatic – signal.

They have been used as archives for Holocene environmental and climatic reconstructions for over a century. The stratigraphy of European peat bogs was one of the first proxy climate records (Godwin, 1975). The pioneering work of Blytt (1876) and Sernander (1908) provided the basis for the first European Holocene climatostratigraphy with the creation of the Blytt-Sernander scheme. Due to the hypothesis of a cyclic regeneration of peat (von Post and Sernander, 1910) and other misconceptions, such as the autogenic succession of peat proposed by Osvald (1923), the potential of peat bogs as climatic archive was not properly exploited until the works of Aaby (1976), Van Geel (1978) and Barber (1981), with the final rejection of the regeneration hypothesis. Barber (1981) demonstrated the major role of climate as an allogenic forcing factor in peat formation. Other factors, such as hydrology, drainage and vegetation are all subordinate to climate.

Today a wide array of proxies are used to reconstruct past environmental, climatic and human history from peat bogs (Berglund, 1987; Charman, 2002; Chambers and Charman, 2004; Chambers et al., 2012). Quantitative macro- and microfossil analysis, such as plant macrofossils (e.g., Barber et al., 1998; Mauquoy et al., 2004; Hughes and Barber, 2004; Chambers et al., 2007; Swindles et al., 2007), pollen, spores and non-pollen palynomorphs (e.g., Fægri and Iversen, 1989; Huntley, Prentice, et al., 1993; Peyron et al., 1998; van Geel et al., 2003; Birks and Birks, 2004; Davis et al., 2003) testate amoebae (e.g., Hendon et al., 2001; Schoning et al., 2005; Warner et al., 2007; Booth, 2008), charcoal (e.g., Moreno, 2000; Tinner et al., 2005; Whitlock et al., 2007), diatoms (e.g., Beyens, 1985; Korhola et al., 2000; Fukumoto et al., 2012), peat humification (e.g., Nilssen and Vorren, 1991; Chambers et al., 2007; Caseldine et al., 2000) and stable isotopes (e.g., Nichols et al., 2009; Kühl and Moschen, 2012; Bilali et al., 2013; Finsinger et al., 2013) are the most widely used proxies for vegetation, climatic and human impact reconstructions.

Peat bogs are also of major interest for studies of soil dust and volcanic ash particles (e.g., Shotyk et al., 2002; Weiss et al., 2002; de Jong et al., 2006; Sapkota et al., 2007; Le Roux et al., 2012), marine aerosols (e.g., Singh and Kanakidou, 1993), major and trace metals of natural and anthropogenic origin (e.g., Shotyk, 1996; Martínez Cortizas et al., 1997; Shotyk et al., 1998; Weiss et al., 2002) and organic pollutants (e.g., Dreyer et al., 2005; Zaccone et al., 2009b).

Each individual proxy has its own strengths and limitations, therefore in palaeoenvironmental studies it is important to apply a multi-proxy approach for a more reliable reconstruction. In this study, pollen and inorganic chemistry are investigated along the core as proxies of climate and environmental changes during the Holocene.

2.1.1 Pollen analysis

Palynology was introduced in 1916 by von Post (von Post, 1916) and started being really applied in the 1930s, with the first work of Erdtman (1934). It soon became one of the most important branches of Quaternary palaeoecology (Bradley, 1999; Birks and Birks, 2004).

Palaeoenvironmental reconstruction from pollen analysis is possible due to the following characteristics of the pollen grains (Bradley, 1999):

- morphological characteristics that make them highly recognizable and identifiable to genus or species level;
- abundant production and wide distribution (anemophilous species);

- excellent preservation in sediments, thanks to their outer layer, the exine, made of sporopollenin, a extremely resistant complex polymer;

- they reflect the past vegetation in an area at a particular time.

Pollen grains are produced by plants and dispersed by insects (entomophilous species) or by wind (anemophilous species) as pollen rain, which may be deposited on lacustrine and peat sediments, where it becomes part of the stratigraphic record and may be preserved for millennia. Different systems of dispersal of pollen lead to a different pollen production, with anemophilous species producing much more pollen with respect to entomophilous and autogamous (self-fertilizing) ones. This, as well as the different degree of pollen preservation, has to be taken into account when dealing with the interpretation of fossil pollen data, for the reconstruction of the past vegetation. Extensive studies on modern pollen rain and modern vegetation carried out in the past decades mainly in North America (Davis and Webb, 1975; Webb and McAndrews, 1976; Webb et al., 1978; Delcourt et al., 1984) and in Europe (Huntley and Birks, 1983; Davis et al., 2003), with the creation of modern pollen data maps, indicate that, despite the problems involved in pollen production, dispersal and preservation, the pollen rain closely reflects the broad geographical patterns of vegetation (Bradley, 1999). Interpreting fossil pollen records requires a clear understanding of the relationship between pollen and the environmental parameter (vegetation, land-use, climate) that it represents. The existence of fossil (FPD) and modern pollen databases (EPD) provides a valid source of information to study past changes in terrestrial vegetation, land-cover and climate at both large and small spatial scales over the Quaternary period (Davis et al., 2003).

Palaeoclimatic reconstruction from fossil pollen is based on the assumption that the vegetation distribution is largely driven by climate. The study of surface pollen samples, mainly from lakes and mires, enables the interpretation of pollen assemblages in terms of climate. The natural vegetation is nowadays affected by human pressure, but the broadscale relationships between pollen and climate are still valid and may provide robust and reliable palaeoclimatic reconstructions (Bradley, 1999).

Pollen analysis, comprehensive of pollen grains, spores and non-pollen palynomorphs, together with micro-charcoal analysis, is a powerful tool, yielding information about vegetation history, climate events and impacts from human activities (mainly land use changes due to cultivation, pastoral activities and forest clearance).

2.1.2 Inorganic geochemistry: atmospheric deposition in peat bogs

In the last few decades numerous geochemical studies using peat bogs have attempted to reconstruct atmospheric deposition of mineral dust, ancient and modern anthropogenic pollution and Holocene climate change (e.g., Martínez Cortizas et al., 1997; Shotyk et al., 2001, 2002; De Vleeschouwer et al., 2007; Sapkota et al., 2007; Allan et al., 2013a; Fagel et al., 2014).

Ombrotrophic peat bogs are excellent natural archives for atmospheric depositions: they are hydrologically isolated from the influence of local groundwater and surface waters and fed solely by atmospheric deposition (Damman, 1986). They extend sufficiently back in time and enable an adequate sampling resolution that allow a detailed study of the Holocene (Shotyk, 1996).

Different types of atmospheric particles are trapped in the peat: soil dust, volcanic ash and anthropogenic aerosols (Givelet et al., 2004). *Sphagnum* mosses, which constitute the dominant vegetation in peat bogs, efficiently trap major and trace elements from the atmosphere, as their high surface-to-volume ratio maximizes interception. Furthermore, *Sphagnum* mosses possess a high cation exchange capacity, which allows the uptake and immobilization of ionic forms of metals, such as lead (Shotyk et al., 2015).

Lead is by far the most studied trace metal in peat bogs for the reconstruction of anthropogenic impacts on the environment, mainly because it is largely recognized as being immobile in ombrotrophic peat bogs (Shotyk et al., 1998; Martínez Cortizas et al., 2002; Le Roux et al., 2004; Novak et al., 2011; Allan et al., 2013b). Moreover, the isotopic composition of lead keeps a fingerprint of the source and it can therefore be used to distinguish between natural and anthropogenic sources (Komárek et al., 2008).

The interpretation of the geochemical data archived in peat bogs require to ascertain the immobility of elements. Indeed, post-depositional migration would lead to the misinterpretation of the data.

The mobility/immobility of trace metals in peat is still a matter of debate and no general agreement has yet been reached on this topic yet. Heavy metal mobility in peat is still imperfectly understood. They are vulnerable to post-depositional migration because of changes in the water table, in pH and/or oxidation/reduction status, elemental uptake by surface vegetation, and the degree of humification (Mighall et al., 2002; Rausch et al., 2005).

The state of the art about mobility and immobility of the heavy metals of interest for this thesis (other than the above-mentioned lead) are briefly discussed below.

The post-depositional behaviour of zinc, often associated to lead in sulfide

minerals and coals (Shotyk et al., 2003, 2005), differs from that of lead and is still under debate. Surface enrichment of zinc has been observed in numerous studies using peat cores, likely due to bioaccumulation by living vegetation (Livett et al., 1979; Rausch et al., 2005). Others have reported zinc to be affected by post-depositional migration, linked, among others, to water table fluctuations and pH conditions (Kempter and Frenzel, 1999; Nieminen et al., 2002; Allan et al., 2013b). In contrast, Novak et al. (2011) proposed that zinc is immobile in ombrotrophic peats since zinc and lead profiles were well correlated. Hence, the interpretation of zinc profiles in ombrotrophic peat cores requires caution.

Arsenic is relatively immobile in peat bogs, as evidenced by several studies where the arsenic profile follows the one of lead, reflecting historical atmospheric deposition from mining and smelting activities (Cloy et al., 2009; Allan et al., 2013b). Other studies pointed out a possible mobility linked with fluctuations of the water table (Zaccone et al., 2008; Rothwell et al., 2009). Therefore, a careful interpretation should be made at sites more subject to water table variations.

Compared to other studies, the post-depositional behaviour of cadmium in peat is poorly understood and underinvestigated. Cadmium is identified as mobile in peat by Rausch et al. (2005), as its vertical profile does not reflect the impacts of smelting and mining activities. In other studies (Coggins et al., 2006; Novák and Pacherova, 2008; Allan et al., 2013b), cadmium is considered mobile in the core. In contrast, the study of Pontevedra-Pombal et al. (2013) suggest the immbolity of Cd, the profile of which shows a similar chronology with the other elements analyzed (As, Ni and Zn).

Copper behaviour in peat bogs is controversial and was considered either immobile and mobile by different studies. Nieminen et al. (2002) showed that copper was preserved in a peat record, whereas Shotyk et al. (2002) and Ukonmaanaho et al. (2004) found that copper could be affected by plant uptake, like zinc. More recently, Rothwell et al. (2010), Novak et al. (2011) and Allan et al. (2013b) demonstrated that copper was immobile in the peat cores.

The multi-proxy approach chosen for this study provides independent evidence about past climate changes and human impacts that characterized the time covered by the peat bog record. In particular, combining data from pollen and geochemical analyses allows us to obtain new insights into variability in the Eastern Italian Alps during the Holocene.

Chapter 3

Research objectives

The Eastern Italian Alps occupy a key position between Central Europe and the Italian peninsula, representing a natural orographic barrier against humidity from the North Atlantic and receiving cold and dry winds from Eastern Europe. The Alpine area represents a strategic location that is highly sensitive to both natural forcings and anthropogenic factors. It is therefore of great importance to reconstruct past climatic conditions, trying to understand how climate and human societies jointly affected and still affect this mountain environment.

The literature offers several attempts at reconstructing past climate variability in the Alps, mainly focusing on the Western sector. For the Eastern sector, studies are available for the Austrian side while the Italian side is much less investigated. Moreover, numerous studies focus on the transition between the Late Glacial and the Holocene, a period of major climatic changes. To understand the current changes in the Alpine environment, it is of primary importance to investigate also the changes that occurred when anthropogenic activities started to impact on the environment and climate. This requires the study of continuous, highly resolved natural records, with a robust chronological control.

The aim of this study is therefore to reconstruct climatic and environmental variations during the Holocene, as well as the impact of human activities, through the investigation of a peat bog located in the Eastern Italian Alps (Dolomitic area).

A multi-proxy approach that includes the investigation of physical, chemical and biological parameters was selected in order to address the following primary objectives and questions:

- establishing if the Coltrondo peat bog represents an ideal natural archive to reconstruct past climate and environmental variations in the Dolomites;

- obtaining a better understanding of Holocene climatic events. Did the Coltrondo peat bog register climatic changes that occurred during the Holocene at regional and global scales?
- describing main anthropogenic impacts. How can this natural archive improve our knowledge about human history in the Comelico area, from the first human settlements to recent times?
- distinguishing between climatic and human signals. Anthropogenic disturbances on the environment are registered by natural archives, often masking the climatic signal. Can we divide the amplitude of Holocene climate natural variability from changes related to anthropogenic impacts?

Chapter 4

Area of study

The Coltrondo peat bog (Veneto, NE Italy, 46° 39' 28.37" N, 12° 26' 59.17" E) is located at 1790 m a.s.l. on the border between Italy and Austria (Fig. 4.1).

It is situated in the Dolomitic area, in the upper sector of the Piave river basin on the left slope of the Padola valley (Comelico area). It has a surface area of 3.7 ha and it is part of a peatland system extended for 14 ha, one of the most valuable naturalistic sites in the region. The area is included in the European Nature 2000 Network in the Special Protection Areas Dolomiti del Cadore e del Comelico, code number IT3230089.

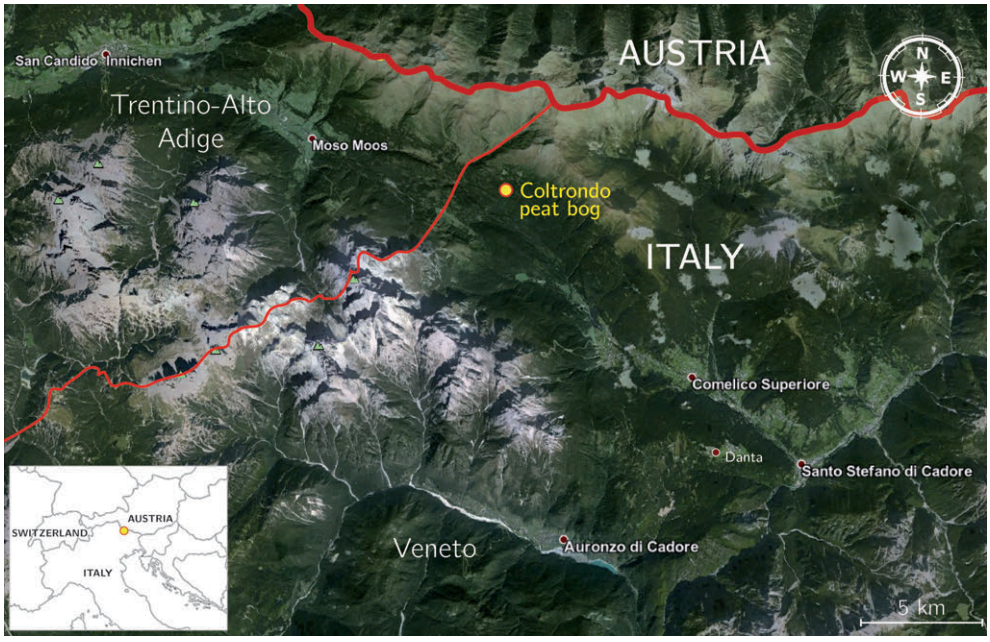

Figure 4.1: Localization of the Coltrondo peat bog.

4.1 Geology and geomorphology

The area is characterized by the Paleozoic crystalline basement, directly overlaid by the Lower Permian volcanic sequence visible on the Col Quaternà. The Coltrondo peat bog rests directly on the Mid Permian Sesto (Sexten) Conglomerate (Dal Cin, 1972) and the Upper Permian red beds (Val Gardena Sandstone) that were deposited in a semiarid setting of alluvial fans, braided streams and meandering rivers (Casati et al., 1982) (Fig. 4.2).

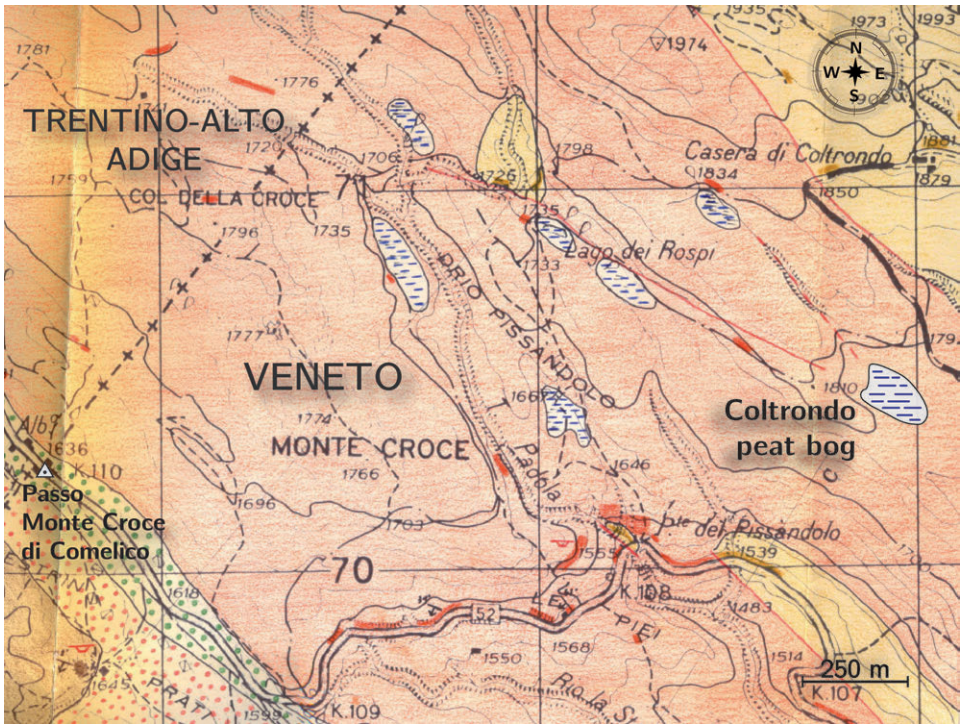

Figure 4.2: Geologic map of the Coltrondo area modified from Surian (1991). Red = Val Gardena Sandstone; yellow = Comelico phylladic schists; green dots = recent alluvial deposits; red dots = slopes deposits; blu dashes = peat deposits.

These lithological features entail strong water retention and enhanced impermeability, favouring the formation of bogs and wetlands. The rounded shapes of the landscape are due to the easy erodibility of the rocks and are mainly caused by the activities of the Piave glacier during the Last Glacial Maximum.

This area is characterized by ore-bearing Devonian-Dinantian carbonates, cropping out continuously for 100 km in the Carnic Alps (Brigo et al., 1988; Brigo et al., 2001). The mineralizations are stratabound to a carbonate

sequence and mainly consist of sulphides, barite and fluorite, associated to gangue that varies regionally (Brigo et al., 2001).

4.2 Modern vegetation

The vegetation of the Comelico area is characterized by the dominance of *Picea* (spruce) forests, extended from lower altitudes up to the treeline, localized approximately at 2000 m a.s.l. *Abies alba* (fir) is also present, but in much lower percentages. *Larix* (larch) also characterizes the arboreal vegetation. It is preferentially located near mountain meadows and in pasture meadows now abandoned by humans. The forest vegetation also contains a low percentage of *Pinus sylvestris* (pine). *Pinus mugo* (arolla pine) is present with quite extensive pure stands on steep slopes.

The modern vegetation has been influenced by centuries of human forestry management, which favoured spruce over fir, pine, larch and especially *Fagus* (beech), present nowadays only as underwood shrub. The general abandonment of pastoral activities in the last few decades favoured the diffusion of shrubs, such as *Rhododendron* and *Vaccinium* (heath family), *Salix* (willow) and *Alnus viridis* (green alder).

Figure 4.3: Coltrondo peat bog: *Sphagnum* mosses carpet with *Calluna vulgaris*.

The Coltrondo peat bog is characterized by a high biodiversity and by the presence of rare and endangered species (e.g., *Drosera intermedia* and *Carex chordorrhiza*). The mire is surrounded by a spruce forest, with the presence of arolla pines growing on the margin of the bog.

The microtopography of the bog is characterized by hummocks and hollows that present a vegetation typical of ombrotrophic peat bogs. The dominant species are *Sphagnum* mosses, mainly *Sphagnum magellanicum*, *S. russowii* and *S. capillifolium*. Other abundant species present on the bog are *Eriophorum vaginatum*, *Vaccinium microcarpum*, *Calluna vulgaris*, *Juniperus communis*, *Andromeda polifolia*, the already cited *Drosera intermedia*, *Tricophorum caespitosum* and *Carex limosa* (Fig. 4.3).

4.3 Modern climate

The study area is influenced by an alpine climate, with temperate summers and cold and prolonged winters. Atmospheric mean temperatures are around 4.5°C with higher temperatures registered generally during July, sometimes August (monthly mean around 11°C – 14°C) (Fig. 4.4).

The annual precipitation of the area averages between 1150 and 1220 mm, with a mean of 110 – 160 rainy days per year, uniformly distributed throughout the year, with the exception of the winter, a relatively dry season (Fig. 4.5). The snow cover can reach up to 400 cm and generally lasts six months, from the end of October until April.

Low temperatures and abundant precipitation are ideal conditions for the existence and maintenance of peatland systems, which indeed characterize the area.

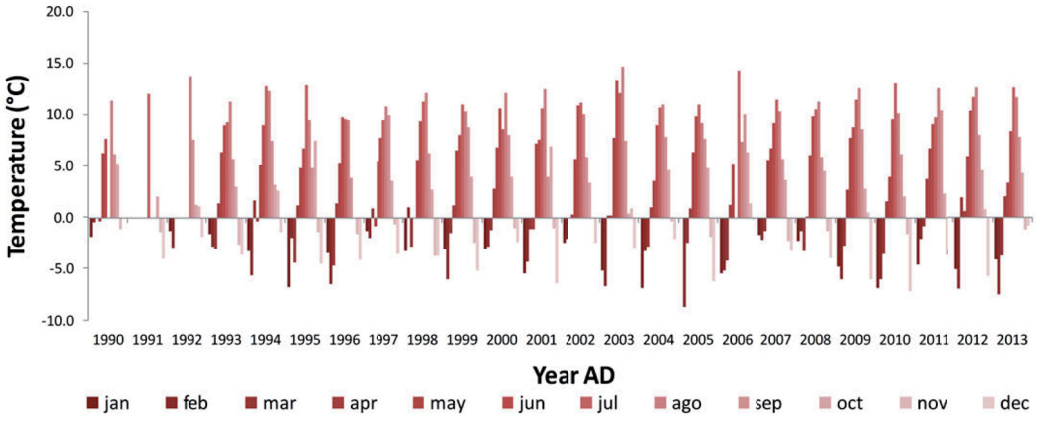

Figure 4.4: Monthly mean temperature measured at the Malga Coltrondo, next to the Coltrondo peat bog, in the interval of time 1990 – 2013 (www.arpa.veneto.it).

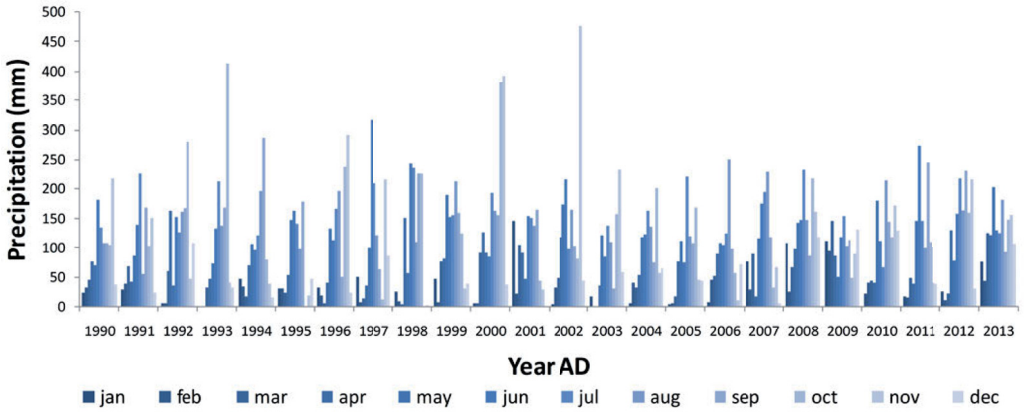

Figure 4.5: Monthly precipitation measured at Passo Monte Croce di Comelico, next to the Coltrondo peat bog, in the interval of time 1990 – 2013 (www.arpa.veneto.it).

4.4 State of the art

4.4.1 Archaeology and historical information

The only pieces of archaeological evidence found in the Comelico area are flint artefacts, dating back to the Mesolithic (Cesco Frare and Mondini, 2005), when nomadic populations, during the hunting season, would reach high mountain environments to hunt for large herbivores.

There are no later archaeological finds, making it difficult to reconstruct with any precision the Prehistory of the area and the human settlements in the Padola valley. The evidence of several necropoles in the nearby Cadore area (Lozzo, Pozzale and Valle) indicate that it was already inhabited by the 7th century BC (Ciani, 1862). This is confirmed by the Venetian inscriptions found at Lagole di Calalzo, dated back to the 7th century BC (Lomas, 2003).

Roman findings are abundant in Cadore, which fell under the Roman rule in 115 BC. In Comelico, hypotheses suggest the presence of a Roman road connecting Auronzo to the Puster valley – Roman settlements are well documented in the near Sesto and San Candido (*Littamum*) (Dal Ri and Di Stefano, 2005) – through the Kreuzbergpass (De Bon, 1938), and recent finds on the Kreuzbergpass (Padovan, 2014) seem to validate this idea. Anyway, no clear proof of human settlement in this area have been found for this period.

After the fall of the Roman Empire, the Cadore area was subjected to a succession of invaders (Ostrogoths, Merovingians, Byzantines and Lombards). Under the Lombards, in the middle of the 6th century, the Comelico

area was probably populated for good (Collodo, 1988).

For the Early Middle Ages, documentation is extremely scarce for the Cadore area. The first documents available date only from the 12th century (Ciani, 1862; Collodo, 1988) and regard the regulation of pastoral activities, which were well established at that time also in the Comelico area. Indeed, pastoral and forestry activities were regulated by rural codes – the so-called *laudi* – containing democratically approved norms (Zanderigo Rosolo, 1982). They provided detailed instructions for the exploitation of summer pastures in mountain environments (*montes*), also indicating the alpine routes ("strade delle peccore") to follow (Fig. 4.6; Cesco Frare, 2011). The first written documentation dates from the 12th century but refers to ancient regulations ("antiquitus", as reported in Cesco Frare, 2011). This suggests the importance of pasture and mountain resources and of their proper management for the subsistence of the inhabitants of these severe mountain environments.

Figure 4.6: Picture taken from Cesco Frare (2011) showing the possible alpine routes for the summer pasture during Middle Ages indicated in the *laudi* for the Comelico area.

From AD 1420, the Cadore and Comelico areas were under the dominion of the Republic of Venice, which increased the mining activities already present in the area and the exploitation of forestry for commercial purposes. This resulted in a general depletion of forestry resources, with fir and beech woods alternatively exploited (Pozzan, 2012).

At the end of 18th century (AD 1797) the Cadore and Comelico areas fell under the domination of Napoleon, then (AD 1814) under the Austrian

control, which lasted until 1866, when Cadore became part of Kingdom of Italy (Fabbiani, 1992). In the first decades of the 20th century the two World Wars had a significant impact on this area. During the first World War, Cadore was one of the principal Italian fronts for the defence against Austria. During the second World War, at Passo Monte Croce di Comelico, a strategic barrier constituted of 12 fortifications was built (AD 1940) to prevent the enemy from penetrating into the Veneto plain.

In the last few decades, the Comelico area has been characterized by a decrease in population and by a general abandonment of traditional, centuries-old practices such as pastoral and agricultural activities.

4.4.2 Mining activities along the centuries

The mineralizations present in the area, providing mainly lead, zinc, iron, copper and traces of silver associated with lead ore, were probably exploited by humans since ancient times. Unfortunately, as in the case of archaeological evidence, metallurgical activities are scarcely documented prior to the Venetian domination, making it difficult to reconstruct the mining history of the Cadore area.

Historians reconstructed the probable evolution of these activities across the centuries, often aided by toponymy. Indeed, place names that refer to metals or their use (e.g., Monte Ferro, Forni Avoltri) may help us localize the main mining sites. Figure 4.7 is a map drawn by Cucagna (1961), with the indication of the main mining sites and places where metallurgical activities were carried out in the past centuries.

The flourishing metallurgic activities carried out by the Romans elsewhere in Europe are not documented in the Cadore area. This does not necessarily mean that the Romans did not exploit the mineral resources of the area. On the contrary, it is more than plausible that they did, as stated by Cucagna (1961) and De Lorenzo (1999), due to their presence in the area and the archaeological discovery of possibly local metal artefacts dated ca. 300 BC.

The lack of documentation does not allow a reliable reconstruction of the mining exploitation. De Lorenzo (1999) mentions a decline after the fall of the Roman Empire and the subsequent invasions, with a new revival from the 11th century. From the 11th century, historical documents indicate the exploitation of the mineral resources in the entire Cadore area and the presence of furnaces for metal processing. The most important metal extracted in this period was iron, but the importance of silver in Medieval economy is not to be overlooked. Therefore, every small lead-silver mining site (e.g., *Argentiera* at Valle Inferna, Auronzo and Salafossa near to Santo Stefano di Cadore) was probably exploited (Vergani, 2003).

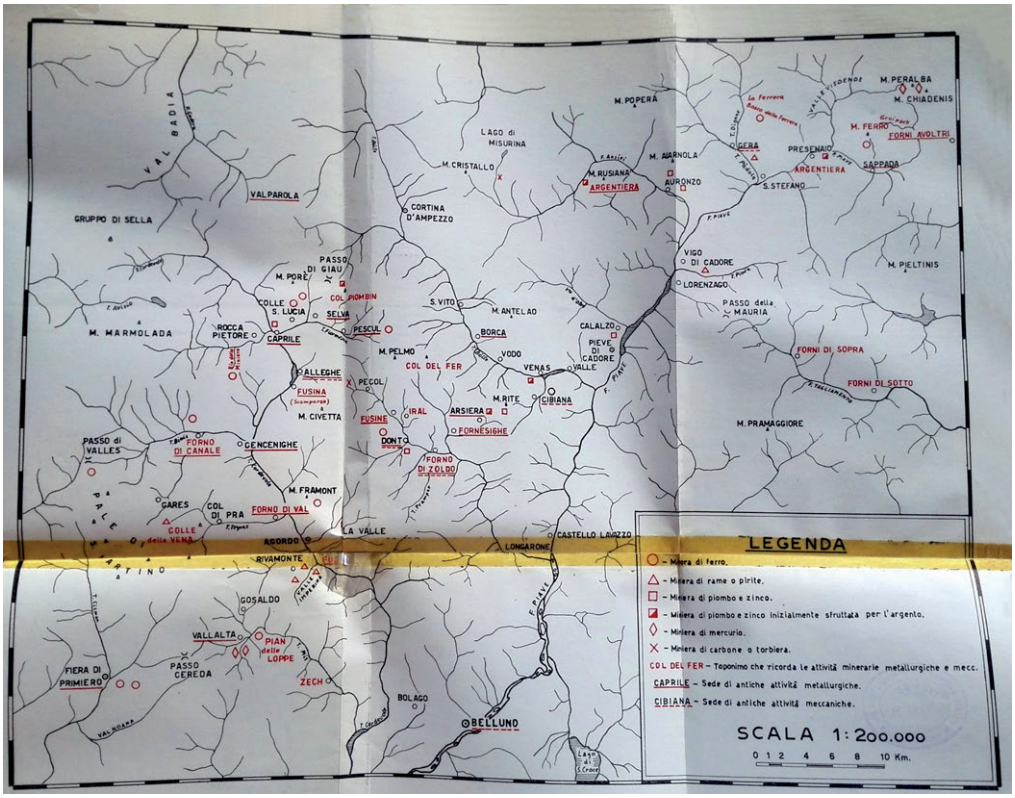

Figure 4.7: Maps of the major mining and metallurgic sites as reconstructed by Cucagna (1961). In the maps not only the mining sites are indicated, but also places where metallurgical activities were carried out, as well as names of places that refer to mining activity.

Under the Republic of Venice, copper and silver metals became more important. The most important copper site in the Cadore area is located in Valle Imperina (see Fig. 4.7), but others ores of lesser importance were present, probably near Santo Stefano di Cadore. It is in this period, between 1460 and 1530, that mining and metallurgic activities registered a significant increase all over Europe, primarily for copper and silver, but also for lead and gold. This surge was followed by a decline, partly due to the depletion of the deposits, but mostly to American exportation of metal (Vergani, 2003). This decline is registered also in the Cadore area and in the nearby Province of Vicenza, where silver extraction had flourished until then. In the following centuries, mining in Cadore saw high-activity periods alternating with periods of abandonment until its irreversible decline from the end of the 18th century, in conjunction with the end of the Republic of Venice and a general economical crisis.

In the 19th and 20th centuries, mining activities continued in Cadore, with different concessions and period of inactivity, mainly for lead and zinc. Remarkably, the Salafossa mine covered, from the 1950s to the end of 1970s, 1/3 of the Italian production of zinc (De Lorenzo, 1999). Today, all the mines of the area are abandoned, mainly due to the depletion of deposits and because they are no longer economically important.

4.4.3 Palynological studies carried out in the area

Few palynological studies have been carried out in the Cadore area. Kral (1986a) in the 1980s studied Sant'Anna Lake and the Danta di Cadore peat bog, the same site studied in recent years by Poto (2013), who investigated the transition from the Last Glacial Maximum to the Holocene, an interval of time not covered by the Coltrondo peat bog. Other works, presented in

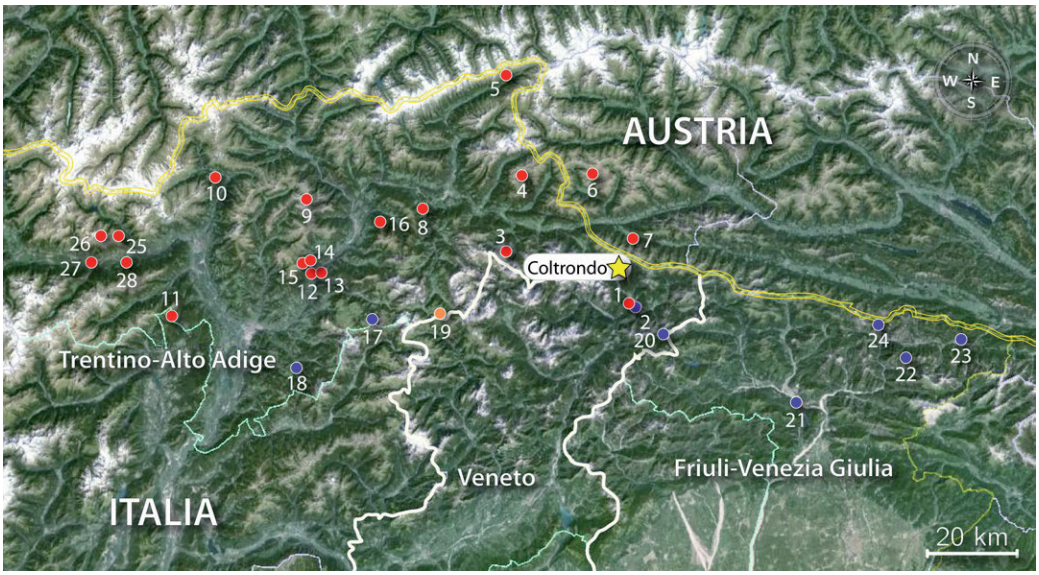

Figure 4.8: Map presenting the Coltrondo site and other palynological studies in the area, for a possible comparison. The yellow star represents the Coltrondo peat bog; the studies marked by a red dot rely on radiocarbon dating, while those marked by a blue dot do not; the study marked by an orange dot do not cover the interval of time of interest for this study. See Table 4.1 for details on each site present on the map.

Figure 4.8 and Table 4.1, reconstruct the vegetation evolution during the Holocene in the Eastern Italian Alps, focussing mainly on South-Tyrol (see Table 4.1 for references), but also also on Friuli-Venezia Giulia (Kral, 1982, no radiocarbon dates) and Austria (Kral, 1988; Oeggl and Wahlmüller, 1994).

The picture of the Eastern Italian Alps outlined by these works, especially studied by Kral and Seiwald, reflect the general trend recorded in the rest of the Alps, with some major climatic oscillations during the Holocene. When humans started to live permanently in the area (the dating of such human settlements varies from site to site), the climatic signal starts to be masked by human activities (mainly pasture and agriculture, but also mining activities), making it difficult to separate climatic events from anthropogenic disturbances.

Most palynological studies around the Coltrondo area date back to the 1980s. No studies use the ^{210}Pb method for the dating of the last ca. 150 years, while the ^{14}C dates are often scarce and characterized by high uncertainty. It is worth mentioning that back in the 1980s, the amount of material needed for the ^{14}C measurements was huge; for instance, Kral (1991) writes of peat material taken from 10 cm for 1 single measurement. Moreover, some studies relied on other works for ^{14}C dating, which led to higher uncertainty in the estimate of the age-depth relationship.

These considerations are taken into account when discussing the pollen data of the Coltrondo peat bog. In particular, the comparison with works from the 1980s will often be supported by more recent works carried out in the Alps. This will ensure a more reliable reconstruction of the climatic, environmental and anthropogenic events registered in the bog.

Table 4.1: List of palynological works in the North-Eastern Italy and Austria, next to the Coltrondo area. ✓ = presence of radiocarbon dates (in brackets the number of ^{14}C dates; * = the study uses some ^{14}C dates from other studies), ✗ = no radiocarbon dates. Moreover, the time interval investigated by the studies is checked: ✓ = it covers the range of the Coltrondo peat bog core, ✗ = out of the Coltrondo peat bog range.

	Site	**Altitude** (m a.s.l.)	**^{14}C dates**	**Interval of time**	**Reference**
1	Lago di Sant'Anna	1390	✓ (2)	✓	Kral (1986b)
2	Danta mire	1420	✗	✓	Kral (1986b)
			✓	✗	Poto (2013)
3	Lake Braies	1492	✓ (4)	✓	Schneider et al. (2010)
4	Rasner Möser	1100	✓ (2)	✓	Kral (1991)
5	Wieser-Werfer	2075	✓ (2)	✓	Kral (1991)
6	Hirschbichl	2140	✓ (3*)	✓	Oeggl and Wahlmüller (1994)
7	Kartitscher Moor	1520	✓ (2)	✓	Kral (1988)
8	Astalm	1955	✓ (1)	✓	Burga and Egloff (2001)
9	Penser Joch	2230	✓ (2)	✓	Burga and Egloff (2001)
10	Kurzmoos	1820	✓ (10)	✓	Stumböck (2000)
11	Totenmoos	1718	✓ (10)	✓	Heiss et al. (2005)
12	Dura-Moor	2080	✓ (6)	✓	Seiwald (1980)
13	Rinderplatz	1780	✓ (4)	✓	Seiwald (1980)
14	Malschötscher Hotter	2050	✓ (4*)	✓	Seiwald (1980)
15	Schwarzsee	2033	✓ (2)	✓	Seiwald (1980)
16	Sommersüß	870	✓ (5)	✓	Seiwald (1980)
17	Großes Moos	1880	✗	✓	Kral (1983)
18	Biotop Wölflmoor	1295	✗	✓	Kral (1986a)
19	Pescosta palaeolake	1521	✓	✗	Borgatti et al. (2007)
20	Malga Varmost	1480	✗	✓	Kral (1982)
21	Cavazzo-Vuarbes	270	✗	✓	Kral (1982)
22	Laghetto di Somdogna	1442	✗	✓	Kral (1982)
23	Malgadi Lussari	1554	✗	✓	Kral (1982)
24	Passo di Pramollo	1551	✗	✓	Kral (1982)
25	Lake Vernagt	1610	✓ (7)	✓	Festi et al. (2014)
26	Lagune mire	2180	✓(9)	✓	Festi et al. (2014)
27	Schwarzboden mire	2150	✓(11)	✓	Festi et al. (2014)
28	Penaud mire	2330	✓(4)	✓	Festi et al. (2014)

Part II

Materials and methods

Chapter 5

Coring, sampling and sub-sampling

The success of a palaeoenvironmental and palaeoclimatic study on peatlands starts with the appropriate selection of the site. Following Givelet et al. (2004), different criteria have been taken into account for the selection of the mire, such as the morphology, the hydrology and the trophic status of the peatland, as well as its location with respect to human activities. The aim was to retrieve an undisturbed peat core that would have preserved high-quality signals of past environment and climate variations. The mineralogy and chemical composition of the mineral substrate were also considered, due to their possible influence on the overlying peat layer as a result of the weathering of minerals and upward migration of ions diffusing into the peat (Shotyk and Steinmann, 1994). Ombrotrophic peat bogs should always be preferred over other peatlands, because they receive water and nutrients exclusively from atmospheric depositions (Clymo, 1983). Furthermore, their rate of organic decomposition is generally lower, resulting in a record with a better time resolution (Givelet et al., 2004).

In June 2011 a vertical core of 250 cm was collected from the Coltrondo peat bog. The superficial layers of the peat, including the acrotelm and the upper part of the catotelm, required a special corer to avoid any kind of compression during the extraction (De Vleeschouwer et al., 2011). For this purpose the first 100 cm were sampled with a 15x15x100 cm Wardenaar corer (Wardenaar, 1987). This modified corer – the normal one is 10x10x100 cm – prevents the compression of the monolith and enables the sampling of enough material for several different analyses, with the possibility to archive part of the core. The deepest layers of the bog were collected with a semicylindrical "D-section" 10x50 cm Belarus corer (Belokopytov and Beresnevich, 1955), using a three-borehole technique, where alternate, overlapping samples are re-

trieved from three different near boreholes, to reduce as much as possible any possible disturbance. The entire core was wrapped in plastic film, brought to the lab and stored at -18°C immediately after collection. It was subsequently cut in frozen conditions into 1 cm slices using a stainless steel band saw, as suggested by Givelet et al. (2004). The outside edges were discarded to avoid any contamination (Fig. 5.1). Each slice was then divided into several squares to obtain different sub-samples. This sub-sampling strategy enabled a multi-proxy approach that included, for each layer, a wide variety of physical, chemical and biological analyses (Fig. 5.2).

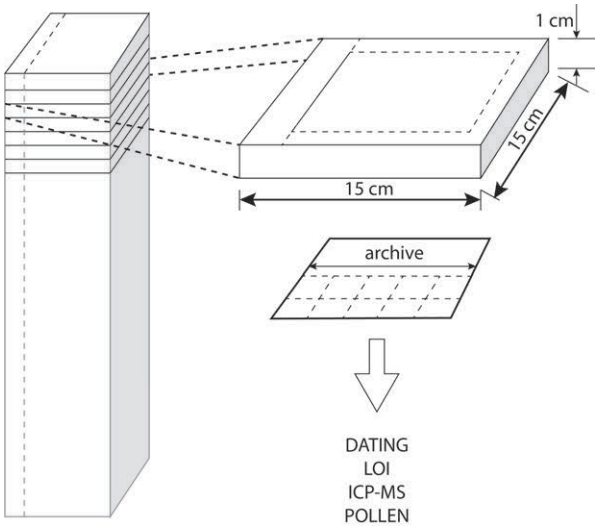

Figure 5.1: Sub-sampling strategy outline.

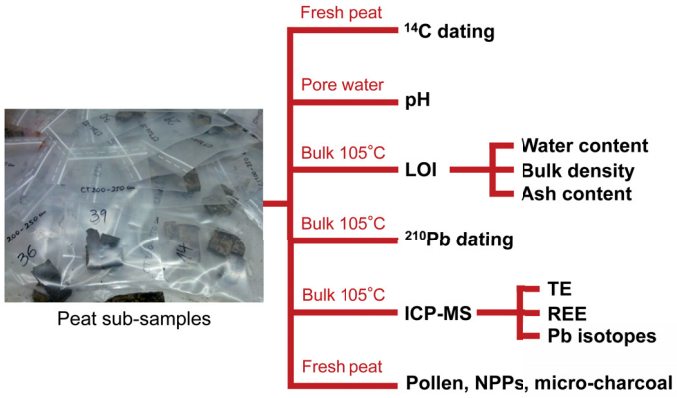

Figure 5.2: Physical, chemical and biological analyses performed for each layer of the core.

Chapter 6

Chronology

The chronology of the core is based on different radiometric techniques, whose aim is to establish a reliable and highly resolved age-depth relationship, the first fundamental feature of a palaeoenvironmental study. ^{210}Pb and ^{137}Cs measurements were performed for the first 40 cm and Accelerator Mass Spectrometry (AMS) ^{14}C dating was applied to the rest of the core.

^{210}Pb dating

The ^{210}Pb dating method is used to date the last 150 years of peat accumulation. ^{210}Pb is a radionuclide naturally present in two fractions: the supported ^{210}Pb, produced by decay of the primeval ^{238}U via intermediate daughters to ^{222}Rn gas in rocks and soils, and unsupported ^{210}Pb produced in the atmosphere by the decay of ^{226}Ra (Appleby and Oldfield, 1978). ^{210}Pb has a relatively short half-life of 22.3 years, and therefore it is detectable for seven half-lives (ca. 150 years).

Other chronological markers are usually measured, such as radionuclides associated with the development of military weapons and with energy production. These kinds of activity can release in the atmosphere ^{90}Sr, ^{134}Cs, ^{137}Cs, ^{239}Pu, ^{240}Pu, ^{241}Np, ^{241}Pu, ^{241}Am and ^{14}C, and if their signals are detectable in the peat sequence, they could be used within ^{210}Pb data.

For this study, samples were selected every cm for the first 40 cm, dried, homogenized and submitted to the Liverpool University Environmental Radioactivity Laboratory. ^{210}Pb and ^{137}Cs were measured by direct gamma assay performed using OrtecHPGeGWL series well-type coaxial low background intrinsic germanium detectors (Appleby et al., 1986). Unsupported and supported ^{210}Pb were detected and the CRS (Constant Rate of Supply) model of radioactive decay through time was used to obtain calendar ages for each depth (Appleby and Oldfield, 1978).

^{14}C dating

There are three main carbon isotopes naturally occurring on Earth: the stable ^{12}C (98.89%), ^{13}C (1.11%) and the unstable and radioactive ^{14}C (0.00000000010%) (Piotrowska et al., 2011). The radiocarbon method is based on the rate of decay of ^{14}C. ^{14}C forms in the upper atmosphere through the effect of cosmic ray neutrons upon ^{14}N. Suddenly formed, ^{14}C is oxidized to $^{14}CO_2$, entering the carbon biogeochemical cycle. Every plant and animal which utilizes carbon in biological food-chains absorb ^{14}C during its life time. As soon as plants and animals die, they stop the metabolic function of carbon uptake and ^{14}C only decays back to ^{14}N, emitting beta particles, and electrons with an average energy of 160 keV. Arnold and Libby (1949) were the first to measure the rate of its decay and they determined that the half-life of ^{14}C beta decay was 5568 ±30 years. The current best value for the half-life is 5720 ±30 years, but the value established in the 1950s is still used and represents the basis for the conventional definition of radiocarbon dating time scale (Piotrowska et al., 2011). After 10 half-lives times, the total amount of radioactive carbon present in a sample become very small: that's why 50-60,000 cal BP represent the limit of the radiocarbon dating technique.

For this study, 7 samples (plant-macrofossil remains and peat bulk samples) were prepared following Piotrowska et al. (2011) for radiocarbon dating. The samples were isolated from the core, cleaned with Milli-Q water to avoid contamination, dried and subsequently sent to the ^{14}CHRONO Centre, Queens University of Belfast, where the analysis was carried out using a NEC compact model 0.5MVAMS. After the creation of a first age-depth model, other 4 samples were prepared and sent to the ^{14}CHRONO Centre, for the refinement of the age-depth relationship.

Since atmospheric ^{14}C concentration varies through time, the radiocarbon dates do not have a linear relationship with calendar ages and therefore require calibration. The INTCAL13 calibration curve (Reimer et al., 2013), defined by absolutely dated records, was used with the *clam* software package (Blaauw, 2010) to obtain an age distribution for each dated depth.

Age-depth model

The age-depth relationship was created by combining the ages obtained from the two different techniques, using the software *clam* (Blaauw, 2010), to estimate the approximate calendar ages for all the undated depths of the core. This was achieved by modelling the accumulation of the peat through a bootstrap technique, whereby a repeated sampling of calibrated distributions is performed, with the calculation of an age-depth model for each repetition,

based on the dated depths, their uncertainties and a linear interpolation age-model; an approximation of the accumulation history of the peat deposit is thus obtained. The best-age estimate for any depth of the core is provided by the weighted mean of all age-model iterations at that depth (Blaauw, 2010).

Chapter 7

Bulk density, water content, organic matter and pH

Physical analyses were performed along all the profile of the peat bog, to determine the bulk density and to estimate water and organic matter content.

Samples were measured with a gauge to assess the volume, selected at 1-cm intervals for the uppermost 100 cm and at 3-cm intervals for the lower part of the peat core. Given the heterogeneity that characterizes peat material within each sample, especially in the poorly decomposed uppermost layers, samples with a larger volume were selected for the first meter to improve the quality of the measurements (Givelet et al., 2004).

Bulk density, estimation of water and organic matter content by loss-on-ignition (LOI) were performed following Chambers et al. (2011). Wet peat samples were placed in a crucible, weighed using a KERN balance Alt 220-4-NM (1 mg resolution) and subsequently dried overnight at 105°C. The dry samples were therefore weighed at room temperature, immediately after cooling in a dessiccator cabin. The crucibles were placed in a muffle furnace at 550°C for 5 hours, cooled in the dessiccator cabin and subsequently weighed at room temperature. Calculations were made as follows:

$$Water\ content\ (\%) = \frac{Weight_{wet} - Weight_{dry}}{Weight_{wet}} * 100$$

$$Bulk\ density\ (g\ cm^{-3}) = \frac{Weight_{dry}}{Volume_{freshsample}}$$

$$Ash\ (\%) = \frac{Weight_{550}}{Weight_{105}} * 100$$

Pore water was extracted from the first 100 cm of the peat bog core, at 1 cm resolution, using the squeezing technique proposed by Shotyk and Steinmann (1994). Peat samples were sealed in polyethylene bags and squeezed by hand with constant pressure to express the pore water. The pH was measured immediately after extraction, using a CRISONmultiprobe MM 40+.

Chapter 8

Geochemical analysis

8.1 ICP-MS technique

The geochemistry of the peat bog was investigated using modern analytical techniques to determine major elements, trace elements and rare earth elements in peat and pore water, as well as their variations through time. The lead isotopic composition of peat samples was also determined. The Inductively Coupled Plasma Mass Spectrometry (ICP-MS) technique, one of the most widely technique used for peat geochemistry (Chambers et al., 2012), was selected for the analyses. It is a powerful multi-elemental technique that allows the measurement of very low concentrations – down to μg kg^{-1} – with low detection limits (Givelet et al., 2004) and it has the great advantage of being linear over at least 6 order of magnitude of concentration (Cairns, 2008).

An ICP-MS consists of six main components, briefly summarized in the following list (Taylor, 2000; Cairns, 2008):

- a sample introduction system, constituted by a pneumatic nebuliser for the conversion of the liquid sample into an aerosol, connected with a spray chamber cooled at 2°C, for the selection of the particles of the aerosol that will enter the plasma torch. Largest droplets falls by gravity and are discharged, while finest droplets are transported into the plasma sample injector;

- an argon plasma torch, to convert the atoms of the elements in the sample to ions. The magnetic field produced by a copper load coil connected to a radio-frequency generator induces the ionization of the argon gas flowing into the torch. These Ar ions collide with other Ar atoms, forming an inductively coupled plasma discharge, reaching

6000-10000°K. The aerosol reaches the plasma and its elements are ionized;

- an interface region between the induced coupled plasma, at atmospheric pressure, and the mass spectrometer, under vacuum conditions. It is constituted by two metallic cones, the sampler and the skimmer cones, which sample selectively the central channel of the plasma when the sample is present and have the fundamental role to reduce the pressure of the ion source;

- ion focusing lens, to separate the ion beam from matrix components, neutral species and photons, which could increase the background signal and cause signal instability. Furthermore they focus the ions to the mass analyser;

- a quadrupole mass analyser that separates ions by their mass to charge ratio (m/z), after ions have been directed into the collision/reaction cell to overcome the problem of polyatomic interferences. In helium mode (collision mode) the interferences are removed based on their physical size. In hydrogen mode (reaction mode) the polyatomic interference reacts with the hydrogen gas increasing its mass number or will pass the positive charge to the hydrogen: in each case their mass will be not detected by the mass spectrometer;

- a detector, called electron multiplier device, able to generate a measurable electric signal from the impact of a single ion, that can be related to the number of atoms of that element in the sample via the use of calibration standards.

ICP-MS measurements were performed at the Ca' Foscari University of Venice, using an Agilent7500cx collision/reaction cell (CRC) inductively coupled plasma mass spectrometer (ICP-MS) equipped with a CETACASX-520 auto-sampler. Among different nebulisers (concentric, micro-flow, cross-flow, v-groove) the v-groove was preferred because it is more tolerant to samples containing high levels of solids or particulate matter, and therefore better suited to working with peat. Since the sample solutions contained hydrofluoridric acid, a v-groove nebuliser HF resistant and a polyethylene spray chamber were chosen. Measurements were carried out using the reaction cell in both helium and hydrogen modes in order to convert interfering species into harmless and non-interfering ones.

8.2 Inorganic geochemistry of peat

Peat samples for geochemical analyses were selected along the core at 1-cm resolution for the first 100 cm and 3-cm resolution for the remaining part of the core. They were dried overnight at 105°C and subsequently milled and homogenized using an agate mortar and pestle (Givelet et al., 2004).

8.2.1 Acid digestion of peat samples

A fundamental step prior to the geochemical analysis is the digestion of the peat samples, achieved through a destructive technique requiring a hot acid mixture. Approximately 100 mg of homogenized powder were weighed into a 20-mL Teflon vessel containing an acid mixture composed of 9 mL HNO_3 (ROMIL, supra-pure grade) and 1 mL HF (ROMIL, supra-pure grade). Hydrofluoridric acid is essential to completely digest the silicate fraction of peat and to release all the trace elements (Givelet et al., 2004).

Samples were dissolved in closed-pressurized digestion vessels in a microwave oven Milestone-Ethos1.

Each run of digestion consisted of:

- increasing temperature up to 220°C in 10 min;
- holding 220°C for 10 min;
- cooling for 2 hours.

After every digestion the solution was controlled to ascertain its transparency and homogeneity. It was therefore transferred into graduated 50-mL polypropylene tubes, filled to the mark with high-purity MilliQ water.

8.2.2 Quality control

Calibration

An external calibration method, based on measurements of calibration standards of known concentration, was used for the conversion of the ICP-MS signal in counts per second (cps) to a concentration in mg kg^{-1} for each analyte.

A 10 mg L^{-1} mother solution was prepared for trace elements and rare earth elements, diluting together two 10 mg L^{-1} multi-elemental standard solutions (IMS-102 containing Ag, Al, As, Ba, Be, Bi, Cd, Ca, Cs, Cr, Co, Cu, Ga, Fe, In, K, Li, Mg, Mn, Na, Ni, Pb, Rb, Se, Sr, Tl, U, V, Zn and

IMS-101 containing Ce, Dy, Er, Eu, Gd, Ho, La, Lu, Nd, Pr, Sm, Sc, Tb, Th, Yb, Y). 5 calibration standards were prepared, ranging from 0.25 to 100 μg L^{-1} in order to cover, for each element, the concentration ranges present in peat samples.

A second 10 mg L^{-1} mother solution for major crustal elements (Fe, Al, Na, K, Ca, Mg, Ti) was also prepared from single standard solutions (ULTRA Scientific, 1000 mg L^{-1}). 3 calibration standards ranging from 400 to 2000 μg L^{-1} were prepared.

Furthermore, to compensate for the drift of the instrument, possibly occurring during the analytical run, continuous online mixing of an internal standard solution was performed during sample introduction, using a 10 μg L^{-1} Rh solution (ULTRA Scientific, 1000 mg L^{-1}).

The external standards normally define highly linear regressions for each analyte, relating signal intensity to concentration. The conversion from cps intensities to concentrations was therefore extrapolated from linear regressions with the y-axis intercept at zero concentration, which was assumed to represent an average blank of the standards, subtracted for calibration. For all the elements $R^2 > 0.97$ was obtained.

Procedural blanks and detection limits

Procedural blanks were determined from the analysis of acidic blank solutions (supra-pure grade HF and HNO_3, ultra-pure water) obtained during the digestion procedure (Section 8.2.1). One procedural blank was prepared for each digestion batch. The mean procedural blanks were used for blank subtraction in order to eliminate the contributions of elements possibly present in the acids and ultra-pure water.

Solution detection limits were calculated as the concentration corresponding to 3 times the standard deviation of the measurement of the procedural blanks. Peat sample detection limits were calculated fixing an average peat sample mass of 100 mg and a final digestion volume of 50 mL (Table 8.1). All values determined in this study were well above the detection limits of the instrument.

Accuracy, precision and reproducibility

The reference material (RM) used for the evaluation of the precision and accuracy of the analytical measures derives from an international interlaboratory study (NIMT/UOE/FM/001, Yafa et al., 2004). A RM sample was present in every digestion batch, for a total of 22 repetitions. Table 8.2 shows the RM values of the trace elements considered in the work of Yafa

Table 8.1: Solution and peat detection limits for peat analytical measurements.

	Solution DL (mg L^{-1})	**Peat DL** (mg kg^{-1})	**Mean peat conc.** (mg kg^{-1})		**Solution DL** (mg L^{-1})	**Peat DL** (mg kg^{-1})	**Mean peat conc.** (mg kg^{-1})
Li	0.014	0.007	1.8	Cd	0.002	0.001	0.107
Be	0.006	0.003	0.115	In	0.0003	0.0002	0.010
Na	6.1	3.0	244	Cs	0.0009	0.0005	0.368
Mg	25	12.3	346	Ba	0.708	0.354	56
K	2.5	1.3	1072	La	0.0019	0.0010	0.979
Ca	58	29	673	Ce	0.0053	0.0027	2.3
Sc	0.182	0.091	3.8	Pr	0.0013	0.0006	0.261
Ti	1.7	0.8	293	Nd	0.0022	0.0011	0.983
V	0.029	0.015	6.8	Sm	0.0007	0.0003	0.214
Cr	0.442	0.221	5.6	Eu	0.0013	0.0006	0.066
Mn	0.091	27	0.046	Gd	0.0268	0.0134	0.340
Fe	9.1	5.7	2115	Tb	0.0002	0.0001	0.032
Co	0.004	0.002	1.2	Dy	0.0004	0.0002	0.157
Ni	0.108	0.054	3.6	Ho	0.0001	0.0001	0.032
Cu	0.355	0.177	14.2	Er	0.0004	0.0002	0.092
Zn	1.2	0.611	8.6	Tm	0.0001	0.0001	0.013
Ga	0.020	0.010	2.8	Yb	0.0003	0.0002	0.086
As	0.089	0.045	0.916	Tl	0.0006	0.0003	0.067
Rb	0.014	0.008	3.5	Pb	0.123	0.061	19.2
Sr	0.112	0.081	10.3	Bi	0.0006	0.0003	0.070
Y	0.003	0.001	0.7	Th	0.0007	0.0004	0.233
Ag	0.008	0.004	0.110	U	0.0013	0.0007	0.220

et al. (2004), the RM mean values and the precision (%) of analytical measurements carried out for this study. The precision is generally equal or less than 10% with the exception of some major elements (Ca = 15.7%, Mg = 33.1%).

The reproducibility was tested by digesting and analysing 3 replicates for 4 samples along the core. Table 8.3 shows the results, presenting for each element the mean concentration of the 3 replicates ± the standard deviation of the measurements (in mg kg^{-1}), and the precision (in %), which is generally below 10%, with a few exceptions for the lanthanides.

8.3 Inorganic geochemistry of pore water

Pore water samples for geochemical analyses were selected along the first meter of the core, at 1-cm resolution. The extraction of pore water – as already explained in Chapter 7 for the pH – followed Shotyk and Steinmann

Table 8.2: Accuracy and precision of RM peat analytical measurements.

	RM concentrations (mg kg^{-1})	**RM found concentrations** (mg kg^{-1})	**Precision** (%)
Na	817 ± 307	868 ± 93	10.7
Mg	582 ± 168	1418 ± 470	33.1
Ca	683 ± 198	449 ± 69	15.4
Ti	357 ± 18	490 ± 33	6.7
V	7.82 ± 1.08	9.39 ± 0.87	9.3
Cr	6.36 ± 0.44	8.22 ± 0.83	10.1
Mn	7.52 ± 0.41	9.11 ± 0.9	9.9
Fe	921 ± 84	938 ± 96	10.3
Co	0.88 ± 0.09	1.05 ± 0.11	10.1
Ni	4.1 ± 0.37	4.3 ± 0.4	9.2
Cu	5.28 ± 1.04	5.18 ± 0.48	9.2
Zn	18.6 ± 1.9	18.9 ± 1.1	5.7
As	2.44 ± 0.55	2.39 ± 0.2	8.5
Cd	0.58 ± 0.08	0.3 ± 0.02	6.5
Pb	174 ± 8	167 ± 14	8.5

(1994). The pore water was transferred into graduated 14-mL polypropylene tubes without being filtered. In some cases it was necessary to combine adjacent samples to allow the subsequent ICP-MS analysis.

8.3.1 Quality control

Pore water analysis followed the same quality control procedures applied to the peat samples analysis (Section 8.2.2):

- the external calibration with the preparation of a multi-elemental standard for trace elements and rare earth elements (IMS-102 containing Ag, Al, As, Ba, Be, Bi, Cd, Ca, Cs, Cr, Co, Cu, Ga, Fe, In, K, Li, Mg, Mn, Na, Ni, Pb, Rb, Se, Sr, Tl, U, V, Zn and IMS-101 containing Ce, Dy, Er, Eu, Gd, Ho, La, Lu, Nd, Pr, Sm, Sc, Tb, Th, Yb, Y) and for major crustal elements (Fe, Al, Na, K, Ca, Mg, Ti – ULTRA Scientific, 1000 mg L^{-1}). The conversion from cps intensities to concentrations was therefore extrapolated from linear regressions with the y-axis intercept at zero concentration, which was assumed to represent an average blank of the standards, subtracted for calibration. For all the elements $R^2 > 0.99$ was obtained;

Table 8.3: Reproducibility of peat analytical measurements. For each sample, the mean concentration ± the standard deviation are expressed in mg kg^{-1}, precision in %.

	Sample 20 cm (mean values±s.d., precision %)	**Sample 70 cm** (mean values±s.d., precision %)	**Sample 96.5 cm** (mean values±s.d., precision %)	**Sample 239 cm** (mean values±s.d., precision %)
Li	1.00 ± 0.01, 1.4	3.13 ± 0.07, 2.1	2.94 ± 0.04, 1.4	3.34 ± 0.09, 2.6
Be	0.051 ± 0.002, 2.9	0.196 ± 0.006, 2.8	0.154 ± 0.001, 0.6	0.51 ± 0.01, 1.9
Na	119 ± 4, 3.4	504 ± 9, 1.7	225 ± 5, 2.3	918 ± 19, 2
Mg	1168 ± 14, 1.2	89 ± 9, 10	129 ± 14, 11.1	106 ± 6, 5.9
K	831 ± 15, 1.8	1707 ± 35, 2.1	1085 ± 23, 2.2	3130 ± 96, 3.1
Ca	1696 ± 27, 1.6	330 ± 70, 21.2	146 ± 4, 2.5	411 ± 66, 16.1
Sc	3.14 ± 0.07, 2.2	9.7 ± 0.3, 2.6	2.58 ± 0.02, 0.9	8.7 ± 0.2, 2.3
Ti	143.0 ± 0.6, 0.4	527 ± 14, 2.6	394 ± 2, 0.5	1110 ± 37, 3.3
V	3.02 ± 0.05, 1.6	11.7 ± 0.1, 1.1	10.06 ± 0.08, 0.8	29.8 ± 0.2, 0.6
Cr	3.4 ± 0.5, 14.6	10.1 ± 0.3, 2.7	8.6 ± 0.2, 2.1	13.2 ± 0.1, 0.9
Mn	7.5 ± 0.2, 3.1	10.0 ± 0.3, 2.5	7.71 ± 0.09, 1.2	63.7 ± 0.4, 0.6
Fe	2245 ± 39, 1.7	1144 ± 14, 1.3	937 ± 14, 1.5	7263 ± 32, 0.4
Co	1.10 ± 0.01, 1	0.805 ± 0.006, 0.8	1.15 ± 0.02, 1.5	2.271 ± 0.007, 0.3
Ni	2.11 ± 0.09, 4.1	7.12 ± 0.08, 1.1	4.01 ± 0.06, 1.4	2.95 ± 0.02, 0.8
Cu	3.62 ± 0.08, 2.2	5.86 ± 0.09, 1.6	5.1 ± 0.3, 6.6	10 ± 2, 23.5
Zn	41 ± 3, 6.6	4.4 ± 0.2, 3.3	3.33 ± 0.07, 2	7.6 ± 0.1, 1.4
Ga	2.5 ± 0.1, 4.5	3.59 ± 0.07, 1.8	2.85 ± 0.06, 2	7.3 ± 0.4, 5.1
As	0.55 ± 0.06, 11.3	0.87 ± 0.05, 5.4	0.70 ± 0.02, 3.4	1.54 ± 0.04, 2.4
Rb	5.59 ± 0.08, 1.4	4.3 ± 0.3, 7.5	3.3 ± 0.2, 4.7	4.2 ± 0.6, 13.3
Sr	21.3 ± 0.4, 1.9	9.9 ± 0.4, 3.7	6.6 ± 0.2, 3	12 ± 1, 9.5
Y	1.96 ± 0.06, 3	0.12 ± 0.01, 10.1	0.19 ± 0.03, 15.5	0.67 ± 0.06, 9.3
Ag	0.083 ± 0.002, 2	0.162 ± 0.005, 2.8	0.072 ± 0.002, 3.1	0.49 ± 0.02, 3.3
Cd	0.75 ± 0.01, 1.7	0.053 ± 0.002, 3.5	0.034 ± 0.001, 2.8	0.075 ± 0.003, 3.5
In	0.013 ± 0, 1.9	0.013 ± 0.001, 4.5	0.009 ± 0, 2.7	0.022 ± 0.001, 2.5
Cs	0.157 ± 0.002, 1.5	0.86 ± 0.02, 2.5	0.352 ± 0.007, 1.9	1.05 ± 0.08, 7.2
Ba	56 ± 2, 3.4	57.8 ± 0.8, 1.3	32.5 ± 0.6, 1.9	120 ± 8, 6.5
La	2.25 ± 0.06, 2.7	0.37 ± 0.05, 13.5	0.31 ± 0.08, 27	1.1 ± 0.1, 12.1
Ce	2.94 ± 0.06, 2	1.0 ± 0.1, 14.3	1.6 ± 0.3, 17.1	2.1 ± 0.3, 13.1
Pr	0.45 ± 0.02, 3.8	0.1 ± 0.02, 14	0.09 ± 0.03, 29.5	0.28 ± 0.03, 10.1
Nd	1.64 ± 0.07, 4	0.34 ± 0.06, 16.3	0.3 ± 0.1, 30.2	1.0 ± 0.1, 11.2
Sm	0.34 ± 0.02, 4.9	0.07 ± 0.01, 18.4	0.08 ± 0.02, 25.3	0.25 ± 0.03, 11
Eu	0.090 ± 0.004, 4.4	0.045 ± 0.002, 4.1	0.026 ± 0.003, 12.7	0.085 ± 0.006, 7.3
Gd	0.438 ± 0.008, 1.9	0.21 ± 0.01, 6.2	0.13 ± 0.02, 13.7	0.36 ± 0.02, 5.3
Tb	0.051 ± 0.003, 6.6	0.009 ± 0.001, 9.2	0.012 ± 0.002, 15.9	0.039 ± 0.004, 11.3
Dy	0.26 ± 0.02, 7.4	0.040 ± 0.002, 5.8	0.063 ± 0.005, 7.8	0.20 ± 0.02, 11.1
Ho	0.056 ± 0.004, 7.4	0.008 ± 0, 3.8	0.014 ± 0.001, 5.5	0.037 ± 0.004, 11.5
Er	0.16 ± 0.01, 8.6	0.026 ± 0.001, 3.1	0.042 ± 0.002, 4.1	0.10 ± 0.01, 11.2
Tm	0.022 ± 0.002, 9.8	0.004 ± 0, 7.3	0.007 ± 0.001, 8.5	0.012 ± 0.002, 14.8
Yb	0.15 ± 0.01, 7.3	0.028 ± 0.003, 12	0.049 ± 0.003, 5.9	0.09 ± 0.01, 13.8
Tl	0.059 ± 0.001, 1.8	0.087 ± 0.001, 1.5	0.032 ± 0.001, 1.7	0.158 ± 0.003, 1.8
Pb	57.1 ± 0.9, 1.5	32.7 ± 0.6, 1.8	9.8 ± 0.1, 1	19.8 ± 0.5, 2.4
Bi	0.130 ± 0.002, 1.5	0.074 ± 0.002, 2.2	0.039 ± 0.001, 2.4	0.109 ± 0.002, 1.5
Th	0.64 ± 0.02, 2.7	0.13 ± 0.02, 18	0.16 ± 0.06, 35.9	0.48 ± 0.09, 17.6
U	0.111 ± 0.003, 2.5	0.427 ± 0.009, 2.2	0.228 ± 0.004, 1.6	0.81 ± 0.03, 3.8

- the internal Rh standard solution to compensate for the drift of the instrument;
- solution detection limits, calculated as the concentration corresponding to 3 times the standard deviation of the acidic blank solutions (Table 8.4);
- accuracy and precision of the analytical measurements, evaluated using rain water certified reference material (TMRAIN-04), provided by Environment Canada, certified for 21 trace elements (Table 8.5).

Table 8.4: Detection limits for pore water analytical measurements.

	Detection limit (μg L^{-1})	**Mean pore water concentration** (μg L^{-1})		**Detection limit** (μg L^{-1})	**Mean concentration** (μg L^{-1})
Li	0.002	0.696	Zn	0.215	13.2
Be	0.002	0.40	Ga	0.001	0.815
Na	3.1	474	As	0.008	1.5
Mg	3.6	505	Rb	0.003	9.4
K	11.6	1938	Sr	0.022	5.5
Ca	8.1	1223	Y	0.002	0.086
Sc	0.023	0.937	Ag	0.001	0.220
Ti	0.2	8.5	Cd	0.002	0.085
V	0.016	0.870	In	0.0004	0.007
Cr	0.067	0.947	Cs	0.001	0.002
Mn	0.013	11	Ba	3.268	0.392
Fe	0.458	71	Pb	0.009	0.420
Co	0.002	0.322	Bi	0.0002	0.243
Ni	0.208	0.678	Th	0.002	0.480
Cu	0.003	0.937	U	0.0002	0.005

8.4 Lead isotopes

Pb isotopes ^{204}Pb, ^{206}Pb, ^{207}Pb and ^{208}Pb were measured using ICP-MS. The samples analysed for major, trace and rare elements were diluted in order to obtain a final lead content < 10 μg L^{-1}.

The Standard Reference Material (SRM) 981 Common Lead Isotopic Standard of the National Institute of Standards and Technology (NIST, Gaithersburg, MD, USA) was dissolved in cold 1:1 (v/v) diluted HNO_3 (65%), which was then diluted to a total lead concentration of 10 μg L^{-1}.

Table 8.5: Accuracy and precision of CRM (TMRAIN-04) pore water analytical measurements.

	CRM concentrations (μg L^{-1})	**CRM found concentrations** (μg L^{-1})	**Precision** (%)
Li	0.39 ± 0.08	0.46 ± 0.02	4.8
Na	90	79 ± 2.5	3
Mg	170	175 ± 45	2.6
Ca	600	609 ± 3	0.5
Ti	0.47	0.61 ± 0.01	1.8
V	0.64 ± 0.12	0.63 ± 0.005	0.7
Cr	0.79 ± 0.17	0.84 ± 0.004	0.4
Mn	6.1 ± 0.78	6.8 ± 0.1	1.7
Co	0.22 ± 0.04	0.23 ± 0.009	3.7
Ni	0.8 ± 0.17	0.9 ± 0.03	3.1
Cu	6.2 ± 0.1	7.1 ± 0.03	0.5
Zn	11.5 - 12.2	11.8 ± 1.0	8.3
As	1.07 ± 0.25	1.54 ± 0.04	2.5
Sr	1.7 ± 0.26	1.73 ± 0.03	1.6
Cd	0.48 ± 0.12	0.68 ± 0.004	0.6
Ba	0.73 ± 0.15	0.84 ± 0.02	1.7
Pb	0.29 ± 0.09	0.38 ± 0.008	2.2
U	0.25 ± 0.06	0.31 ± 0.007	2.1

During the analysis, 5 replicates for each sample were performed. The certified material was analysed every 4 samples, in order to correct for mass discrimination effects.

The precision of all measurements gave for each ratio calculation an RSD <0.4%, which was sufficient for our data to be used.

Measurements of the certified referenced peat material do not include data about lead isotope ratios, and accuracy could therefore not be clearly defined during this analysis. In order to understand if the calculated isotope ratio values are in an acceptable range, in the discussion of the results they are compared with other measurements of lead isotopes from peat bog samples.

Chapter 9

Biological analysis

Analyses of pollen, non-pollen palynomorphs (NPPs) and micro-charcoal were carried out at the Botanical Institute of the Innsbruck University. Samples were selected at 10-cm intervals for a first exploratory analysis of the core, then at 5-cm intervals along the first 125 cm of the peat profile. Finally, the resolution for the last 100 cm was improved to 2 – 3 cm. 55 samples were counted overall.

9.1 Pollen extraction

Methods for the preparation of pollen, NPPs and micro-charcoal followed standard techniques. The volume of each sample was measured and a defined amount of exotic pollen spores (*Lycopodium clavatum* tablets) was added for the calculation of palynological concentrations and influx (Stockmarr, 1971). The peat material was sieved and the fraction 7-150 μm was chemically treated following the standard protocol by Erdtman (1960) and Seiwald (1980).

The main phases consist of:

- chlorination with sodium chlorate ($ClNaO_3$) and hydrogen chloride (HCl) to oxidize lignin;
- acetolysis, with acetic anhydride ($C_4H_6O_3$) and sulfuric acid (H_2SO_4) in a ratio of 9:1 to hydrolyse cellulose and hemicellulose;
- hydrofluoric acid (HF), if necessary, to dissolve silicates.

The more resistant elements, such as pollen grains, spores and micro-charcoal particles were therefore isolated. The slides for the subsequent identification and counting were coloured by fuchsine and mounted in glycerine.

9.2 Analysis of pollen samples

The quantification of pollen, spores and micro-charcoal was carried out using an Olympus BX50 light microscope at the standard magnification of 400x and at a 1000x magnification for critical determinations. The reference collection of the Botanical Institute of Innsbruck University, standard identification keys (Punt, 1976; Punt and Clarke, 1980, 1981, 1984; Punt et al., 1988; Moore et al., 1991; Fægri et al., 1993; Beug, 2004) and pollen atlas (Reille, 1992) were used for the identification of the pollen grains and spores.

To obtain a statistically robust dataset, at least 1000 pollen grains were counted for each pollen spectrum (Berglund and Ralska-Jasiewiczowa, 1987), excluding pollen from aquatic and wetland plants.

Cerealia refers to Poaceae pollen grains larger than 40 μm, and were determined based on pollen morphology (Beug, 2004).

Parallel to pollen quantification, non-pollen palynomorphs (NPPs) and micro-charcoal particles were also considered. NPPs were identified following van Hoeve and Hendrikse (1998), van Geel et al. (2003) and, for the nomenclature, Miola (2012).

Micro-charcoals were identified as angular, black and opaque particles, and grouped in three size classes: < 50 μm, 50-100 μm and > 100 μm.

9.3 Palynological data presentation

Pollen taxa were grouped in Arboreal Pollen (AP) and Non-Arboreal Pollen (NAP) accordingly to the Alpine Palynological Database (ALPADABA) of the University of Bern (Switzerland), and the following sub-groups were created (Table 9.1):

- Climax trees (AP), local vegetation thriving in the area which surrounds the peat bog, mainly characterized by conifers;
- Other trees and shrubs (AP), deciduous trees and shrubs from local and extra-local sources;
- Herbs (NAP), local and extra-local grasses and herbs;
- Human Impact Indicators (NAP), herbs related to anthropogenic intervention (Behre, 1981).

The software *Tilia* (Grimm, 2011, version 1.7.16) was used to calculate the percentage, expressed over the terrestrial pollen sum (TPS). The high

abundance on/around the peat bog of Cyperaceae, *Pinus* and *Calluna vulgaris* may lead to their over-representation, therefore they were excluded from the TPS. The percentage of aquatic and wetland plants, spores, NPPs and micro-charcoal particles were calculated as a percentage of TPS. The to-

Table 9.1: Pollen taxa sub-groups for the Coltrondo peat bog.

Pollen sub-groups	**Pollen taxa**
Climax trees	*Abies*, *Fagus*, *Larix*, *Picea*, *Pinus cembra*
Other trees and shrubs	*Acer*, *Carpinus betulus*, *Fraxinus excelsior*-type, *Fraxinus ornus*, *Ostrya*-type, *Quercus robur*-type, *Tilia*, *Ulmus*, *Alnus*, *Betula*, *Castanea*, *Corylus*, *Ephedra fragilis*, *Hedera helix*, *Junglans*, *Juniperus*-type, *Lonicera*, *Morus alba*, *Olea europea*, *Populus*, *Rhamnus frangula*, *Salix*, *Sambucus nigra*-type, *Sorbus*-type, *Vitis*
Herbs	*Ambrosia*, *Anemone nemorosa*-type, Apiaceae, Asteraceae, Brassicaceae, Caryophyllaceae, Cichoriaceae, *Cirsium*, *Clematis*, Crassulaceae, *Echium*, *Epilobium*, Ericaceae, Fabaceae, *Filipendula*, *Geum*-type, *Helianthemum*, *Knautia*, Liliaceae, *Lotus*-type, *Lysimachia*, *Achillea*-type, *Melampyrum*, *Mentha*-type, Poaceae, Polygonaceae, *Potentilla*-type, Ranunculaceae, *Ranunculus acris*-type, *Rhinanthus*-type, Rosaceae, Rubiaceae, *Sanguisorba minor*-type, *Saxifraga oppositifolia*-type, *Saxifraga granulata*-type, *Saxifraga stellata*-type, Scrophulariaceae, *Senecio*-type, *Soldanella*-type, *Thalictrum*, Valerianaceae, *Veronica*-type, *Xanthium*
Human Impact Indicators	*Aconitum*-type, *Artemisia*, Campanulaceae, Cannabaceae, Cerealia, *Centaurea cyanus*, Chenopodiaceae, Gentianaceae, *Plantago lanceolata*-type, *Plantago major-media*-type, *Rumex acetosa*, *Rumex acetosella*, *Secale*, *Trifolium*, *Urtica*

tal concentration of pollen grains in the peat samples and the influx (pollen grains cm^{-2} yr^{-1}) were also determined for all taxa. Local pollen assemblage zones (lpaz) were determined with CONISS clustering, using a square root transformation of terrestrial pollen taxa percentages (Grimm, 1987). The palynological diagrams of the relative occurrence and influx of selected pollen, spores, NPPs and micro-charcoals were constructed using the software *Tilia* (Grimm, 2011, version 1.7.16).

Chapter 10

Data analysis

10.1 Normalization of the chemical profiles to Ti and calculation of enrichment factors

The element profiles were normalized to titanium (Ti), an element that is considered to be immobile, conservative, resistant to chemical weathering in acidic solutions (Nesbitt and Markovics, 1997), and with limited anthropogenic sources. Ti may be therefore viewed as an indicator of the abundance and distribution of lithogenic dust in the peat profile. The normalization provides deeper insight in the atmospheric metal deposition, compensating for natural variations in dust supplied to the peat bog and for bulk density differences along the profile (Shotyk, 1996; Shotyk et al., 2002; Weiss et al., 2002; Krachler et al., 2003b).

Scandium (Sc) is also well known for its stability against weathering and is widely used for normalization (e.g., Shotyk, 1996; Shotyk et al., 2002). The correlation between Ti and Sc in this core is highly significant (Pearson correlation coefficient 0.75, $p<0.01$). Ti was chosen over Sc for its higher concentrations in the peat samples, and because it displays a higher correlation with the ash content (Pearson correlation coefficient = 0.92, $p<0.01$).

Normalization of elemental concentrations is the basis for the calculation of the enrichment factor (EF). The EF represents the number of times an element is enriched in a sample with respect to the abundance of that element in the Earth's crust (Shotyk, 1996) and it may therefore provide useful information about metal depositions from anthropogenic sources.

EF is calculated as

$$EF_M = \frac{([M]/[Ti])_{sample}}{([M]/[Ti])_{UCC}}$$

where [M] and [Ti] refer to the total concentration (mg kg^{-1}) of elements and Ti in the peat sample and in the Earth's Upper Continental Crust (UCC; Wedepohl, 1995). The interval 120 – 170 cm (ca. 3720 – 6100 cal BP) was initially chosen as reference peat baseline for the calculation of EFs, because thought to be unaffected by humans. At these depths anyway, the Cu profile shows a peculiar profile, with some peaks possibly related to anthropogenic disturbances. Therefore, UCC values were preferred to determine the EF of all the elements considered.

10.2 Statistical analysis

Statistical analyses were performed using SPSS 20 and Canoco 5 software packages.

Geochemical data were firstly examined by means of descriptive statistics to summarize information through minimum and maximum values, 25° and 75° percentiles, and mean and median values, the most common statistical indexes of position and data distribution.

Linear correlation (Pearson correlation coefficient) was calculated using SPSS 20 to measure the strength of the linear association between variables. Data presented are significantly correlated with $p<0.05$ and highly significantly correlated with $p<0.01$.

Chemical data were normalized through a log transformation and standardization to z-scores – an important step when dealing with variables covering several orders of magnitude. Pollen data for statistical analyses were square-root transformed. The criterion for the selection of taxa to be included in the analyses was their presence in at least 3 samples.

Factor analysis by principal component analysis (PCA) was performed with SPSS 20 separately for chemical and pollen data, to order the data and summarize the variability in few components, grouping similarly distributed elements together.

To order the data obtained from the different proxies investigated, PCAs on pollen data were realized with Canoco 5, with physical, chemical and biological data as supplementary data. We chose to perform 3 PCAs, accordingly to the different phases encountered in the history of the peat bog and of the area studied.

Part III

Results and discussions

Chapter 11

Peat bog stratigraphy

The Coltrondo bog was drilled in June 2011 and 4 sections were extracted. The first meter was retrieved with the Wardenaar corer (Wardenaar, 1987), while other 3 sections, each one long 50 cm, with the Belarus corer (Belokopytov and Beresnevich, 1955). The drilling reached the mineral substrate, constituted by Val Gardena Sandstone. The core covers the entire peat bog history since its initiation. Figures 11.1 and 11.2 show the 4 sections of the core.

The first section is characterized by living plants in the first centimetres, followed by a part of really low decomposed peat down to 30 cm, probably the boundary between the acrotelm and the catotelm. At depth of ca. 31 cm a narrow stratum of more compact and dark peat is visible. After that, the Wardenaar section is characterized by the prevalence of fibrous peat down to ca. 90 cm, with two strata rich in wood remains, at depth of ca. 38 – 40 cm and between 45 and 50 cm.

The last part of the first section is characterized by darker fibrous peat, the same observable in the first section (100 – 150 cm) retrieved with the Belarus corer.

The two sections covering 150 – 200 cm and 200 – 250 cm are both characterized by fibrous peat.

The last 20 cm of the final section are characterized by a reddish color, due to the transition between peat to peaty soil, mixed with small Val Gardena Sandstone clasts.

The absence of lacustrine sediments at the bottom of the core suggests that the initiation of the bog followed a process of paludification, with the formation of peat directly over the mineral substrate (see Section 17.1, Part IV).

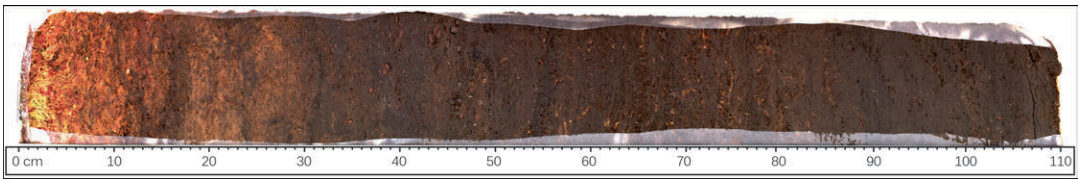

Figure 11.1: The first section of the core retrieved with the Wardenaar corer.

Figure 11.2: The three sections retrieved with the Belarus corer.

Chapter 12

Chronology of peat accumulation

12.1 Lead-210 dating

The samples from the first 40 cm of the peat bog core were analysed for total ^{210}Pb, unsupported ^{210}Pb, supported^{210}Pb and for ^{137}Cs. Table 12.1 reports their concentrations, in Bq kg^{-1}.

Table 12.1: Fallout radionuclide concentrations in the uppermost layers of the Coltrondo peat core. The concentration of total ^{210}Pb, unsupported ^{210}Pb, supported ^{210}Pb and ^{137}Cs is reported in Bq kg^{-1}.

Depth (cm)	**Total ^{210}Pb** (Bq kg^{-1})	**Unsupported ^{210}Pb** (Bq kg^{-1})	**Supported ^{210}Pb** (Bq kg^{-1})	**^{137}Cs** (Bq kg^{-1})
3.6	570 ± 57	570 ± 57	0.0 ± 0.0	369 ± 13
4.5	745 ± 91	745 ± 91	0.0 ± 0.0	274 ± 19
5.5	412 ± 59	412 ± 59	0.0 ± 0.0	147 ± 10
6.6	416 ± 56	416 ± 56	0.0 ± 0.0	254 ± 12
7.6	571 ± 42	571 ± 42	0.0 ± 0.0	466 ± 11
8.5	574 ± 65	574 ± 65	0.0 ± 0.0	346 ± 16
9.6	426 ± 41	426 ± 41	0.0 ± 0.0	248 ± 9
13.7	370 ± 38	370 ± 38	0.0 ± 0.0	238 ± 8
17.8	306 ± 39	306 ± 39	0.0 ± 0.0	103 ± 7
21.9	256 ± 51	256 ± 51	0.0 ± 0.0	83 ± 9
26	153 ± 33	153 ± 33	0.0 ± 0.0	53 ± 6
28.1	106 ± 17	99 ± 17	6 ± 2	29 ± 3
30.1	62 ± 19	56 ± 19	6 ± 2	48 ± 3
33.5	30 ± 5	23 ± 5	6 ± 2	30 ± 1
37.5	32 ± 10	26 ± 10	6 ± 2	19 ± 1

In Figure 12.1 is easily visible that there is a negligible difference between total and unsupported ^{210}Pb, this reflecting the trophic status of the peatland. In ombrotrophic bogs, indeed, which receive water and nutrients only from atmospheric depositions, it is assumed that the unsupported fraction of ^{210}Pb present in the atmosphere is the main component of the total ^{210}Pb, rather than the supported fraction present in rocks and soils (Appleby et al., 1997). Unsupported ^{210}Pb concentrations declined relatively uniformly with depth, with an apparent steepening of the gradient below 20 cm, partly due to the higher density of the deeper layers (see Chapter 13).

A significant fraction of the ^{137}Cs in the core derives from fallout from the 1986 Chernobyl nuclear reactor explosion. Some irregularities are visible in the first 8 cm of the core, where living plants are present. Cs follows the same pathways of biophilic elements, such as K, and these irregularities in the uppermost layers are therefore related to the biological activity of the surface vegetation. It is however almost certain that the high concentrations above 14 cm are largely attributable to Chernobyl fallout.

The CRS model applied to calculate ^{210}Pb dates suggests a relatively constant net dry mass peat accumulation rate over the past 100 years, with a mean value of 0.024 ± 0.005 g cm^{-2} y^{-1} and places 1986 at a depth of around 12 cm (Fig. 12.2). Table 12.2 presents the chronology of the first 40 cm of the Coltrondo peat bog, resulting from ^{210}Pb and ^{137}Cs.

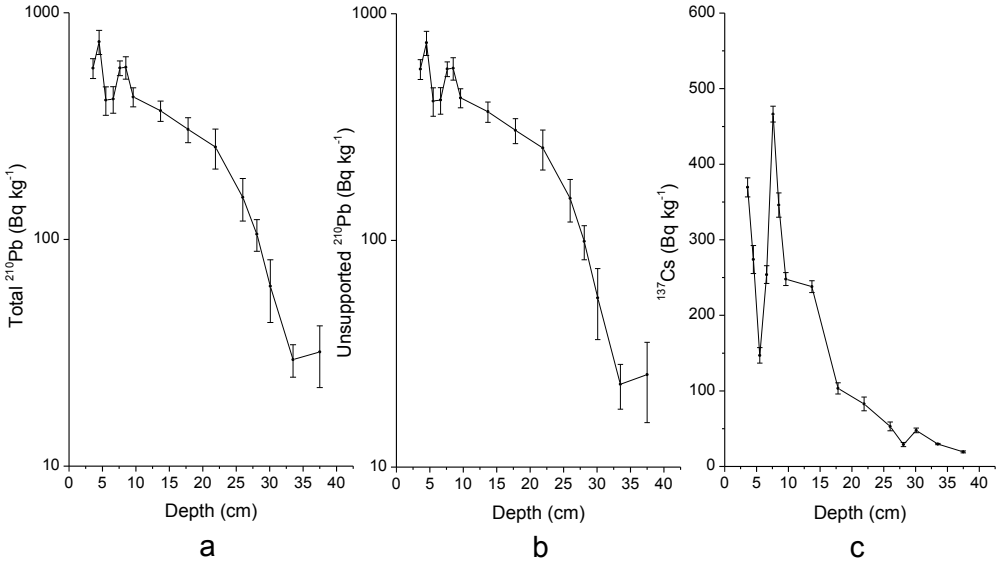

Figure 12.1: Fallout radionuclide in the upper layers of the Coltrondo peat bog, showing (a) total ^{210}Pb, (b) unsupported ^{210}Pb and (c) ^{137}Cs concentrations versus depth.

Table 12.2: ^{210}Pb chronology of the uppermost layers of the Coltrondo peat core with the calculated sedimentation and accumulation rate.

Depth (cm)	**Date** AD	**Sedimentation rate** (cm yr^{-1})	**Accumulation rate** (g cm^{-2} yr^{-1})
0.0	2011 ± 0		
3.6	2005 ± 2	0.69	0.029
4.5	2003 ± 2	0.49	0.017
5.5	2001 ± 2	0.51	0.022
6.6	1999 ± 2	0.54	0.028
7.6	1997 ± 2	0.51	0.023
8.5	1995 ± 2	0.49	0.028
9.6	1992 ± 2	0.34	0.017
13.7	1981 ± 3	0.46	0.026
17.8	1969 ± 4	0.36	0.020
21.9	1960 ± 5	0.51	0.029
26	1950 ± 6	0.54	0.033
28.1	1944 ± 7	0.34	0.024
30.1	1935 ± 8	0.19	0.025
33.5	1910 ± 10	0.12	0.018
37.5	1886 ± 12	0.17	0.026

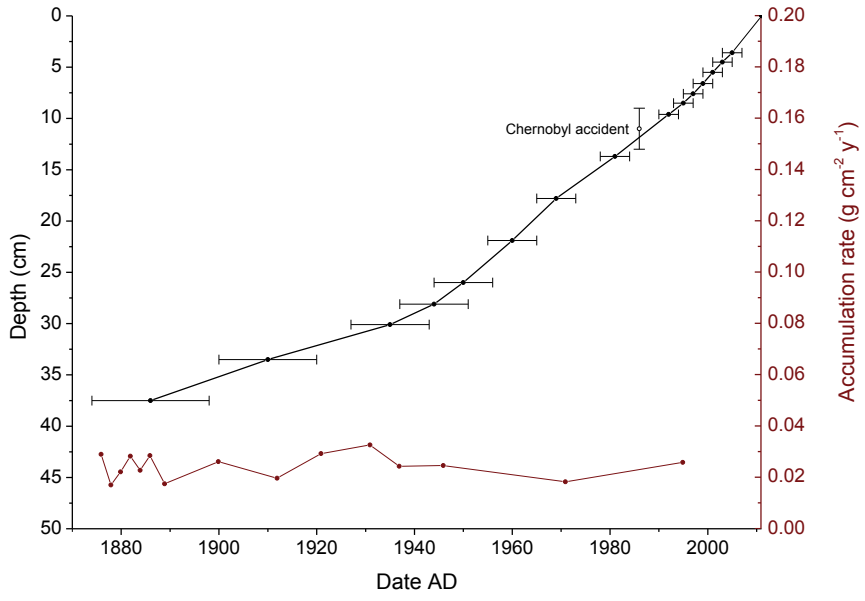

Figure 12.2: Radiometric chronology showing the ^{210}Pb dates in black and peat accumulation rate in dark red, and the approximate 1986 depth suggested by the ^{137}Cs.

12.2 Radiocarbon dating

A total of 11 samples were radiocarbon dated at the ^{14}CHRONO Centre. Table 12.3 presents the ^{14}C ages BP (Before Present, with present = AD 1950), the final result of the calibration, expressed as the range in which the probability to find the calibrated ages is 95%, and the best value. The analysed fraction is also listed.

Table 12.3: ^{14}C ages and ^{14}C calibration, with the estimated and the best values. Analysed fraction is also reported.

Depth (cm)	**^{14}C age** (BP)	**Estimated 2σ range** (cal BP)	**Best value** (cal BP)	**Analysed fraction**
45.7	469 ± 27	493-535	515	cone
62.5	885 ± 27	680-755	716	wood
73	899 ± 26	785-901	842	peat
73	942 ± 26	785-901	842	wood
100.1	922 ± 25	2439-2516	2477	wood
115.5	3180 ± 29	3360-3451	3406	peat
135.5	4229 ± 31	4653-4850	4773	peat
148.5	4891 ± 45	5506-5719	5630	peat
167	5259 ± 39	5936-6174	6041	wood
211.5	6019 ± 36	6762-6950	6860	peat
239	6790 ± 43	7854-7687	7635	wood

The wood fragments samples at depths 62.5, 73 and 100.1 cm have a very similar ^{14}C age, 885 ± 27, 942 ± 26 and 922 ± 25 respectively. At depth of 73 cm also a peat bulk sample was dated that shows a correspondent ^{14}C age (899 ± 26) with the wood remain retrieved at the same depth. For the final age-depth model the samples at depth 62.5 and 100.1 cm were not considered, since they probably come from the same woody fragment found at 73 cm.

In the Figure 12.3 the calibrations of the ^{14}C ages using the calibration curve by Reimer et al. (2013) (green line) are reported. For each plot, the y-axis shows the ^{14}C ages BP while the x-axis shows the asymmetric and multi-peaked calibrated distributions reduced to 2 σ calibrated ranges.

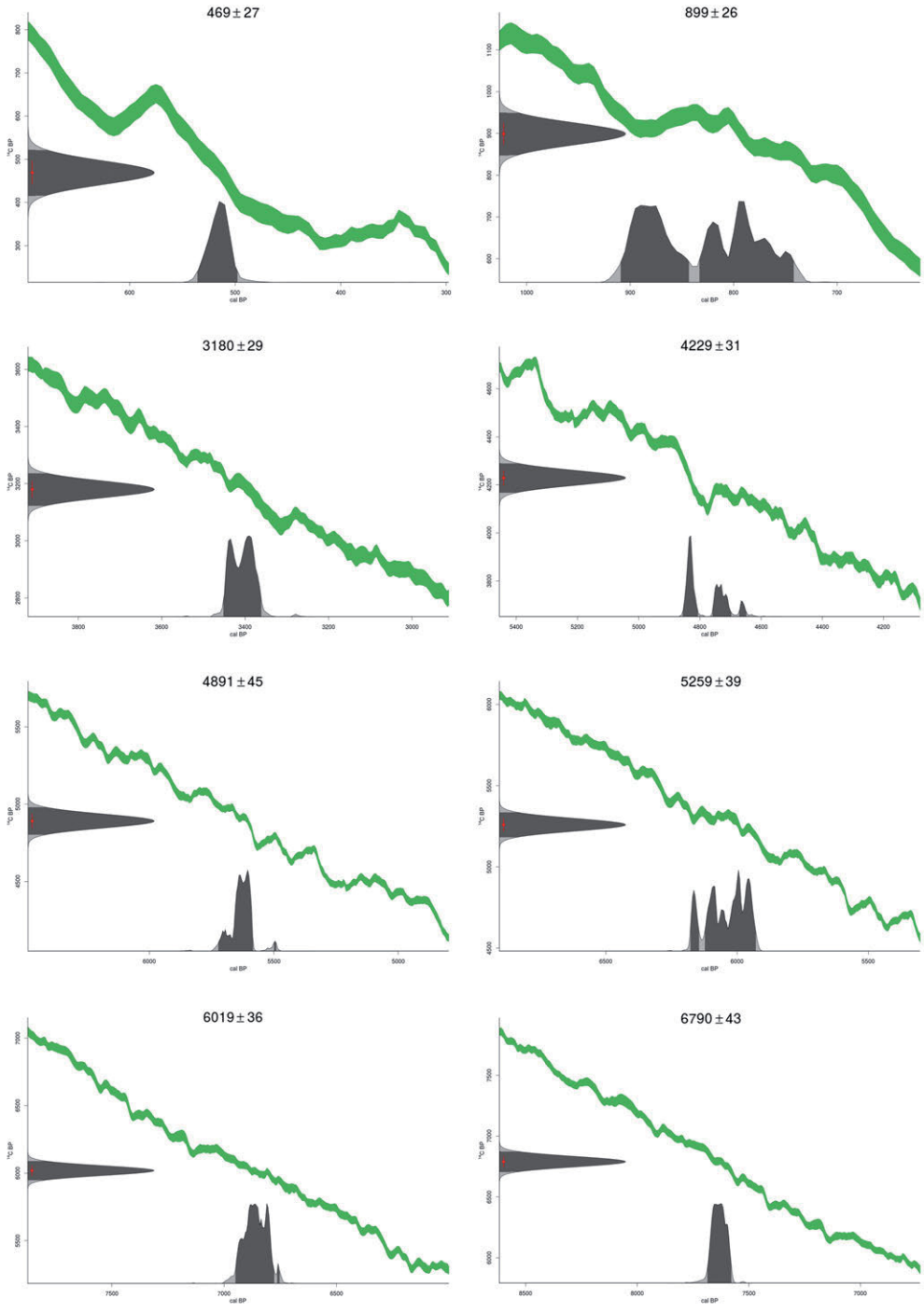

Figure 12.3: Calibrations of the ^{14}C ages BP. The y-axis shows the ^{14}C ages BP while the x-axis shows the asymmetric and multi-peaked calibrated distributions reduced to 2 σ calibrated ranges, calculated using the calibration curve of Reimer et al. (2013) in *clam*.

12.3 Age-depth model

The age-depth model was created combining the ^{210}Pb ages and the ^{14}C ages and was extrapolated down to 250 cm. It suggests that the sedimentation of the Coltrondo peat started ca. 7900 cal BP (Fig. 12.4), covering the Middle and Late Holocene.

The bog grew at a mean sedimentation rate of 0.046 cm yr^{-1} from 7900 to 5700 cal BP, followed by a prolonged phase of relatively constant slow peat growth (mean value of 0.016 cm yr^{-1}) lasting until 920 cal BP (Fig. 12.4). A period of high accumulation (0.080 cm yr^{-1}) lasted for the next 340 years, after that the sedimentation returned to lower values (ca. 0.020 cm yr^{-1}). The last 120 years are characterized by a much faster growth (0.120 – 0.685 cm yr^{-1}).

All dates appearing in the following chapters are cited in calendar year before AD 1950 or cal BP, unless otherwise mentioned, within the 95% confidence interval.

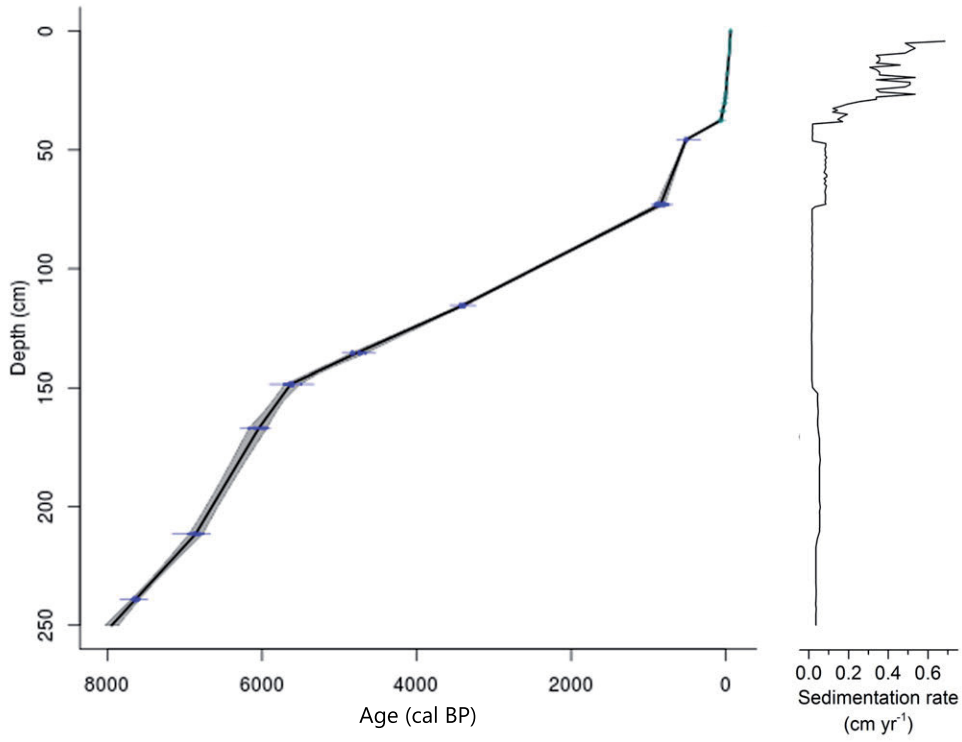

Figure 12.4: The *clam* age-depth model based on linear interpolation between the data levels and the sedimentation rate profile in cm yr^{-1}.

Chapter 13

Physical properties of the peat and pore water pH

The bulk density, the ash and the water content determined for the Coltrondo peat bog are depicted in Figure 13.1.

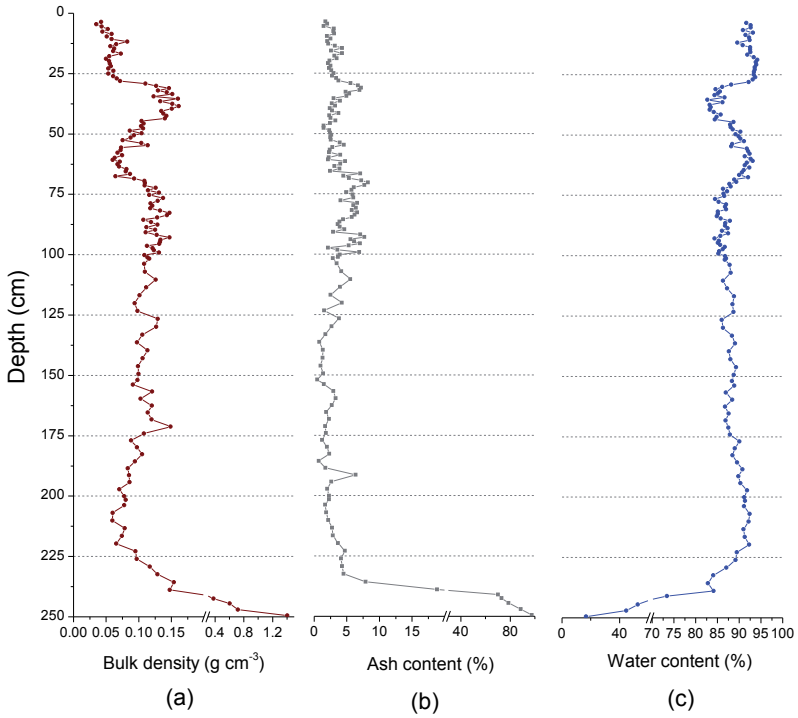

Figure 13.1: The physical properties of the peat measured by LOI technique. (a) Bulk density expressed in g cm^{-3}, (b) ash content in % and (c) water content in %.

The bulk density measured along the profile ranges between 0.04 and 0.16 g cm^{-3}, with a mean value of 0.10 g cm^{-3}, down to 239 cm. The lowest values are registered in the uppermost layers of the peat bog, followed by an increase, from 29 to 55 cm (mean value of 0.12 g cm^{-3}). The bulk density remains then fairly constant, registering a slight increasing trend down to 239 cm. The bottom of the core (the last 10 cm) registers a severe increase, with values ranging from 0.26 up to 1.41 g cm^{-3}. This is due to the approaching of the bedrock and the transition between peat to peaty soil (Charman, 2002), characterized by the presence of sandstone's clasts (Val Gardena Sandstone). The bulk density is negatively correlated with the water content (Pearson coefficients of -0.98, $p<0.01$). This is in agreement with observations previously reported by Boelter (1969) and Zaccone et al. (2009a), who observed that the variation in water holding capacity of peat is negatively correlated to the bulk density.

The ash content of peat represents the inorganic material remaining as dry ash after combustion at 550 °C. It may reflect the input of non-organic material from atmospheric depositions, variations in the peat accumulation rate, as well as decomposition processes occurring in the peat (Zaccone et al., 2012). In the Coltrondo peat bog, the ash content follows the trend of the bulk density, their correlation is indeed highly significant, with a Pearson coefficient of 0.54 ($p<0.01$). The values are low along the profile until the depth of 239 cm, with a mean value of 3.5%. Some peaks and periods of enhanced ash content are present, well in accordance with the increase in concentration of titanium (Ti) and other lithogenic elements described in the Section 14.1. The last 10 cm of the core are characterized by a strong increase, up to 97% at 250 cm when the mineral substrate is reached. The variations of ash content are generally not related to changes in the accumulation rate and, moreover, the ash content is highly correlated with lithogenic elements recorded in the bog profile (see Section 14.1), this reflecting a more exogenous origin of the inorganic material present in the bog.

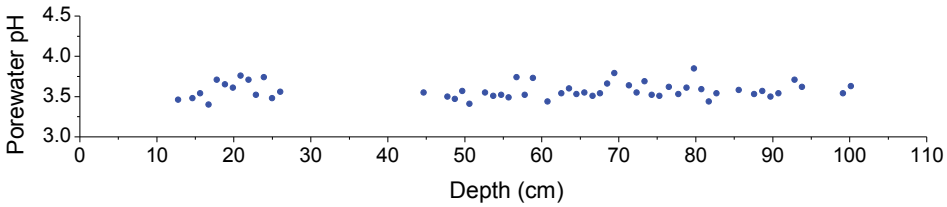

Figure 13.2: Pore water pH measured in the first 100 cm of the peat bog profile. pH values are always <4.

The Figure 13.2 shows the pore water pH values, always <4, ranging

between 3.40 to 3.85. These fairly constant low values are typical of habitats dominated by *Sphagnum* spp. and indicates oligotrophic conditions and acidic waters (Charman, 2002). The acidity of pore water is mainly driven by hydrological sources: in ombrotrophic bogs, fed only by rainwater, acidic conditions are most likely, while in minerotrophic mires the influence of groundwater tend generally to increase the pH. Furthermore, the high cation exchange capacity of *Sphagnum* mosses participates in the lowering of the pH, with the removal of cations and the replacement with hydrogen ions (Rydin et al., 2013). A significant contribution to lowering the pH may derive also by organic acids (Gorham et al., 1984).

Chapter 14

Geochemical analysis

14.1 Geochemical element profiles in peat

Discrete samples for ICP-MS analysis were collected along the profile of the peat bog core for a total of 145 samples, 98 in the first 100 cm (1 cm resolution) and 47 for the remaining part (3 cm resolution). This focus on the first metre allowed us to reach a higher resolution for the last 2000 years, i.e. from the moment when human presence is thought to have started impacting more severely on the environment.

The concentration of major, trace and rare earth elements was determined. Table 14.1 presents the descriptive statistic of the elements: minimun and maximum values, 25° and 75° percentiles, mean and median values are reported. Figures 14.1, 14.2, 14.3, 14.4 and 14.5 depict the concentration (in mg kg^{-1}) of all the elements considered versus depth (in cm). The elements present concentrations that differ by several order of magnitude. Major elements, such as sodium (Na), magnesium (Mg), potassium (K), calcium (Ca) and iron (Fe), considered the main components of the Upper Continental Crust (Wedepohl, 1995) present the highest concentrations, in the range of thousand of mg kg^{-1}, while trace elements and rare earth elements register much lower concentrations.

A principal component analysis was performed for a first ordination of the profiles: the 3 components explain 79% of the total variance, grouping elements with a similar distribution. In Table 14.2 the loadings of the three components for each element are presented and in Figure 14.6 the scores of each component against depth are depicted.

The first component (PC1, 40% of the total variance) is characterized by large positive loadings of lanthanides, thorium (Th), yttrium (Y), Mg, Ca and by medium positive loadings of zinc (Zn), strontium (Sr), cadmium

Table 14.1: Descriptive statistic of the geochemical elements analysed.

	Min (mg kg^{-1})	**25°Perc** (mg kg^{-1})	**Median** (mg kg^{-1})	**Mean** (mg kg^{-1})	**75°Perc** (mg kg^{-1})	**Max** (mg kg^{-1})
Li	0.137	0.725	1.2	1.8	2.4	10.4
Be	0.032	0.058	0.096	0.115	0.154	0.572
Na	39	109	178	244	319	2832
Mg	53	102	177	346	332	2348
K	115	524	901	1072	1329	11084
Ca	99	217	430	673	1026	2201
Sc	0.443	2.0	3.1	3.8	4.8	23
Ti	30	122	219	293	392	3638
V	1.3	3.3	5.2	6.8	9.2	57
Cr	1.2	3.0	4.5	5.6	7.4	28
Mn	1.8	5.7	8.6	27	17	800
Fe	458	891	1311	2115	2477	9143
Co	0.260	0.759	1.0	1.2	1.3	3.2
Ni	1.5	2.1	2.8	3.6	4.8	10.1
Cu	2.4	4.3	5.5	14.2	8.3	265
Zn	1.7	3.0	4.0	8.6	8.9	50
Ga	1.1	2.0	2.5	2.3	3.3	13.0
As	0.190	0.595	0.769	0.916	1.2	2.7
Rb	0.510	2.1	3.0	3.5	4.4	20
Sr	3.1	6.7	8.1	10.3	11.9	23
Y	0.067	0.154	0.362	0.675	1.0	3.0
Ag	0.031	0.069	0.087	0.110	0.124	0.840
Cd	0.013	0.030	0.046	0.107	0.084	0.760
In	0.001	0.005	0.009	0.010	0.013	0.036
Cs	0.041	0.164	0.271	0.368	0.511	2.732
Ba	19.4	36	47	56	64	167
La	0.079	0.332	0.601	0.979	1.447	5.675
Ce	0.306	1.2	2.2	2.3	3.2	7.7
Pr	0.028	0.113	0.196	0.261	0.400	1.2
Nd	0.109	0.372	0.741	0.983	1.5	4.2
Sm	0.026	0.080	0.166	0.214	0.341	0.766
Eu	0.017	0.034	0.054	0.066	0.095	0.168
Gd	0.076	0.161	0.251	0.340	0.493	0.960
Tb	0.005	0.013	0.026	0.032	0.049	0.098
Dy	0.024	0.063	0.125	0.157	0.240	0.490
Ho	0.005	0.013	0.027	0.032	0.049	0.102
Er	0.015	0.039	0.074	0.092	0.139	0.310
Tm	0.002	0.006	0.010	0.013	0.019	0.043
Yb	0.015	0.041	0.065	0.086	0.128	0.295
Tl	0.007	0.028	0.048	0.067	0.070	0.514
Pb	0.691	3.7	16.1	19.2	30	72
Bi	0.009	0.032	0.046	0.070	0.073	0.276
Th	0.047	0.136	0.233	0.335	0.516	1.6
U	0.044	0.126	0.191	0.220	0.276	1.4

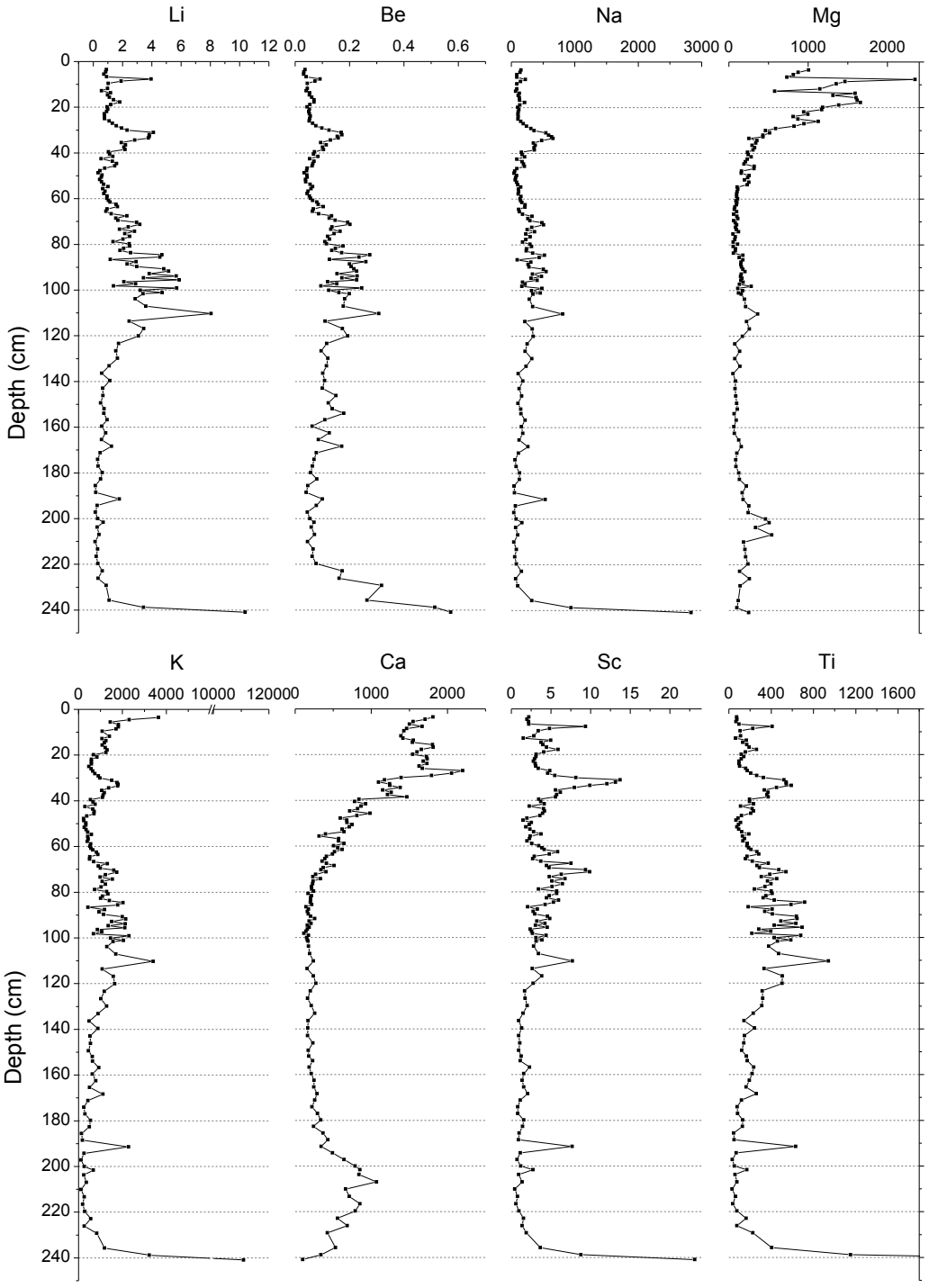

Figure 14.1: Geochemical elements concentration in mg kg^{-1} versus depth (cm): Li, Be, Na, Mg, K, Ca, Sc, Ti.

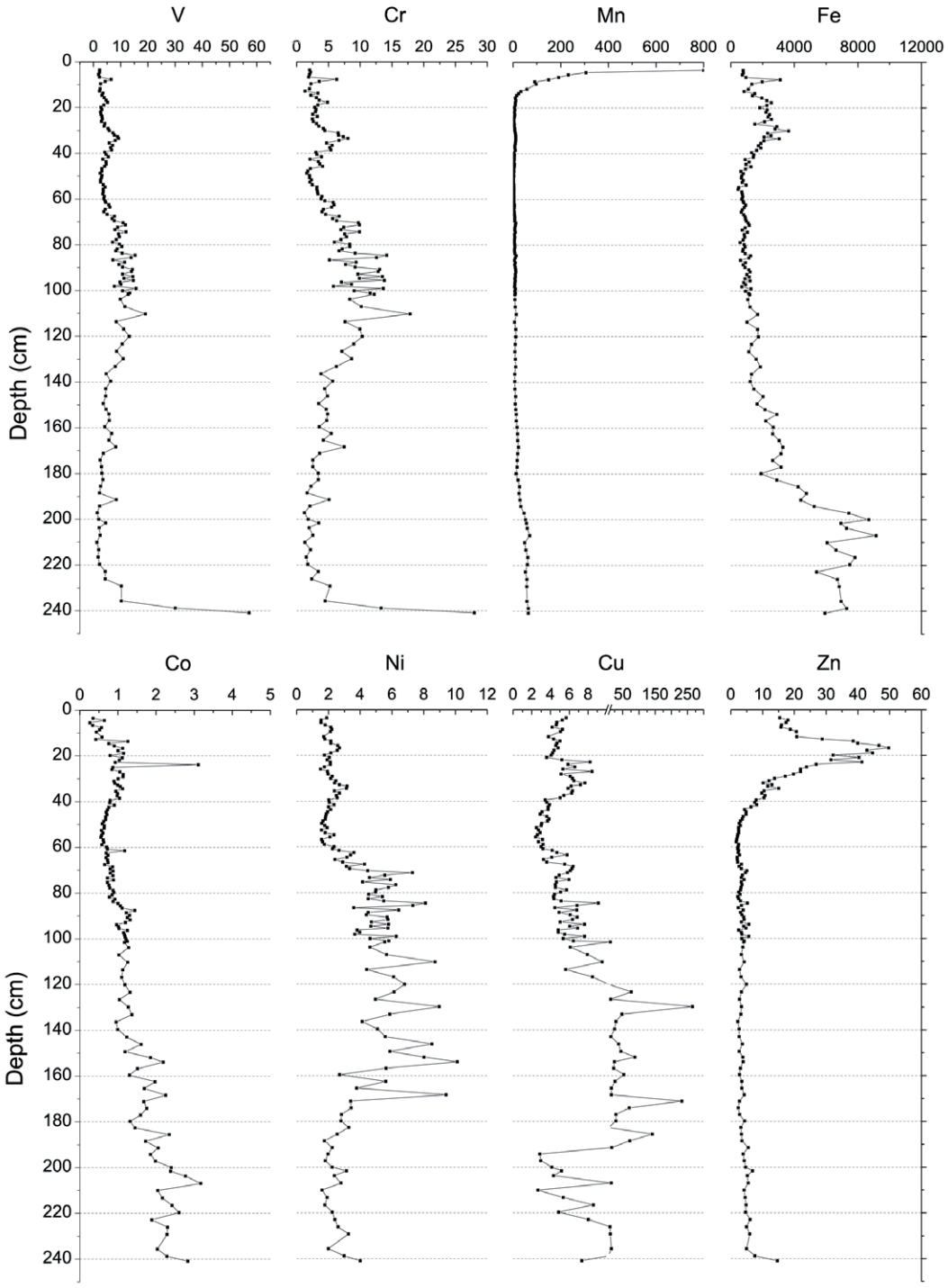

Figure 14.2: Geochemical elements concentration in mg kg^{-1} versus depth (cm): V, Cr, Mn, Fe, Co, Ni, Cu and Zn.

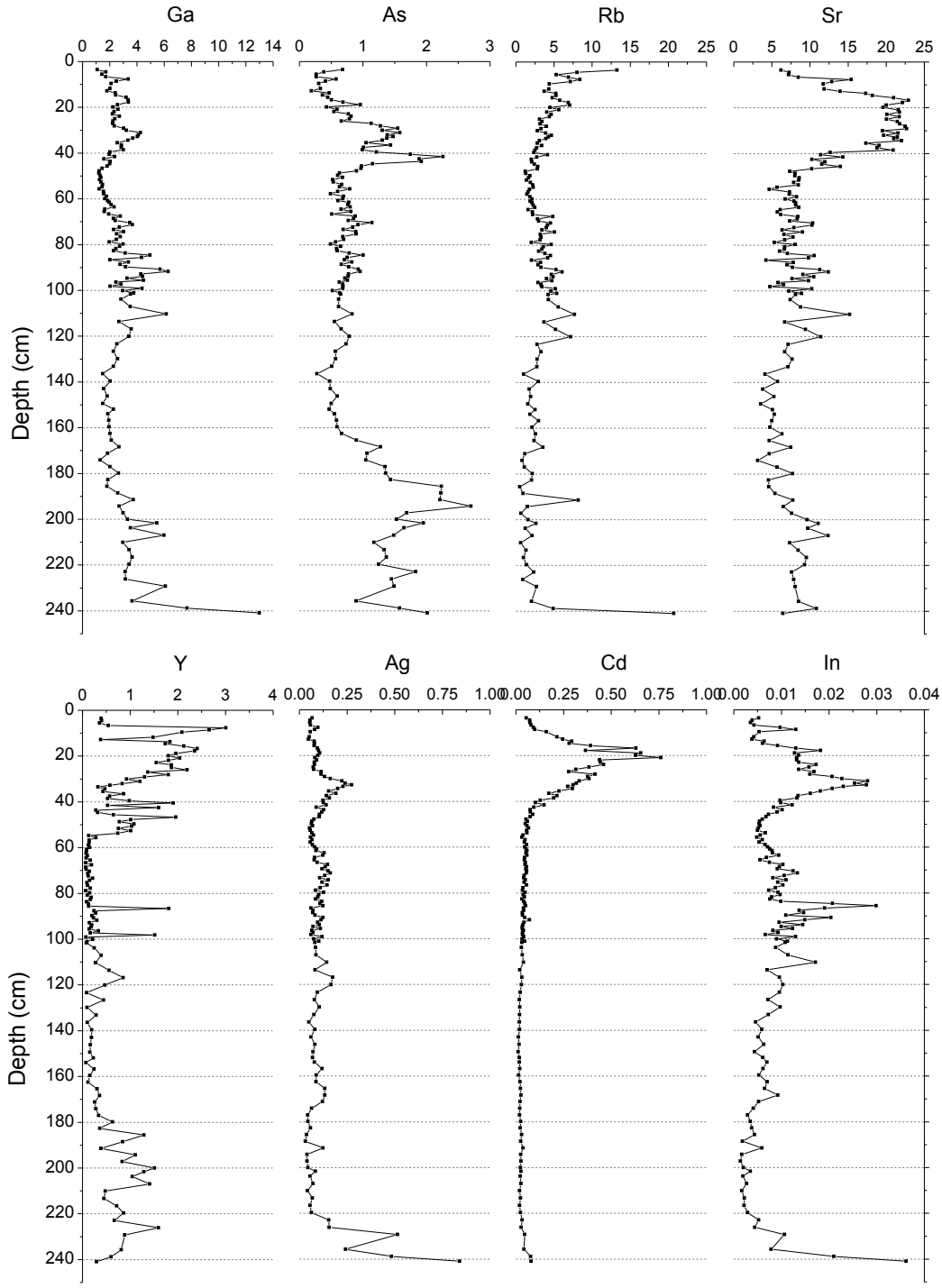

Figure 14.3: Geochemical elements concentration in mg kg^{-1} versus depth (cm): Ga, As, Rb, Sr, Y, Ag, Cd and In.

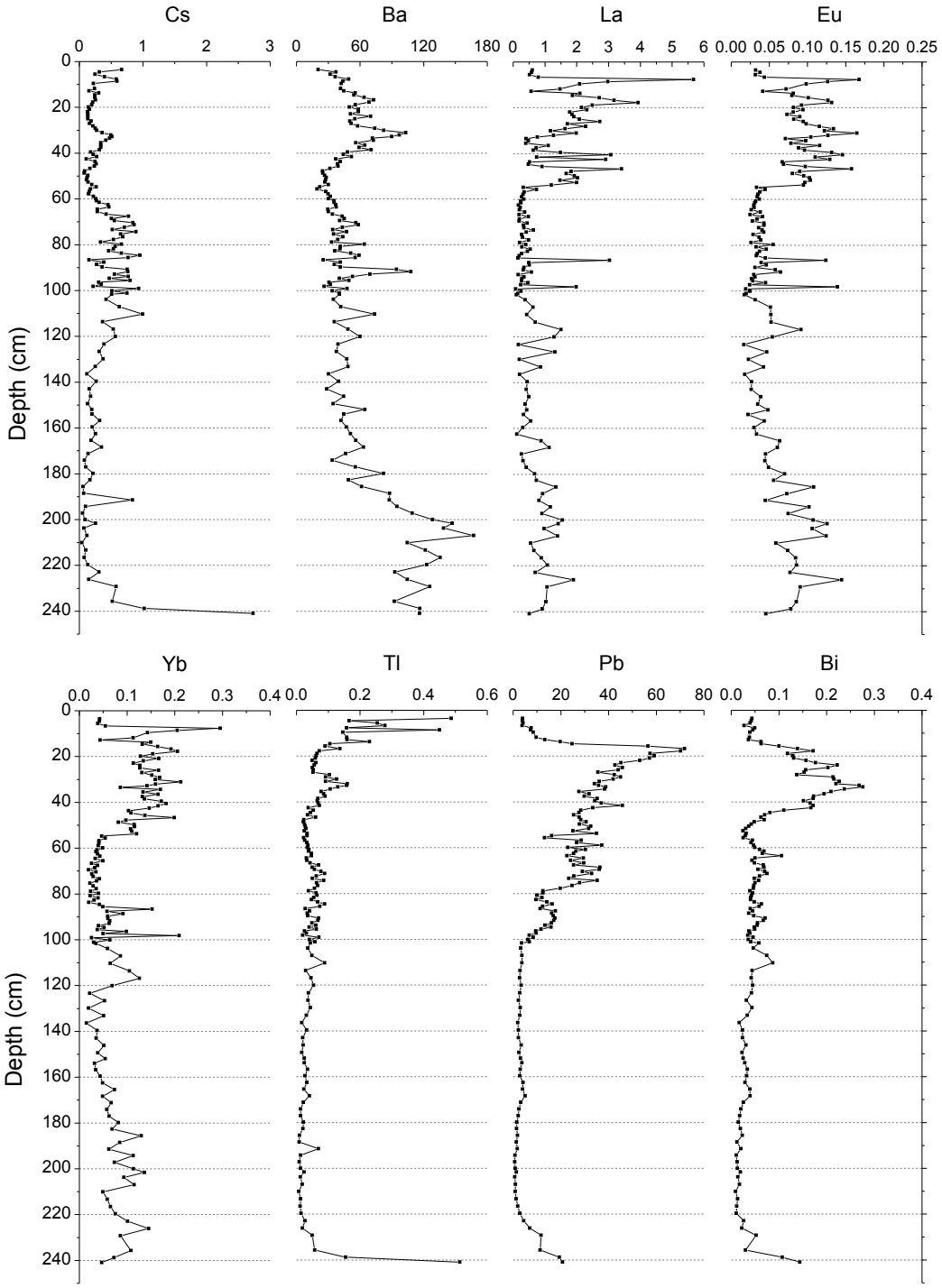

Figure 14.4: Geochemical elements concentration in mg kg^{-1} versus depth (cm): Cs, Ba, Tl, Pb and Bi. For rare earth elements (REE) we report La as light REE, Eu as middle REE and Yb as heavy REE.

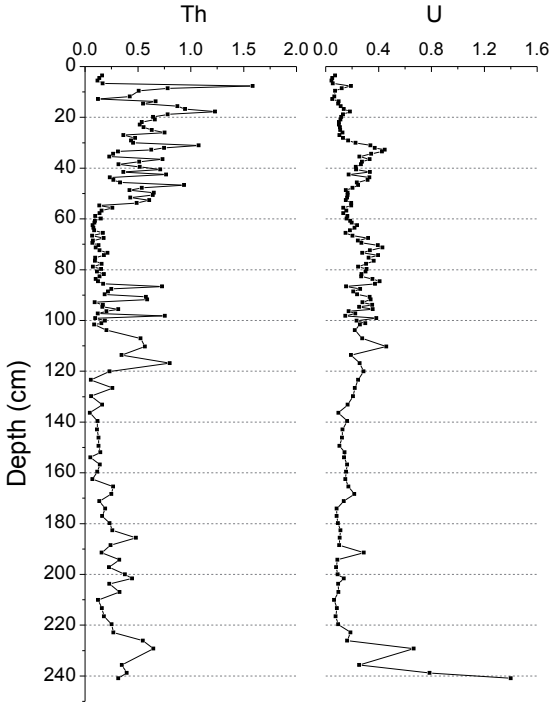

Figure 14.5: Geochemical elements concentration in mg kg^{-1} versus depth (cm): Th and U.

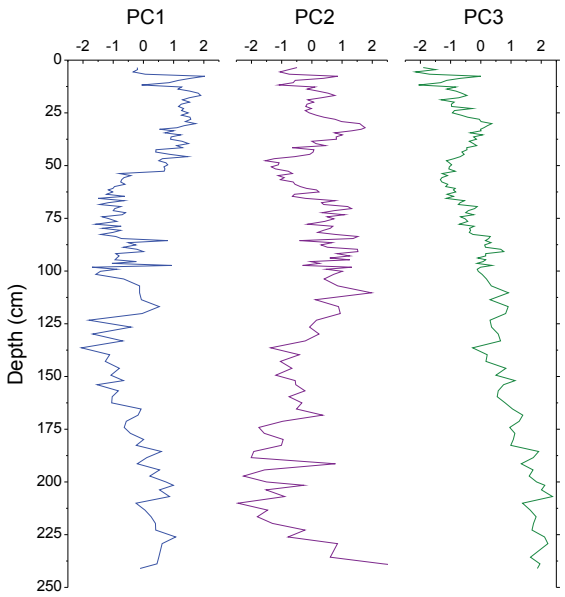

Figure 14.6: Scores of the extracted principal components.

Table 14.2: Loadings of the elements in the three components extracted by PCA (PC1, PC2, PC3). Communality is the proportion of variance of each element explained by the three principal axis.

	PC1	PC2	PC3	Communality
Li	-0.164	**0.936**	-0.161	0.93
Be	-0.359	**0.755**	0.431	0.89
Na	-0.213	**0.939**	0.077	0.93
Mg	**0.825**	0.036	-0.204	0.72
K	-0.142	**0.870**	-0.165	0.80
Ca	**0.759**	-0.140	-0.336	0.71
Sc	0.156	**0.863**	-0.316	0.87
Ti	-0.251	**0.935**	0.043	0.94
V	-0.364	**0.862**	0.177	0.91
Cr	-0.436	**0.839**	0.138	0.91
Mn	0.116	-0.080	0.395	0.18
Fe	0.370	-0.084	**0.780**	0.75
Co	0.006	-0.012	**0.895**	0.80
Ni	**-0.621**	0.450	0.303	0.68
Cu	-0.292	-0.090	**0.503**	0.35
Zn	**0.690**	0.233	-0.211	0.57
Ga	0.077	**0.683**	**0.565**	0.79
As	0.279	0.106	**0.617**	0.47
Rb	0.123	**0.753**	-0.272	0.66
Sr	**0.697**	0.423	-0.212	0.71
Y	**0.948**	-0.169	0.089	0.93
Ag	0.092	**0.813**	0.165	0.70
Cd	**0.688**	0.335	-0.476	0.81
In	0.151	**0.867**	-0.214	0.82
Cs	-0.328	**0.875**	-0.074	0.88
Ba	0.347	0.203	**0.714**	0.67
La	**0.900**	-0.162	0.011	0.84
Ce	**0.794**	-0.246	0.145	0.71
Pr	**0.935**	-0.180	0.061	0.91
Nd	**0.943**	-0.186	0.078	0.93
Sm	**0.950**	-0.173	0.129	0.95
Eu	**0.945**	-0.063	0.173	0.93
Gd	**0.931**	-0.106	0.134	0.90
Tb	**0.948**	-0.145	0.145	0.94
Dy	**0.946**	-0.157	0.147	0.94
Ho	**0.950**	-0.116	0.132	0.93
Er	**0.961**	-0.108	0.108	0.95
Tm	**0.925**	-0.013	0.105	0.87
Yb	**0.954**	-0.012	0.077	0.92
Tl	0.231	**0.677**	-0.447	0.71
Pb	0.305	0.444	**-0.576**	0.70
Bi	0.421	**0.644**	-0.405	0.76
Th	**0.910**	0.124	0.043	0.85
U	-0.197	**0.818**	0.137	0.73

(Cd). Ni is explained by a negative loading. This first axis mainly explains the trend registered by lanthanides, Th and Y (all loadings >0.9, except for cerium (Ce) with a value of 0.79), characterized by higher concentrations for the first 54 cm, followed by a severe drop down to 100 cm. A subsequent increasing trend is registered, whit a final decrease in the last 10 cm of the core (Fig 14.6, PC1). These elements (rare earth elements, REE) are generally found to be correlated with other conservative elements (e.g., Krachler et al., 2003b; Aubert et al., 2006; De Vleeschouwer et al., 2009; Allan et al., 2013a; Fagel et al., 2014), as the ones explained by the second component of the PCA, but this is not the case for the Coltrondo peat bog.

The first component of the PCA explains also Mg and Ca, both macronutrients, essential elements for plants. Their high concentrations registered in the uppermost part of the core are likely due to plant uptake, binding and recycling of these elements.

Sr shows a highly significant correlation with Ca in the peat deposit (Pearson correlation coefficient 0.76, $p<0.01$), with higher concentrations in the first layers of the bog. Ca and Sr register an increase in the bottom layers of the core (183.7 – 240 cm), likely due to the influence of the groundwater (Kylander et al., 2005). Dissolution and upward migration of Ca and Sr from the bedrock have probably occured.

The great ability of *Sphagnum* mosses to exchange cations (e.g., Mg^{2+} and Ca^{2+} ions for H^{+}) may also result in accumulation of heavy metal pollutants such as Cd, due to the lack of sufficient selectivity by the mosses (Brown and Bates, 1990). This may be occured in the Coltrondo peat bog, presenting higher concentrations of Cd in the upper part (0 – 40 cm) and a peak registered at 20.8 cm of depth (0.76 mg kg^{-1}). Also Zn shows a similar trend, in this case it has to be taken into account that Zn is also a micronutrient for plants, which recycle it into the root layers. Anyway Zn shows a similar profile to lead (Pb) in these uppermost layers (see later in this Section), possibly due to Pb – Zn ores and their exploitation until recent times (1980s).

Figure 14.6 shows an increment of the scores of the first component (PC1) in the deeper part of the bog, similar to the one registered by PC3. Indeed, all the elements explained by this axis (lanthanides, Th, Y, Mg, Ca, Zn, Sr and Cd) present an increase in their concentrations at the bottom of the core, possibly related to the upward migration of these elements from the underlying substrate.

The second component (PC2, 27% of the total variance) groups together most of the litophilic elements analysed: lithium (Li), beryllium (Be), Na, K, scandium (Sc), titanium (Ti), vanadium (V), chromium (Cr), rubidium

(Rb), caesium (Cs) and uranium (U). Gallium (Ga), silver (Ag), indium (In) and thallium (Tl), calcophilic elements, are also explained by this second component, generally with lower loadings.

The lithophilic elements present remarkably similar profiles (only the trend is considered, not the absolute values of the concentration, that vary greatly among different elements), reflecting the mineral content of the peat due to deposition of atmospheric dust, possibly deriving from erosional processes and, for the deepest layers of the bog, accounting for the transition to the mineral substrate. There is, indeed, a highly significant correlation between these elements and the ash content measured at the same depths (Pearson coefficients: Li = 0.6, Be = 0.8, Na = 0.9, K = 0.8, Sc = 0.69, Ti = 0.92, V = 0.89, Cr = 0.67, Rb = 0.51, Cs = 0.81, U = 0.88, $p<0.01$). All profiles are characterized by high values at the bottom of the core, followed by a drop between 240 and 230 cm, at the transition to peat. Profiles are then characterized by a peak at 191.4 cm and higher values in the interval between 136.4 and 65.5 cm with a peak at 110.3 cm. Another important increase is registered between 50 and 30 cm culminating at 31 cm. The concentrations then decrease registering a final peak at 7.6 cm. Such similar trends demonstrate the conservative behaviour of these elements in the peat record.

Cr, often related to anthropogenic emissions (e.g, Krachler et al., 2003a) follows in this study the trend of other lithogenic elements, showing a high correlation with all of them (e.g., Ti = 0.86, $p<0.01$). In this bog, as in the one studied by Zaccone et al. (2008), Cr probably derives from erosional processes as the other conservative elements rather than from anthropogenic sources.

Both K and Rb, biophyle elements with similar physicochemical properties, both present higher concentrations in the uppermost layers of the bog, as a result of the biological activity of surface vegetation. The same pattern is visible also in Cs, that follows the same pathways as K in *Sphagnum* spp. (Vinichuk et al., 2010). Below 20 cm of depth their concentration largely follows lithogenic elements, indicating they predominantly derives from weathering processes.

Regarding the calcophilic elements explained by the second axis of the PCA, Ag behaves similarly to the lithogenic elements, while Tl and In present some peculiarities. Tl shows higher concentrations in the first centimetres (up to 0.5 mg kg^{-1}), probably because easily absorbed by plants from atmospheric depositions (Kabata-Pendias and Szteke, 2015), and then it follows lithogenic elements. In presents higher concentrations in the first 50 cm, with a peak of 0.03 mg kg^{-1} at 31 cm, showing a similar behaviour to Bi in this part; they are known indeed to form alloy. After another peak between 80

to 100 cm (0.03 mg kg^{-1}), it follows the trend of the lithogenic elements.

The last component (PC3, 12% of the total variance) is characterized by positive loadings of iron (Fe), cobalt (Co), arsenic (As) and barium (Ba). This component partly explains also gallium (Ga), copper (Cu) and, with a negative loading, lead (Pb). All the elements listed with positive loadings present an increase in concentration in the deeper layers of the bog. This increase is possibly related to the upward migration of these elements from the underlying substrate to the peat layers.

Fe is a dynamic element in peat bogs, affected by post-depositional processes (Steinmann and Shotyk, 1997; Zaccone et al., 2007; Novak et al., 2011). The Fe concentration shows a slightly continual increase from 100 cm onward, with a severe increase below the depth of 180 cm, registering peaks of approximately 9000 mg kg^{-1}, well in accordance with the fact that Fe is one of the component of the Val Gardena Sandstone.

Co is highly correlated with Fe (Pearson coefficient 0.80, $p<0.01$) and registers a similar trend, with higher concentrations in the deeper layers (with a maximum of 3.2 mg kg^{-1}), possibly due to upward migration from the mineral substrate.

The same reason may explain the behaviour in the deeper layers of Ba, with higher concentrations below 180 cm of depth, and of As, presenting increasing concentrations starting from 140 cm, with the highest values registered below 180 cm (2.7 mg kg^{-1}). Furhtermore, As presents high values in the first 50 cm of the core, with a peak at depth of 41.5 cm (2.3 mg kg^{-1}), probably due to the ability of *Sphagnum* mosses to accumulate heavy metal pollutants (Brown and Bates, 1990) and, as stated by Zaccone et al. (2008), because it may be taken up by plants, due to its similar chemical behaviour to phosphorous (P).

Cu, considered immobile in peat in the most recent studies (e.g., Novak et al., 2011; Allan et al., 2013b), shows really high peaks between 120 and 190 cm, reaching concentrations up to 265 mg kg^{-1} (at depth of 130 cm). The upper part of the core registers much lower values in the order of ca. 5 mg kg^{-1}. The bottom layers (ca. 190 – 240 cm) register a slight increase with respect to the superficial part, registering concentrations up to 14 mg kg^{-1}). It does not seem possible to explain the high peaks of Cu only with upward migration from the bedrock, otherwise the highest concentrations would be at the very bottom of the core, as it is for other elements. These high concentrations may be possible related to anthropogenic disturbances linked to mining activities; further studies will be performed to investigate the origin of these depositions.

Pb presents high values in the uppermost layers of the core (with a peak

at 16.7 cm of 72 mg kg $^{-1}$), followed by a decreasing trend down to 100 cm. Below this depth the concentration of Pb remains constantly low. Pb is considered an immobile element in the peat (e.g., Shotyk et al., 1998; Le Roux et al., 2004) and its concentration may reflect the human atmospheric contamination.

14.2 Geochemical element profiles in pore water

Pore water in the first 100 cm of the profile was extracted mainly to achieve information about the trophic status of the peat bog, measuring the pH and determining Ca and Mg content. Indeed, pH and the ratio Ca/Mg are important parameters to define peatlands ombrotrophy.

The Ca/Mg ratio in pore water is compared to the same ratio in rainwater (Fig. 14.7: in an ombrotrophic peatland the ratio in the pore water is lower or comparable to the one in the rainwater, while in a minerotrophic peatland, influenced by the groundwater, the ratio in the pore water is higher, due to the additional input of Ca from non atmospheric sources (Shotyk, 1996). Ca/Mg ratio in pore water was therefore compared to the one determined during the "LIFE Nature Programme Danta: Project to safeguard the integrity of Danta di Cadore peat bogs", considered to be indicative of the precipitation in the studied area. The results are discussed together with all the other indicators of ombrotrophic/minerotrophic conditions in Chapter 16.

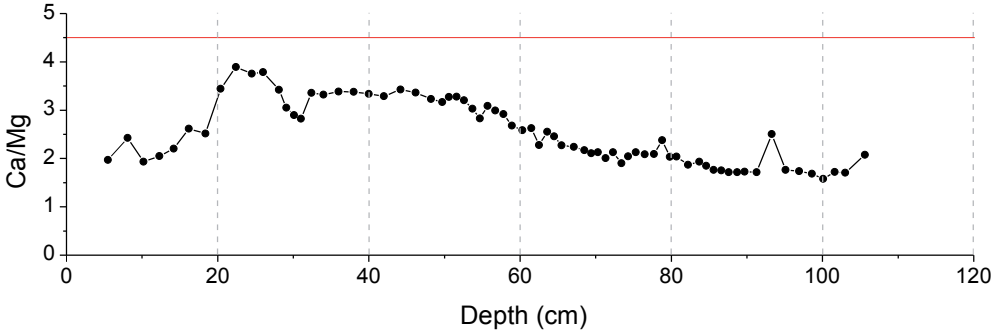

Figure 14.7: Ca/Mg ratio in the pore water of the first 100 cm of the peat bog core, compared with the same ratio in the rainwater (red line) determined during the "LIFE Nature Programme Danta: Project to safeguard the integrity of Danta di Cadore peat bogs".

The analysis of Ca and Mg was performed using ICP-MS technique, simul-

taneously with other chemical elements, for a total of 30 elements analysed. Figures 14.8, 14.9 and 14.10 report the concentration of the elements in μg L^{-1} against depth (cm).

The lithogenic elements show a peak at ca. 30 cm of depth, also registered in the solid peat, as well as the higher concentrations of biophylic elements in the uppermost layers of the peat (Mg, K, Ca, Mn, Zn and Rb). Trace elements related to human activity also show similar profiles to the ones registered in the peat samples, as As, In, Ba and Pb. The similar behaviour of many elements to the ones registered in the solid peat samples suggest their immobility in the core.

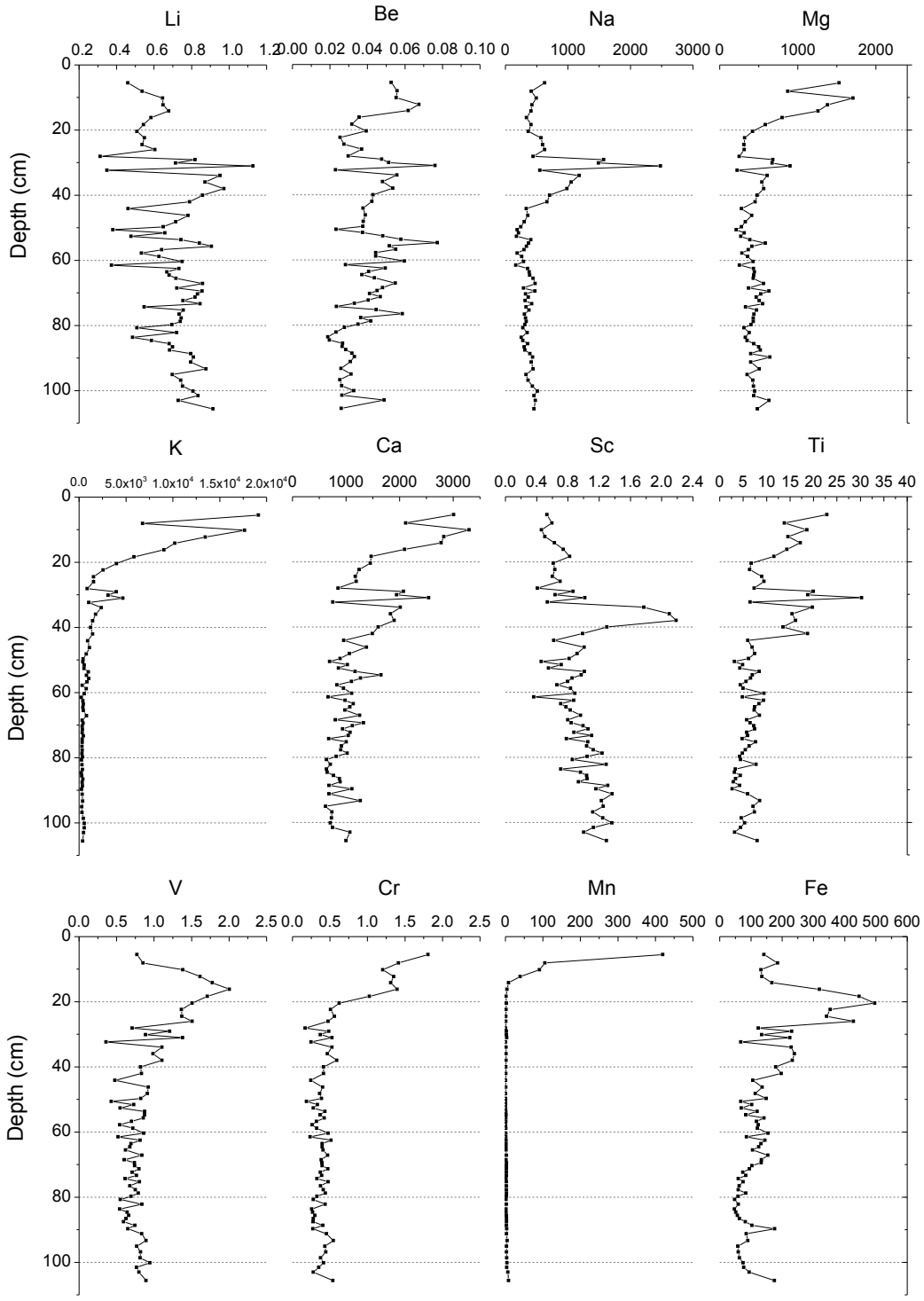

Figure 14.8: Pore water geochemical elements concentration in μg L^{-1} versus depth (cm): Li, Be, Na, Mg, K, Ca, Sc, Ti, V, Cr, Mn and Fe.

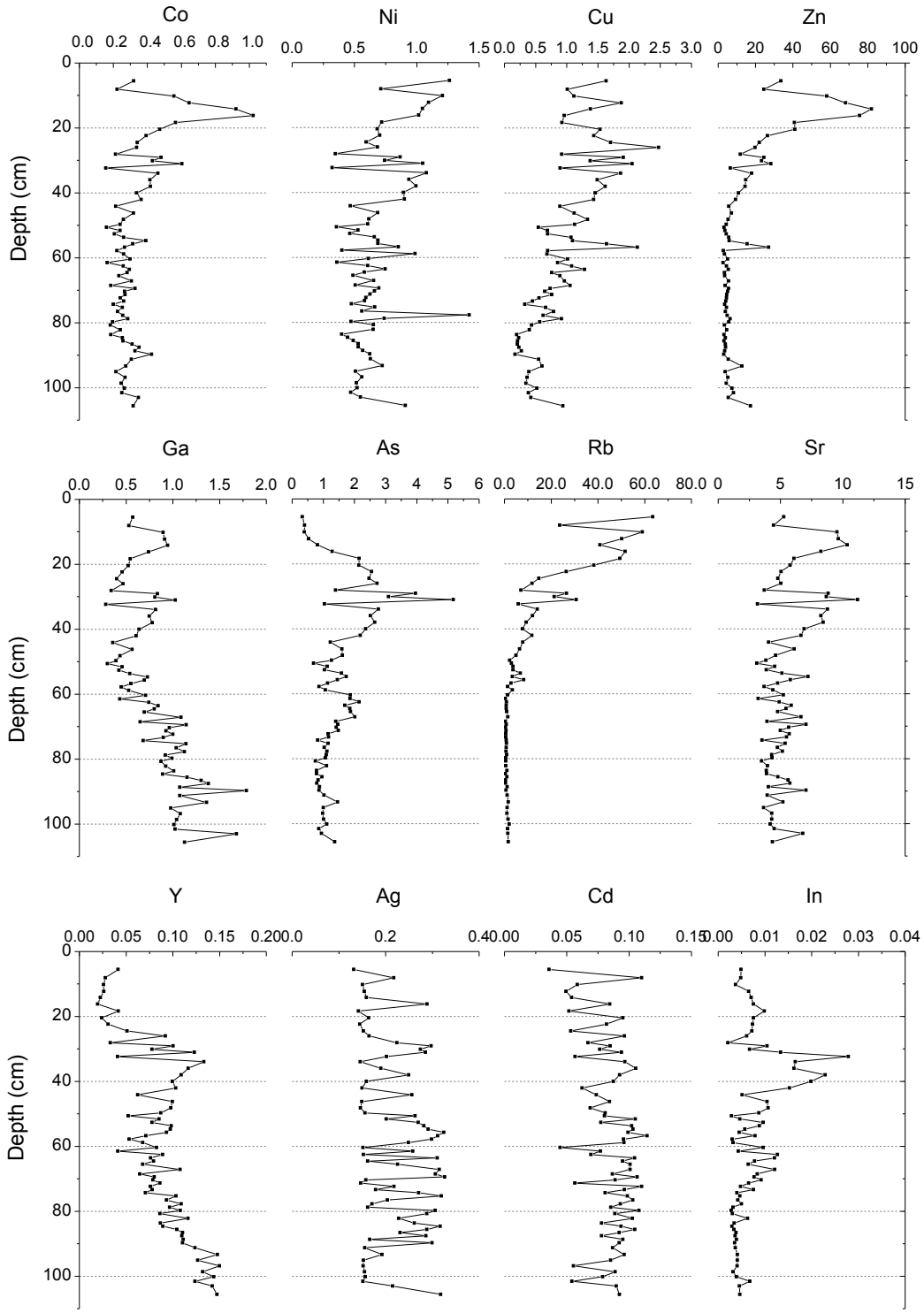

Figure 14.9: Pore water geochemical elements concentration in μg L^{-1} versus depth (cm): Co, Ni, Cu, Zn, Ga, As, Rb, Sr, Y, Ag, Cd and In.

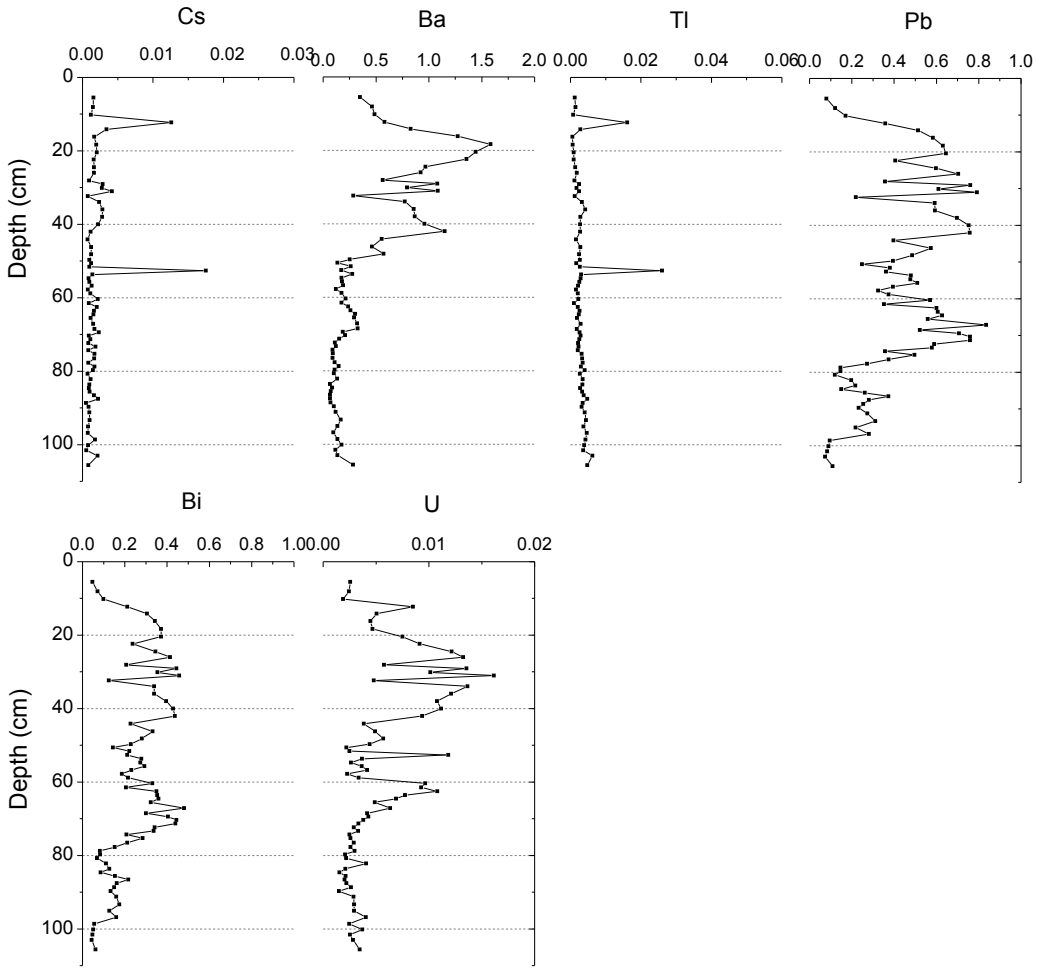

Figure 14.10: Pore water geochemical elements concentration in μg L^{-1} versus depth (cm): Cs, Ba, Tl, Pb, Bi and U.

14.3 Enrichment Factor

The enrichment factor allowed us to detect the human impact on the peat bog, as well as the influence of the living vegetation in the uppermost part of the core.

Biologic enrichment in the surface layers

In Figure 14.11 the EF of Mg, K, Ca, Mn, Rb are presented. These elements are macro- and micro- nutrients for plants and are essential to their growth (Strasburger et al., 1995). The high EFs registered in the superficial zone is related to plant uptake and recycling of nutrients.

The zone of biologic influence covers ca. the first 30 cm in which ca. 7.5 cm are constituted by living vegetation (mainly *Sphagnum* mosses) and the remaining part by recently dead vegetation and roots from plants growing on the surface.

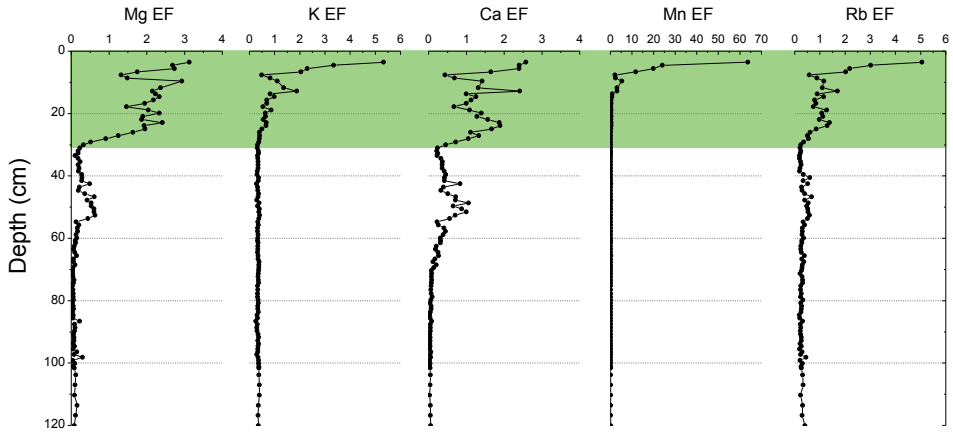

Figure 14.11: Enrichment factor of Mg, K, Ca, Mn and Rb. The green rectangle represents the zone influenced by biological activity.

Anthropogenic enrichment

Trace elements related to human activities were selected and their enrichment factors with respect to the Earth's crust was calculated, for the last ca. 3700 years (0 – 120 cm). In the Figure 14.12 the more significant EF profiles are drawn (Pb, Zn, As, Ag, Cd and Cu EFs) and different phases, based mainly on Pb EF profile, are defined.

Phase 1: 85.6 – 101.6 cm (619 BC – AD 350)
During this first phase all metals show really low EF values; it is possible

to distinguish a slight increase in the Pb EF, likely related to the Roman mining activity. The end of this phase is characterized by a drop in the Pb EF (from 11 to 4). This decrease is also visible in the EF profile of the other elements. At that time the Roman empire was declining, with the subsequent abandonment of mining sites present all around Europe (e.g., Shotyk et al., 1998; Brännvall et al., 1999). This decrease in EF values may be therefore a consequence of this event.

Phase 2: 70.3 – 85.6 cm (AD 350 – AD 1140)
During the Early Middle Ages Pb EF shows values comparable to the ones of Earth's crust, with a slight increase from ca. 79 cm (AD 760), up to 14. Ag EF presents a similar trend, while for the other elements peat samples do not show a significant enrichment with respect to Earth's crust values. This increase is coeval with the drop in the $^{206}Pb/^{207}Pb$ isotopic ratio (see Section 14.4), possibly related to mining activity carried out in the near mines, as for examples the Salafossa site, mainly exploited for Pb and Zn in the following centuries, as testified by historical documents.

Phase 3: 54.7 – 70.3 cm (AD 1140 – AD 1330)
An important increase in the Pb EF is registered in this phase, visible also in the As, Ag and Cu EFs, possibly related to the mining activities developed in the area at that time, as evidenced by historical documents (Cucagna, 1961). The Pb EF determined by Poto (2013) in the peat bog next to Danta di Cadore also registers a slight increase during this period. During this time all around Europe a general increase in population and an economic growth are registered, with the expansion of mining activities due to the discovery of new ore deposits and the reopening of old mines (Brännvall et al., 1999).

Phase 4: 38.5 – 54.7 cm (AD 1330 – AD 1830)
In this phase the highest EF values of the Middle Ages are reached. Pb EF registers values up to 50, As and Ag show the highest EFs of the entire profile, reaching values of 42 and 49, respectively. Peat samples at these depths are enriched also with Cd, Co and Cu. Also Zn EF shows a slight increase, with values up to 3.4. The likely explanation is the prosperous mining activities in the Cadore and, more generally, in the Belluno area at that time, during the domination of the Republic of Venice (Vergani, 2003). A general favourable condition for mining activities is registered in all Europe during this period of time (Brännvall et al., 1999; Vergani, 2003). During the 16th century the decrease in the EF may be ascribed to the discovery of America and the consequent exploitation and importation of American metal resources (Brännvall et al., 1999; Vergani, 2003), while the decrease registered at the end of this phase is well in accordance with the decline of the Republic of Venice and the abandonment of several mining sites (Cucagna, 1961). A similar trend, when radiocarbon dating uncertainties are taken into

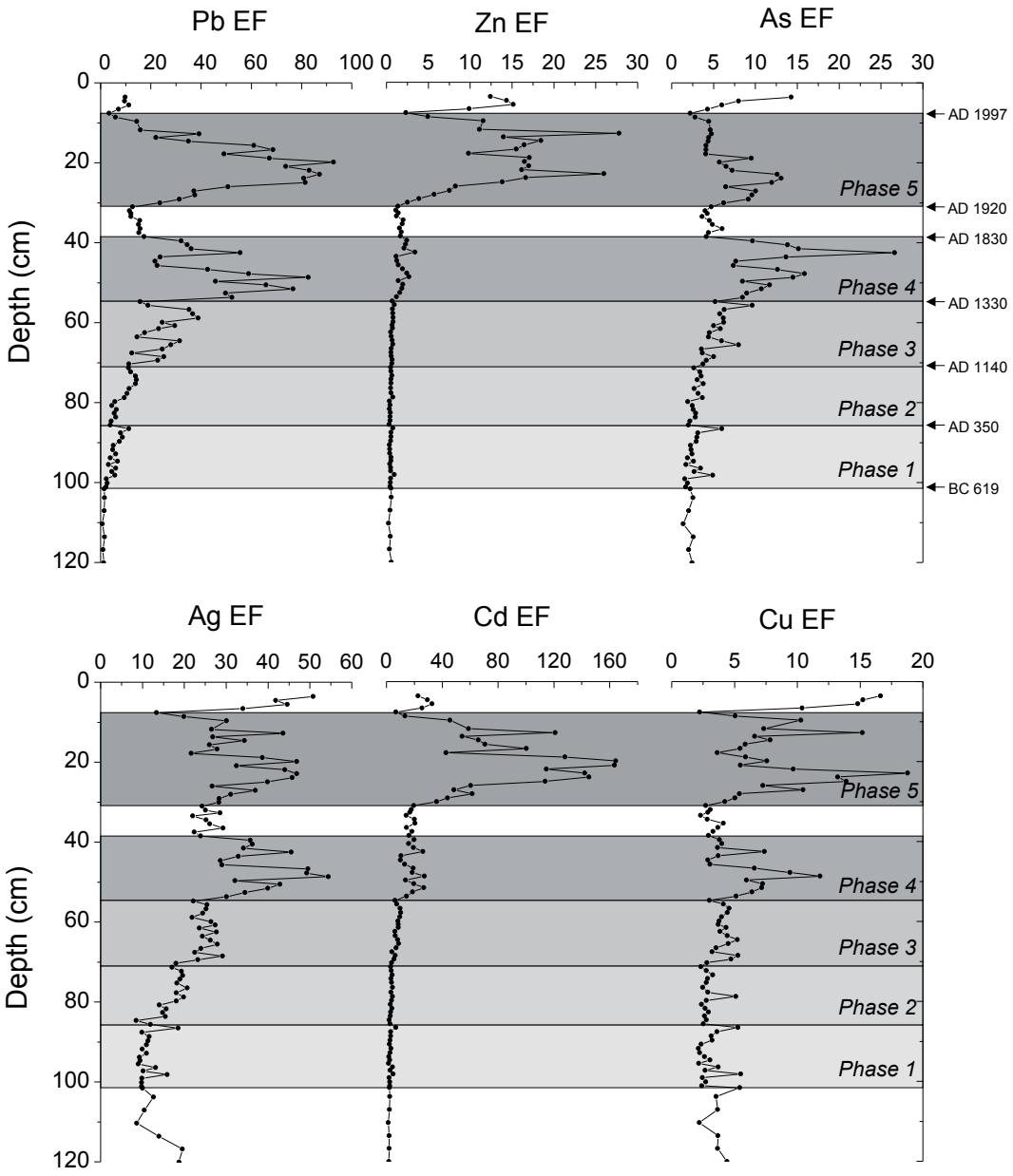

Figure 14.12: Enrichment factor of Pb, Zn, As, Ag, Cd and Cu. 5 different phases are defined: *Phase 1*: 619 BC – AD 350, *Phase 2*: AD 350 – 1140, *Phase 3*: AD 1140 – 1330, *Phase 4*: AD 1330 – 1830, *Phase 5*: AD 1920 – 1997.

account, is visible in the Danta peat bog (Poto, 2013), that also registers the prosperous activities during the Venetian domination, the decrease followed by the American exportation, and the final decrease during the decline of the Republic of Venice.

Phase 5: 7.6 – 32.0 cm (AD 1920 – AD 1997)
The last phase is characterized by high enrichment factors for all the elements considered. Pb EF shows a severe increase, reaching a peak of 93 at 20 cm of depth (AD 1964). A steep decrease follows in the subsequent years, reaching at depth 7.6 cm (AD 1997) a really low value, comparable to the one of the Earth's crust. This higher enrichments are mainly attributable to the advent of the industrialization and to the introduction, during the 1950s, of leaded gasoline. The phasing out of leaded gasoline, the abandonment of mining activities in the area, and a more attention to the environment by the institutions may explain the steep decrease in the last decades. Danta Pb EF (Poto, 2013) registers for this period of time an increase that can be related with the one of the Coltrondo peat bog, with the same peak at ca. AD 1964, followed by a decrease in the last decades.

The other EF profiles of the Coltrondo bog follow the Pb EF, presenting their own characteristics. Zn EF presents two peaks, at 22.8 (AD 1958) and 12.8 (AD 1983) cm of depth. In this period of time, the Salafossa mining site located in the Comelico area, is active and the Zn mineral processing accounts for 1/3 of the Italian production (De Lorenzo, 1999), possibly explaining this high EF values. Anyway this interpretation is to be considered with caution, since the increase of Zn EF in this superficial layers may be due to i.e. bioaccumulation by living vegetation, as reported in other studies (e.g., Rausch et al., 2005). As EF presents high values between 32.0 and 18.8 cm (AD 1920 – AD 1967), followed by a decrease in the last part. This trend may be related, as suggested by Shotyk (1996), to the increase in coal burning with the advent of the industrial revolution and to the use in agriculture of pesticides containing lead arsenates. Ag, Cd and Cu also present a severe increase attributable to the industrialization, followed by a decrease to more natural values in the last part.

14.4 Pb isotope analysis

Lead has three radiogenic isotopes (^{206}Pb, ^{207}Pb, ^{208}Pb) and one non radiogenic (^{204}Pb), all naturally occurring. The lead isotope ratios of rocks and soil and dust derived from them vary from place to place, therefore they can be used as a fingerprint of their source. The isotopic ratios are indeed widely used mainly for distinguishing between natural and anthropogenic

sources of this metal (e.g., Shotyk et al., 1998; Martínez Cortizas et al., 1997; Komárek et al., 2008).

$^{206}Pb/^{204}Pb$, $^{207}Pb/^{204}Pb$, $^{208}Pb/^{204}Pb$, $^{208}Pb/^{206}Pb$ and $^{206}Pb/^{207}Pb$ were calculated along the core of the Coltrondo peat bog. Figure 14.13 shows the profile of $^{206}Pb/^{207}Pb$, the concentration of Pb in mg kg^{-1}, the lead flux in $\mu g\ cm^{-2}\ yr^{-1}$ and the enrichment factor of lead (discussed in detail in the Section 14.3). The lead flux was calculated as follows:

*Pb flux = [Pb] * bulk density * sedimentation rate*

with Pb concentration expressed in $\mu g\ g^{-1}$, bulk density in $g\ cm^{-3}$ and the sedimentation rate in $cm\ yr^{-1}$.

Three main phases were defined to help in the identification of possible natural and anthropogenic Pb sources (Fig. 14.13). Three-isotope plots (Fig. 14.14) were drawn, to trace variations in Pb isotope ratios along the peat bog core, evidencing the different phases.

The comparison with historical information (Cucagna, 1961; Vergani, 2003) and other studies on lead isotopes carried out in Europe (see Table 14.3 and Figure 14.15) permitted to distinguish between natural and anthropogenic sources and individuate possible sources of human-induced lead contamination.

Phase 1 (101.6 – 240 cm) covers ca. 5120 yr (7690 – 2570 cal BP). $^{206}Pb/^{207}Pb$ ratio has an average value of 1.201 ± 0.004, really low Pb fluxes (mean value $0.017 \pm 0.031\ \mu g\ cm^{-2}\ yr^{-1}$) and a negligible Pb enrichment factor. The high radiogenic values that characterize this phase (always >1.19) are typical of pre-anthropogenic natural values (Klaminder et al., 2003).

The green rectangle in Figure 14.15 shows the similarity of $^{206}Pb/^{207}Pb$ versus $^{208}Pb/^{206}Pb$ ratios measured in the Coltrondo peat bog, with other uncontaminated sites in Europe (Switzerland and France) and with the mean values of the Upper Continental Crust (see Table 14.3 for lead isotopic values and references) and the Matmata loess from the Southern Tunisia. The Saharan Desert is a possible natural long distance source of dust to Europe (Shotyk et al., 1998; Kylander et al., 2005; Kylander et al., 2010; Shotyk et al., 2015).

This phase is characterized by pre-contamination peat with atmospheric lead likely represented by a mixture of local and regional sources, with the occasional input of long distance soil dust.

Phase 2 (38.5 – 101.6 cm) covers part of the Iron Age, the Roman Times, the Middle Ages and part of the Modern Time (2570 cal BP – AD 1830).

This phase is characterized by a general increase of lead fluxes and enrichment factor. Three sub-phases may be individuated according to the lead

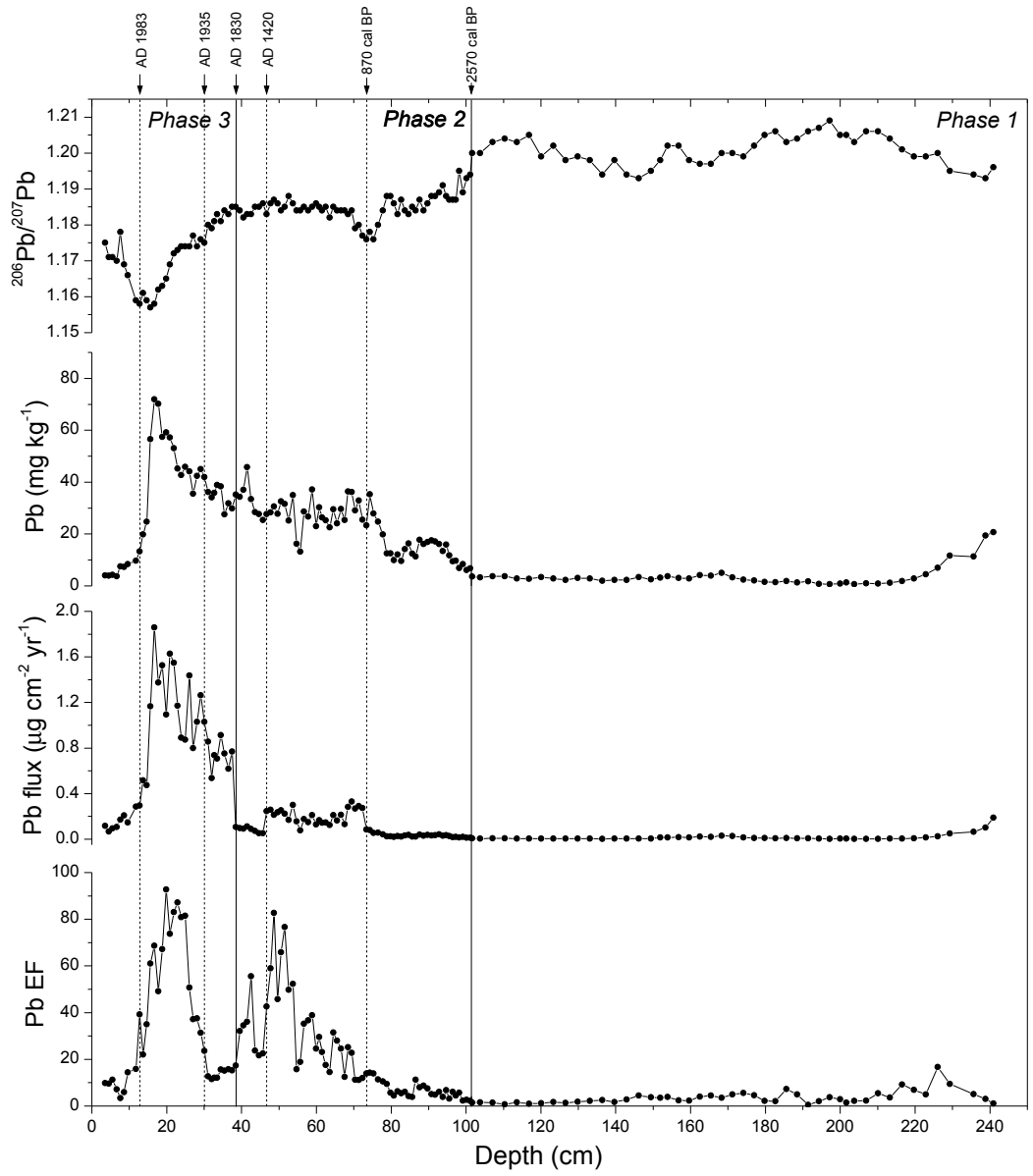

Figure 14.13: $^{206}Pb/^{207}Pb$ ratio, Pb concentration (mg kg^{-1}), Pb flux (μg cm^{-2} yr^{-1}) and Pb EF. The graphs are divided in 3 main phases (solid lines). Phase 2 and Phase 3 are further subdivided in sub-phases (dashed lines).

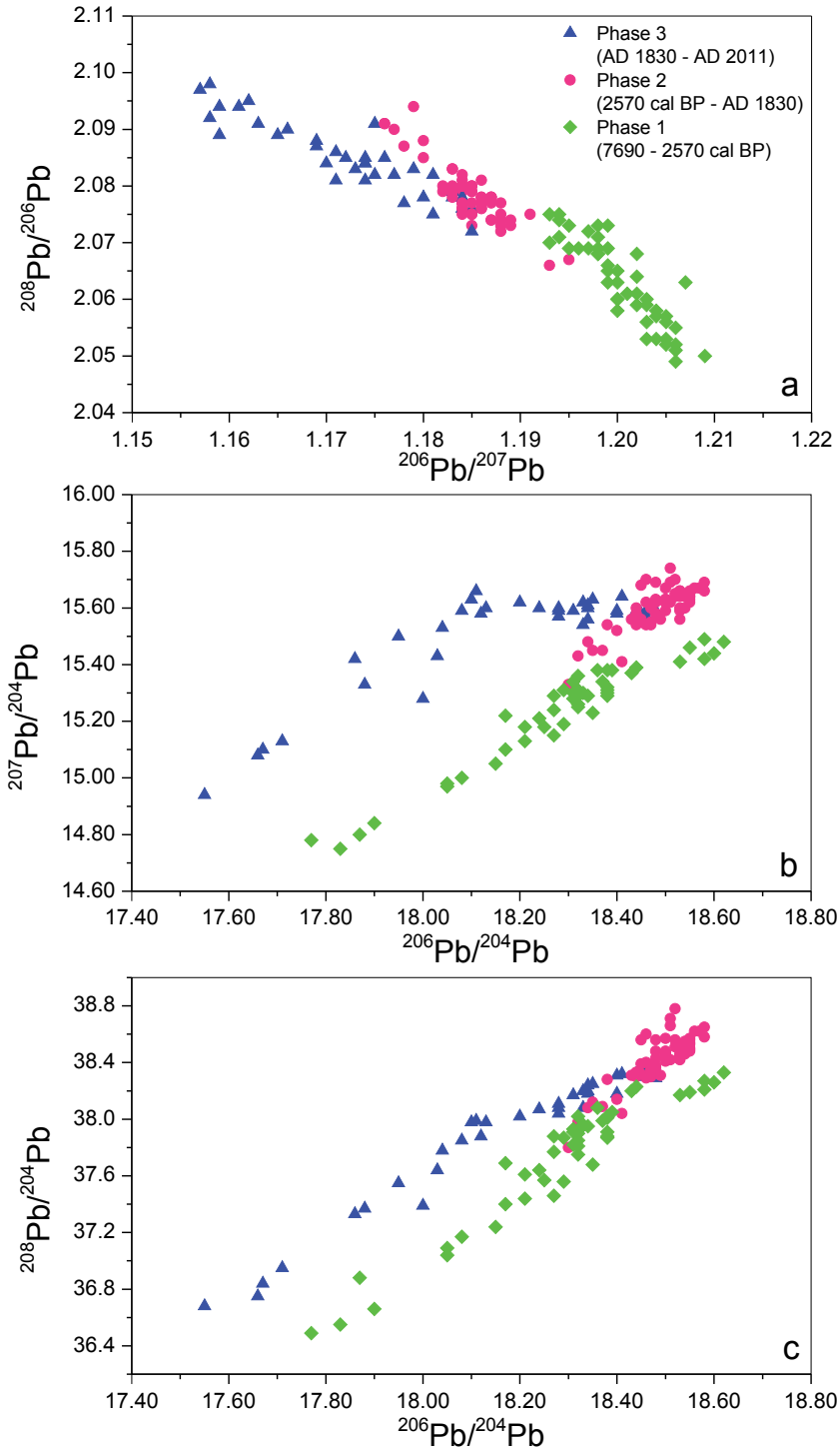

Figure 14.14: Three-isotope plots of (a) $^{206}Pb/^{207}Pb$ vs. $^{208}Pb/^{206}Pb$, (b) $^{206}Pb/^{204}Pb$ vs. $^{207}Pb/^{204}Pb$ and (c) $^{206}Pb/^{204}Pb$ vs. $^{208}Pb/^{204}Pb$.

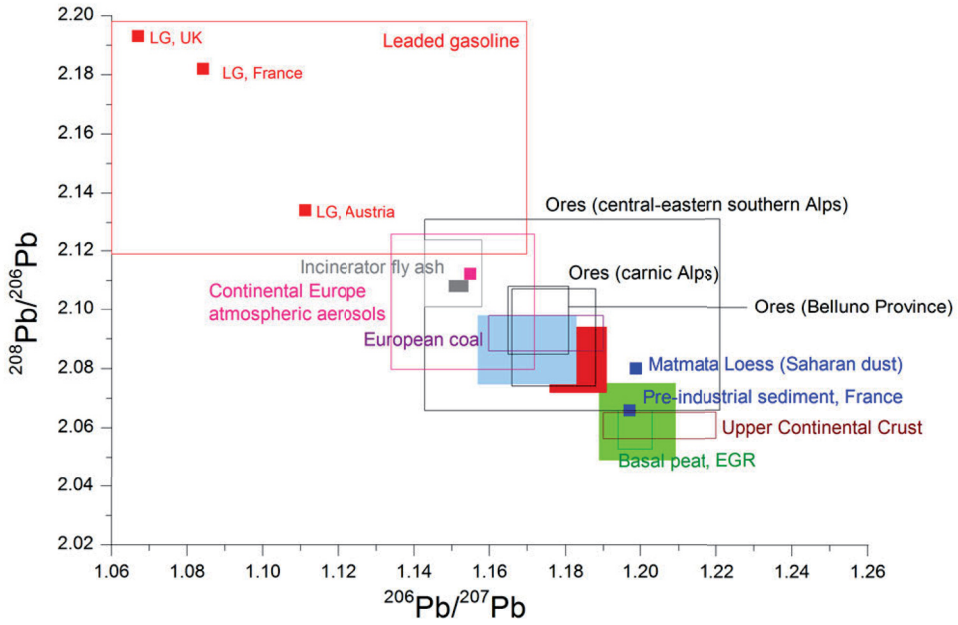

Figure 14.15: Three-isotope plot of $^{206}Pb/^{207}Pb$ vs. $^{208}Pb/^{206}Pb$ of this study (full coloured rectangles) with other studies (empty rectangles and points). The green, red and light blue rectangles represent the 3 main phases individuated for this study: a pre-contamination period, an early contamination period and the industrialized time, respectively. For comparison with other studies of the pre-contamination period the isotopic values of the basal peat of (Étang de la Gruère (EGR) in the Jura Mountains of Switzerland (Shotyk et al., 2001) and of pre-industrial sediment in France (Monna et al., 1997) are depicted. As possible natural sources the loess from the Sahara Desert (Grousset et al., 1994) and the Upper Continental Crust (Kramers and Tolstikhin, 1997) are visible in the graph. Mining deposit isotopic values of the area of the Belluno Province (Ros, 2008), the Carnic Alps (Giunti, 2011) and central-Eastern southern Alps (Nimis et al., 2012) are drawn, as a comparison with the early contamination period. For the industrialized period, study of coal combustion (Kylander et al., 2005; Komárek et al., 2008), atmospheric aerosols in the continental Europe (Monna et al., 1997; Flament et al., 2002), waste incinerator ash (Monna et al., 1997; Hansmann and Köppel, 2000; Carignan et al., 2005; Kylander et al., 2005) and leaded gasoline (Hopper and Ross, 1991; Leistel et al., 1997; Monna et al., 1997; Monna et al., 1999; Hansmann and Köppel, 2000; Novák et al., 2003) are considered. In Table 14.3 the Broken Hill Mine Ore from Australia is also listed, the values are not reported here, because off the graph.

flux, the first one from 101.6 up to 73.4 cm (2570 – 870 cal BP), characterized by an increase in the Pb flux from 0.012 μg cm^{-2} yr^{-1} up to 0.085 μg cm^{-2} yr^{-1}. A second sub-phase (46.7 – 73.4 cm, AD 1085 – AD 1420) presenting higher values, with a mean of 0.205 $\pm$ 0.064 μg cm^{-2} yr^{-1}, and a final interval (38.5 – 46.7 cm, AD 1420 - AD 1830) characterized by a decrease in the Pb flux down to 0.083 $\pm$ 0.023 μg cm^{-2} yr^{-1}. The Pb flux decrease in the last sub-phase may be linked to the evolution of the peat bog that registers in this interval a drop in the sedimentation rate.

The ^{206}Pb/^{207}Pb values are less radiogenic in this phase, with a mean value of 1.185 $\pm$ 0.004 and a significant drop (1.179 $\pm$ 0.003) between 68.5 and 76.5 cm (AD 895 – AD 1160) possibly indicating a different provenance of atmospheric lead.

The red rectangle in Fig. 14.15 presents the range of ^{206}Pb/^{207}Pb and ^{208}Pb/^{206}Pb ratios in this phase. The values are remarkably similar to the ones registered for mining deposits in the Carnic Alps (Giunti, 2011), and looking at a broader scale to values that characterize ores in the Central-Eastern Southern Alps (Nimis et al., 2012). The values reported for mining sites in the Belluno province near to the Coltrondo peat bog (Salafossa, Col Piombin and Cibiana mines; Ros, 2008), present a slightly different range, characteristic of the isotopic values of peat samples from the interval between 68.5 and 76.5 cm, mentioned above. Therefore the possible explanation of the isotopic drop registered for these depths may be related to the local exploitation of near mining sites. This ^{206}Pb/^{207}Pb range more typical of the mines in the Belluno province, characterizes also the peat bog studied by Poto (2013) located near the major mining sites for Medieval and Modern times, between ca. AD 800 to industrial time.

The isotopic signature of the Coltrondo peat samples in this phase may be likely explained more as a mixture derived from local and regional mining sites, that from the Iron Age onward have began to be exploited, as it is documented for the rest of Europe (e.g., Renberg et al., 1994; Martínez Cortizas et al., 1997; Shotyk et al., 1998; Brännvall et al., 1999).

Phase 3 (0 – 38.5 cm) covers an interval of time up to present days (AD 2011). The lead flux presents the highest values registered in the profile, with a maximum of 1.858 μg cm^{-2} yr^{-1} reached at 16.7 cm (AD 1972), followed by a severe decrease. The same trend is visible in the enrichment factor, even if it presents a significant drop between 38.5 to 31.0 cm, not evidenced in the flux profile. This decrease is more likely explained due to the peak of Ti (and other lithogenic elements) registered at these depths more than due to a reduction of human disturbance.

According to the ^{206}Pb/^{207}Pb values, this phase may be subdivided in

different parts: a first one (30.1 – 38.5 cm, AD 1830 – AD 1935) characterized by a severe decrease reaching values of 1.175, a second one where another drop is registered (from 12.8 to 30.1 cm, AD 1935 – AD 1983) reaching the lowest value of 1.157, and the last one, from 12.8 cm to the top of the core, characterized by a constant increase in the isotopic signature. This trend is visible in the near bog of Danta di Cadore (Poto, 2013) and in many other lead isotopes studies carried out in European peat bogs (e.g., Shotyk et al., 1998, 2003; Bindler et al., 2004; Farmer et al., 2005; Kylander et al., 2005).

The sub-phases individuated may be explained as a fingerprint of different anthropogenic lead sources (see Fig. 14.15, the light blue rectangle represents the isotopic values of the Coltrondo peat bog). With the on-set of the industrialization in Europe, the exploitation of mining sites and the combined metallurgic activities increased, and the use of coal combustion began (Komárek et al., 2008). Afterwards, other sources of lead started impacting severely on the atmosphere and the environment, such as the leaded gasoline (introduced in Europe around AD 1945 and in Italy in AD 1955) and, more recently, the waste incineration, producing fly ash considered as an average industrial signature (Monna et al., 1997). The peat bog accurately registers the introduction of leaded gasoline in Italy, visible by a steep decrease in the $^{206}Pb/^{207}Pb$ values, starting from 23.9 cm (AD 1955). The cessation in the use of leaded gasoline is the major responsible for the recent increase in $^{206}Pb/^{207}Pb$ ratio to less radiogenic values (Farmer et al., 2005). In Italy the phasing out of leaded gasoline started in the 1970s, with consecutive reductions of lead concentration in gasoline from 1974 to 1992. The most important decreases dated back to the 1980s (Bono et al., 1995), when the $^{206}Pb/^{207}Pb$ ratio of the Coltrondo bog starts to increase.

Table 14.3: Pb isotope signatures of Pb natural and anthropogenic sources in Europe. Empty rectangles: isotopic ranges from other studies; coloured rectangles: this study (see text for full details).

Source	**Site**	^{208}**Pb**/^{206}**Pb**	^{206}**Pb**/^{207}**Pb**	**Reference**
Natural sources				
Matmata Loess (Holocene)	Southern Tunisia	2.0801	1.1988	Grousset et al. (1994)
Upper continental crust (UCC)		2.0653 - 2.0564	1.19 - 1.22	Kramers and Tolstikhin (1997)
Pre-industrial sediments	Frace	2.066	1.197	Monna et al. (1997)
EGR Basal peat (305-405 cm)	Switzerland	2.053 - 2.066	1.194 - 1.203	Shotyk et al. (2001)
Mining deposit				
Ores	Italian Eastern Alps	2.066 - 2.131	1.143 - 1.221	Nimis et al. (2012)
Ores	Carnic Alps	2.074 - 2.107	1.166 - 1.188	Giunti (2011)
Ores	Belluno Province	2.085 - 2.108	1.165 - 1.181	Ros (2008)
Anthropogenic sources				
European coal		2.086 - 2.098	1.16 - 1.19	Kylander et al. (2005)
				Komárek et al. (2008)
Atmospheric aerosols	Continental Europe	2.08 - 2.1256	1.1342 - 1.1719	Flament et al. (2002)
Industrial emissions	France and UK	2.112	1.155	Monna et al. (1997)
Incinerator fly ash	Continental Europe	2.1070 - 2.1236	1.143 - 1.1547	Monna et al. (1997)
				Hansmann and Köppel (2000)
				Carignan et al. (2005)
				Kylander et al. (2005)
Broken Hill Mine Ore	Australia	2.2283	1.03983	Martínez Cortizas et al. (2002)
				Kylander et al. (2005)
Leaded gasoline		2.1188 - 2.1980	1.06 - 1.17	Leistel et al. (1997)
				Monna et al. (1999)
				Hansmann and Köppel (2000)
				Novák et al. (2003)
Leaded gasoline	Austria	2.134	1.111	Hopper and Ross (1991)
Leaded gasoline	France	2.182	1.084	Monna et al. (1997)
Leaded gasoline	UK	2.193	1.067	Monna et al. (1997)

Chapter 15

Pollen analysis

55 samples for palynological analyses were collected along the profile of the peat bog core, for the reconstruction of the vegetation evolution and its interaction with human and climatic events. A total of 114 pollen taxa were encountered, together with micro-charcoal particles (subdivided in 3 size classes: < 50 μm, 50-100 μm and > 100 μm) and non-pollen palynomorphs (in this thesis not all NPPs will be shown and discussed).

The pollen diagram presented in Figures 15.1 and 15.2 displays a selection of the most important and abundant taxa. Each profile presents the percentage values of the taxum, relatively to the total pollen sum. In Figure 15.1 the groups presented in the Part II, Material and Methods (Section 9.3) are shown as a summary of the vegetation: Climax trees, Other trees and shrubs, Herbs and Human impact indicators.

Micro-charcoal particles are also presented in the pollen diagram calculated as percentages of the total pollen sum. These particles give information about natural and human-induced fire events. By subdividing the micro-charcoal particles in different size groups may be possible to distinguish local fires, occurred next to the bog, from regional ones. Indeed, big and heavy particles do not fly long distances, as smaller and lighter ones do. The influx values (micro-charcoal particles cm^{-2} yr^{-1}), discussed in the Section 15.1 during the description of the pollen assemblage zones, are shown in Figure 15.3.

Pollen indicators of human activities were grouped in settlement, cultural and pasture indicators (Table 15.1) to allow an interpretation and discussion of the human impact on the peat bog. This subdivision was realized following and comparing Behre (1981, 1986), Oeggl (1994) and Festi (2012), the last two works focused on the Alpine environment.

The following Section will give a detailed description of the different pollen assemblages individuated along the peat bog core. The reconstruction of the

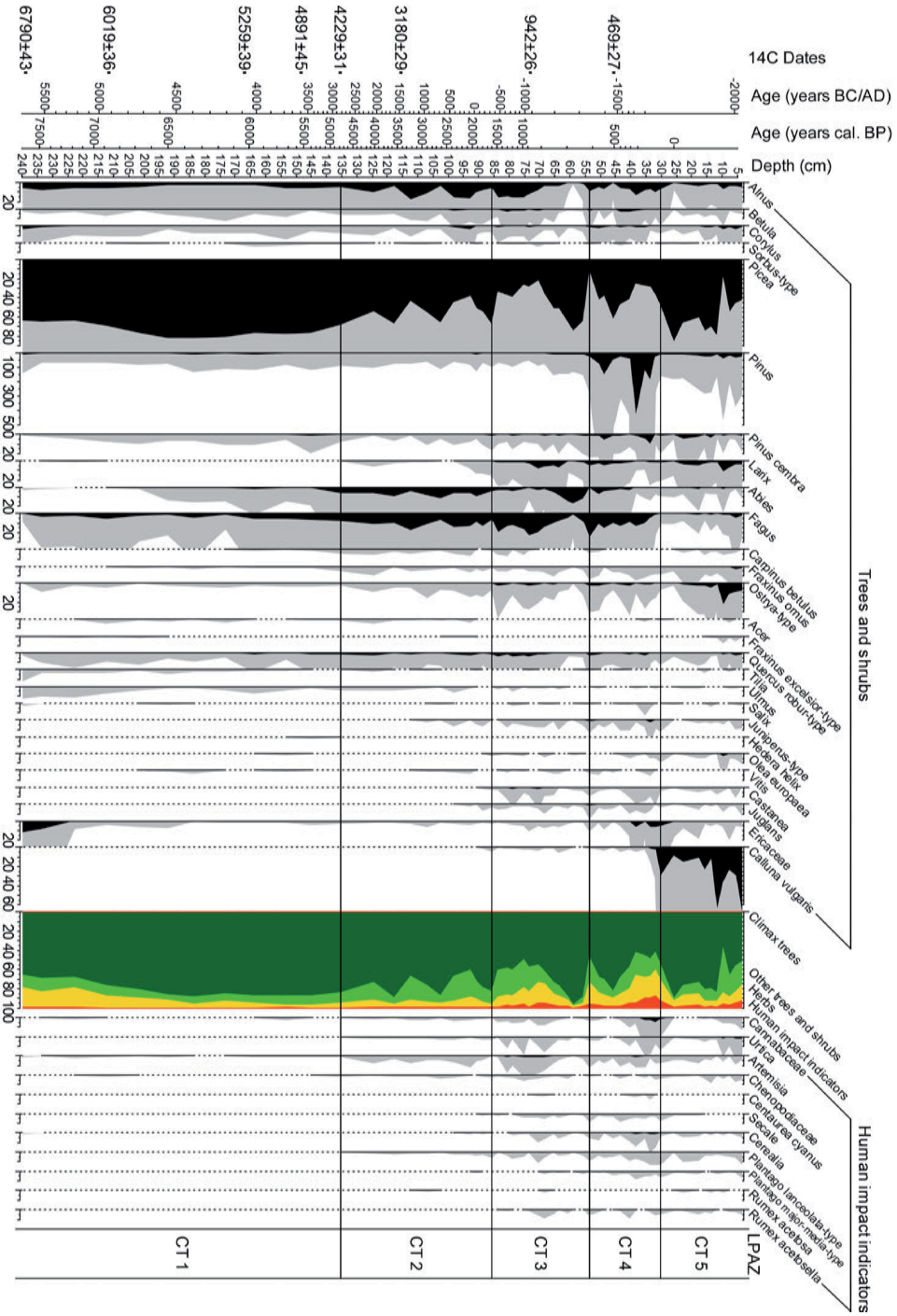

Figure 15.1: Simplified pollen diagram showing percentage values of trees, shrubs and human indicators. Unless otherwise noted, main tick represent 10%.

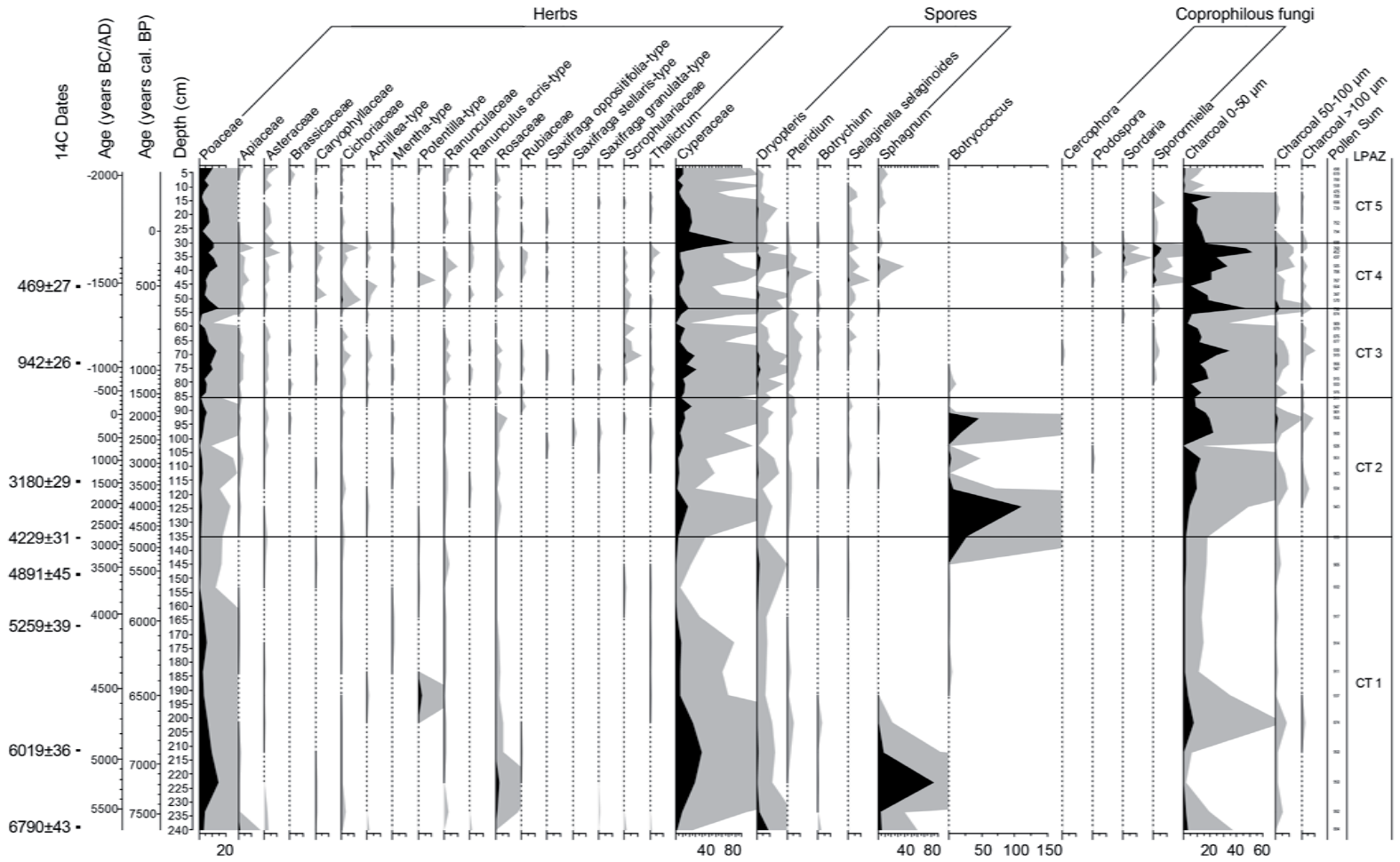

Figure 15.2: Simplified pollen diagram showing percentage values of herbs, spores, algae, coprophilous fungi and micro-charcoal particles. Unless otherwise noted, main tick represent 10%.

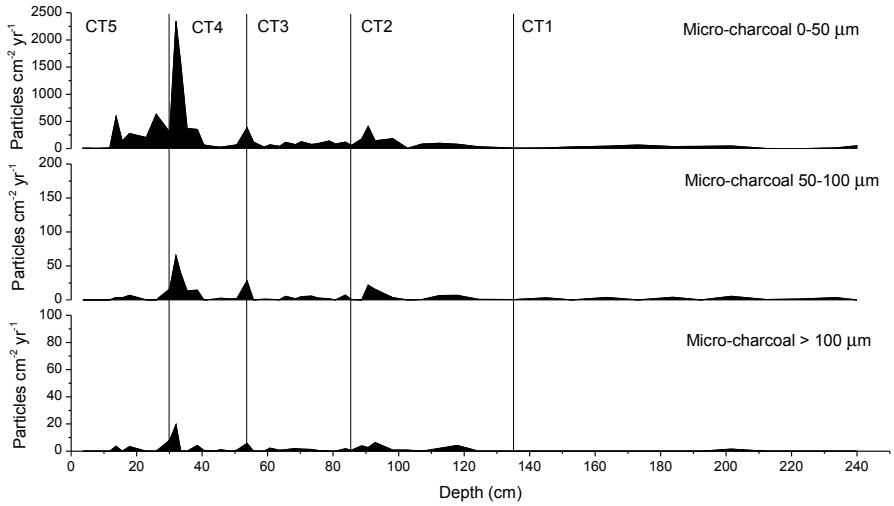

Figure 15.3: Three-size classes of micro-charcoal particles, influx values (particles cm^{-2} yr^{-1}) are shown.

vegetation history and the climatic and human events detectable in the pollen diagram will be discussed in the Part IV.

Table 15.1: Subdivision of pollen markers for human activity in settlement, cultural and pastoral indicators, following and comparing Behre (1981, 1986), Oeggl (1994) and Festi (2012).

	Human impact indicators
Settlement indicators	*Artemisia*, Cannabaceae, Chenopodiaceae, *Urtica*
Cultural indicators	*Secale*, Cerealia, *Castanea*, *Juglans*
Pasture indicators	*Aconitum*-type, Campanulaceae, Gentianaceae, *Plantago alpina*, *Plantago lanceolata*, *Plantago major-media*-type, *Rumex acetosa*, *Rumex acetosella*, *Trifolium*

15.1 Local pollen assemblage zone description

Five local pollen assemblage zones (lpaz) are statistically significant for the Coltrondo peat bog. Here they are presented, each one characterized by the name, the depth interval, the lithological composition, the chronological interval, the chronozone, the archaeological period and the main vegetational changes occured at the upper limit of each zone. Arboreal pollen (AP), non-arboreal pollen (NAP), spores, micro-charcoal and non-pollen palynomorphs (NPP) are described separately. Table 15.2 summarizes the main features of each zone.

lpaz CT1: *Picea* zone

Depth: 239.9 - 135.3 cm

Lithology: peat

Age: 7660 - 4765 cal BP (5710 - 2815 BC)

Chronozone: Atlantic p.p. - Subboreal p.p.

Archeological period: Neolithic p.p. - Copper Age p.p.

Lower limit: mineral substrate

Upper limit: decrease of *Picea* - increase of *Fagus* and *Abies*

AP: *Picea* pollen dominates with percentages values of about 65% at the bottom (239.9 - 222.9 cm, 7660 - 7180 cal BP), increasing up to about 80% from 222.9 to 173.1 cm (7180 - 6150 cal BP) registering the highest values along all the core. The curve shows a decrease (77%) from 163.5 cm on (5970 cal BP). *Alnus* is present with values of about 6% between 239.9 to 201.6 cm (7660 – 6680 cal BP), decreasing to 3% at depths 192.3 - 163.5 cm (6500 - 5970 cal BP) to rise again (6%) at the end of the lpaz (152.9 cm, 5740 cal BP). *Pinus* pollen type presents an average percentage value of 9% (calculated on the pollen sum), while *Pinus cembra* is present with lower values (average 0.7%). *Fagus* achieves values of about 3% showing two subsequent increases, 6% at 163.5 cm (5970 cal BP) and 6.6% at 145.1 cm (5410 cal BP), both with the concomitant decrease of *Picea*. At 145.1 cm there is also the increase of *Abies* pollen type up to 2%. Regarding the shrubs, Ericaceae shows considerable values, up to 13% at the bottom (239.9 - 233.5 cm, 7660 - 7480 cal BP). Other present pollen types are: *Betula* and *Corylus* occuring constantly with low percentages, *Quercus robur*-type with percentages of about 1%, *Tilia* and *Ulmus* with higer values at the bottom of

the core (239.9 - 222.9 cm, 7660 - 7180 cal BP), *Ostrya*-type, *Acer*, *Fraxinus ornus*, *Carpinus betulus*. *Sorbus*-type, *Lonicera*, *Hedera helix*, *Salix*, *Vitis* and *Olea europea* also occur.

NAP: Poaceae pollen grains register an average percentage value of about 5% with a peak of 15% at 222.9 cm (7180 cal BP), the maximum percentage value along all the core, and a second one of 6% at 173.1 cm (6150 cal BP), both concomitantly with lower values of *Picea*. Herbaceous taxa occur with very low percentages (Apiaceae, *Artemisia*, Asteraceae, Caryophillaceae, Cichorioideae, Ranunculaceae, *Thalictrum*). Higher values of Rosaceae pollen grains are present at the bottom (229.9 cm, 7180 cal BP), reaching 3.3%, and a peak of *Potentilla*-type up to 3.4% is registered at 192.3 cm of depth (6500 cal BP). Cyperaceae pollen type is always present, with considerable high values between 229.9 to 201.6 cm (7180 - 6680 cal BP, up to 40% calculated on the pollen sum). *Scheuchzeria palustris* appears, together with the green algae *Botryococcus* from 183.7 cm on (6345 cal BP).

Spores: presence of bryophytes and pterydophytes spores, with a notable peak of *Sphagnum* (over 85%, calculated on the pollen sum) at 229.9 cm (7180 cal BP).

Micro-charcoal: low influx values of micro-charcoal particles are registered along all the assemblage zone.

lpaz CT2: *Picea* - *Fagus* zone

Depth: 135.3 - 85.6 cm

Lithology: peat

Age cal. BP: 4765 - 1605 (2815 BC - 345 AD)

Chronozone: Subboreal p.p. - Subatlantic p.p.

Archeological period: Copper Age p.p., Bronze Age, Iron Age, Roman Time

Upper limit: decrease in *Picea* - increase in *Fagus*, *Larix*, Poaceae and other herbs

AP: *Picea* pollen grains show a decreasing trend but still dominate the profile with an average percentage of 56%. Three major peaks are registered at depth 117.9 cm (68%, 3570 cal BP), 102.7 cm (67%, 2635 cal BP) and 85.6 cm (69%, 4765 cal BP). *Alnus* pollen type is present with an average of 10%, showing increasing values (up to 18%) concomitantly with the decrease of *Picea*. *Fagus* pollen grains increases, reaching about 18% at 112.5

cm (3230 cal BP). *Abies* is present with values of about 8%, with some decreases at the same time of *Picea* decreases. *Pinus* pollen type presents an average percentage of 8% (calculated on the pollen sum), while *Pinus cembra* registers lower values (average 0.7%, as in CT1). There are the first findings of *Larix* pollen grains with an increase in the last part of this zone (up to 1.5%), from depth 92.9 cm on (2040 cal BP). *Quercus robur*-type is present with higher percentages with respect to CT1, of about 2.2%, as well as *Betula* (1%), *Corylus* (1%), *Ostrya*-type (0.8%), *Fraxinus ornus* (0.3%) and *Carpinus betulus* (0.3%). Other pollen types present are: *Sorbus*-type, *Acer*, *Ulmus*, *Tilia*, *Vitis*, *Salix*. There is the first appearance of *Juniperus*-type at depth 107.1 cm (2900 cal BP), *Juglans* (92.8 cm, 2038 cal BP) and *Castanea* (88.7 cm, 1970 cal BP). Ericaecae pollen is present along all the zone with an average percentage of 0.2%.

NAP: there is a constant presence of Poaceae with a percentage of about 2.4%, with higher values between 92.8 to 88.7 cm (2040 cal BP - 1790 cal BP) reaching a percentage of 6%. An increase in the percentage of herbaceous taxa (*Artemisia*, Cannabaceae, *Plantago lanceolata*-type, *Urtica*, Apiaceae, Asteraceae, Chenopodiaceae, Cichorioidae, Ranunculaceae, Rosaceae) is registered, with a cumulative percentage of 1.4%. Cyperaceae are present with an average value of 10.5%. There is the first occurrence of Cerealia (92.8 cm, 2040 cal BP) and *Secale* (88.7 cm, 1790 cal BP).

This second zone is characterized by a high abundance of the green algae *Botryococcus* that reaches values of 112% (calculated on the pollen sum) at depth 124.4 cm (4020 cal BP) and of 47.6% at depth 92.8 cm (2040 cal BP).

Spores: presence of bryophyte (mainly *Dryopteris*) and pterydophyte spores (mainly *Pteridium* and *Selaginella selaginoides*).

Micro-charcoal: low influx values are registered. In the last part an increase is visible, with a peak at 90.7 cm (1910 cal BP).

lpaz CT3: *Picea* - *Fagus* - Poaceae zone

Depth: 85.6 - 53.7 cm

Lithology: peat

Age cal. BP: 1605 - 610 (345 - 1340 AD)

Chronozone: Subatlantic p.p.

Archeological period: Late Antiquity, Middle Ages p.p.

Upper limit: decrease in *Picea* - increase in *Pinus*, *Fagus*, Poaceae and human impact indicators

AP: *Picea* pollen type diminishes from 83.7 to 70.3 cm (1490 - 810 cal BP) reaching a value of 22%. There is a subsequent increase up to 75.5% at 58.9 cm (675 cal BP). *Alnus* pollen shows percentage values of 16% between 83.7 and 75.3 cm (1490 - 980 cal BP) and then decreases to reach values of 2% at the end of the zone. *Fagus* reaches in this zone the highest values along all the profile, 23.5% at depth 73.4 cm (870 cal BP). Subsequently there is a decrease and at depth 58.9 cm (675 cal BP) it reaches 2.2%. At the end of the zone it starts to increase again. *Larix* is present with percentage values of about 3% (peaks up to 9% at 70.3 cm, 810 cal BP). *Abies* pollen type shows an increase up to 17% from 65.5 to 58.9 cm (755 - 675 cal BP) followed by a decrease at the end of the zone. *Pinus* pollen type presents a percentage of about 10% (calculated on the pollen sum) and *Pinus cembra* registers values of 1%. Pollen from *Betula* has a higher percentage compared to previous pollen assemblage zones, reaching 3%. *Quercus robur*-type, *Ostrya*-type and *Fraxinus ornus* register a similar trend with an higher presence from the bottom of the zone to 63.6 cm (730 cal BP) with an average percentage of 3%, 2% and 0.5% respectively, followed by a decrease at depth 58.9 cm (675 cal BP). *Castanea* and *Juglans* pollen type show a constant present with percentages of 0.8% and 0.5% respectively. Other pollen taxa are: *Corylus*, *Sorbus*-type, *Lonicera*, *Carpinus betulus*, *Acer*, *Ulmus*, *Salix*, *Olea europea*, *Vitis*. Regarding shrubs, *Juniperus*-type is present with percentages of about 0.5%, Ericaceae with percentages of 0.4% and *Calluna vulgaris* also appear with values of 0.2%.

NAP: Poaceae pollen grains always dominate among non-arboreal pollen, in this zone with a mean percentage of 7% with a peak of 17% (68.5 cm, 790 cal BP). There is a general increase of herbaceous taxa: Cannabaceae, *Artemisia*, *Plantago lanceolata*-type, *Urtica*, *Rumex acetosella*, *Centaurea cyanus*, Apiaceae, Asteraceae, Chenopodiaceae, Cichorioideae, Ranunculaceae, *Achillea*-type, Rosaceae, Rubiaceae, Scrophulariaceae, *Thalictrum*. Sporadic presence of *Rumex acetosa*, Brassicaceae, *Ranunculus acris*-type, *Mentha*-type, *Saxifraga oppositifolia*-type, *S. stellaris*-type and *S. granulata*-type. Cerealia and *Secale* pollen are registered in this zone, with a higher percentage at 68.5 cm, the same depth where Poaceae shows a peak and several other herbs register higher values (Cannabaceae, *Rumex acetosella*, *Urtica*, Scrophulariaceae). Cyperaceae is present with a mean percentage of 15%.

Spores: a general small increase is also registered for bryophytes and pterydophytes spores (*Dryopteris* and *Pteridium*). Occurence of *Botrychium*, *Selaginella selaginoides* and *Sphagnum*.

Micro-charcoal: constant occurrence of micro-charcoal particles, with an increase at the end of the zone.

NPP: *Sporormiella* occurs in this zone, with values of 0.1%.

lpaz CT4: *Picea* - *Fagus* - *Pinus* zone

Depth: 53.7 - 30.1 cm

Lithology: peat

Age cal. BP: 610 - 15 (1340 - 1935 AD)

Chronozone: Subatlantic p.p.

Archeological period: Middle Ages p.p., Modern Time p.p.

Upper limit: increase in *Picea* and *Calluna* - decrease in *Pinus*, *Fagus*, decrease in cultural indicators and herbaceous taxa

AP: *Picea* pollen increases from the bottom of the zone to 45.7 cm (515 cal BP) reaching 64%. There is a subsequent decrease down to 25% (38.5 cm, 119 cal BP) and then *Picea* starts to increase again. *Fagus* pollen is present with a mean percentage of 11%, showing a decreasing trend reaching 1% at the end of the zone. *Pinus* registers considerable values in this zone, with three main peaks at 48.7 cm (156%, calculated on the pollen sum), 38.5 cm (450%, calculated on the pollen sum) and 33.5 cm (197%, calculated on the pollen sum). At these depths wood remains are individuated in the core. *Pinus cembra* also shows higher values in this zone, with two peaks at 48.7 cm (6%, 550 cal BP) and 33.5 cm (10%, 40 cal BP). *Alnus* is present with a mean percentage of 8%. *Abies* and *Larix* show a similar profile, with a decreasing trend, with *Abies* reaching a really low percentage at the end of the zone (0.9%). *Betula* pollen reaches here the maximum values of all the profile, with 2.4% at 38.5 cm (119 cal BP), while *Corylus* pollen type is constantly present with a mean value of 1.5%. Other taxa present: *Ostrya*-type (1.8%), *Quercus robur*-type (1.7%), *Fraxinus ornus* (0.8%). *Ulmus*, *Salix*, *Vitis*, *Olea europea* also occur with lower values. *Castanea* and *Juglans* present values of 0.8% and 0.6% with a slight increase at the top of the zone. Between shrubs, Ericaceae dominates at the end of the zone, with values of 6.4%; as well as *Calluna vulgaris* pollen that starts to increase in the last part of the zone.

NAP: Poaceae pollen dominates the NAP, with mean values of 9.5%. Lower values (6.5%) are registered between 50.6 cm to 40.5 cm (575 – 230 cal BP, AD 1375 – 1720). The general increase of herbaceous taxa registered in the former zone is evident and more pronounced in CT4: Cannabaceae, *Artemisia*, *Plantago lanceolata*-type, *Plantago major-media*-type, *Urtica*, *Rumex acetosella*, *Centaurea cyanus*, Apiaceae, Asteraceae, Brassicaceae, Caryophyllaceae, Chenopodiaceae, Cichorioideae, *Achillea*-type, *Mentha*-type, Ranunculaceae, *Ranunculus acris*-type Rosaceae, Rubiaceae, Scrophulariaceae,

Thalictrum. Sporadic presence of *Saxifraga oppositifolia*-type. Cannabaceae and Cerealia pollen register in this zone the highest values, between 38.5 to 30.1 cm (119 - 15 cal BP, AD 1831 - 1935) up to 5.3% and 1.4% respectively. *Secale* also reaches its maximum in this zone, at 43.6 cm (400 cal BP, AD 1550) with 0.8%. Cyperaceae increases at the end of the zone reaching its maximu value of 95% (calculated on the pollen sum).

Spores: higher presence of bryophytes and pterydophytes spores (*Dryopteris*, *Pteridium*, *Selaginella selaginoides*, *Sphagnum*). Occurence of *Botrychium*.

Micro-charcoal: highest influx values of micro-charcoal are registered in this zone, at the bottom (53.7 cm, 610 cal BP, AD 1340) and then again in the upper part of the zone 32 cm (AD 1921).

NPP: coprophilous fungi are present, in the last part of the zone with higher values, the most abundant is *Sporormiella*, followed by *Sordaria*, *Podospora* and *Cercophora*.

lpaz CT5: *Picea* - *Calluna* zone

Depth: 30.1 - 3.6 cm

Lithology: peat

Age cal. BP: 15 - -55 (1935 - 2005 AD)

Chronozone: Subatlantic p.p.

Archeological period: Modern Time p.p.

Upper limit: surface of the bog

AP: *Picea* pollen type increases in this zone, reaching values up to 87% with a decrease at the top of the zone. The shrub *Calluna vulgaris* shows considerable values, with a mean percentage of 34% (calculated on the pollen sum) and some major peaks, at 11.8 and 3.6 cm (99% and 72% respectively, calculated on the pollen sum). High percentages of *Larix* characterizes this zone, up to 7.5% at depth 7.6 cm, the end of the 90's. *Pinus* pollen presents an average percentage of 26% (calculated on the pollen sum), while *Pinus cembra* registers values of 1.8%. *Alnus* is present with lower percentages with respect to former zones, mean values of 3.5%. *Abies* and *Fagus* pollen type strongly decrease; *Fagus* registering an increase at the end of the zone, as well as *Corylus*, reaching 4% at 5.5 cm, and *Ostrya*-type 12% at depth 7.6 cm). Other taxa present are: *Carpinus betulus*, *Fraxinus excelsior*-type, *Olea europea*, *Castanea*, *Juglans* and *Betula*. Sporadic occurrence of: *Sorbus*-type, *Acer*, *Tilia*, *Ulmus* and *Salix*. Lower percentages of *Juniperus*-type and Ericaceae with respect to CT4.

NAP: Poaceae and the other herbs register a general decrease in this zone. Herbaceous taxa present are: Cannabaceae, *Plantago lanceolata*-type, *Plantago major-media*-type, *Urtica*, *Artemisia*, Asteraceae, Chenopodiaceae, Ranunculaceae, Rosaceae and Cichorioideae. *Secale* disappears while the curve of Cerealia decreases. There is the sporadic occurrence of *Rumex acetosa*, Brassicaceae, Apiaceae, Caryophyllaceae, *Mentha*-type, Rubiaceae, *Saxifraga oppositifolia*-type, *S. granulata*-type and *Thalictrum*.

Spores: general decrease of bryophytes and pterydophytes spores, *Pteridium* disappears.

Micro-charcoal: micro-charcoal particles are present up to 13.7 cm (AD 1980), then there is a severe reduction and they almost disappear.

Table 15.2: Main characteristics of the local pollen assemblages of the Coltrondo peat bog.

lpaz	**Depth** (cm)	**Age cal BP** (Age AD/BC)	**Chronozone**	**Archeological period**	**AP/NAP** (average values)	**Main taxa**
CT5 *Picea-Calluna* zone	30.1-3.6	15–55 (1935-2005 AD)	Subatlantic p.p.	Modern Time p.p.	AP 86% NAP 14%	*Picea*, *Calluna vulgaris*, *Larix*, *Ostrya*-type, Poaceae
CT4 *Picea-Fagus-Pinus* zone	53.7-30.1	610-15 (1340-1935 AD)	Subatlantic p.p.	Middle Ages p.p., Modern Time p.p.	AP 76% NAP 24%	*Picea*, *Pinus*, *Fagus*, *Abies*, *Larix*, *Alnus*, *Juniperus*-type, Poaceae, Cerealia, *Secale*, *Plantago lanceolata*-type, Cannabaceae, *Urtica*, *Artemisia*, Cichorioideae
CT3 *Picea-Fagus-* Poaceae zone	85.6-53.7	1605-610 (345-1340 AD)	Subatlantic p.p.	Late Antiquity, Middle Ages p.p.	AP 87% NAP 13%	*Picea*, *Fagus*, *Abies*, *Larix*, *Alnus*, *Quercus robur*-type, *Ostrya*-type, *Juniperus*-type, Poaceae, Cerealia, *Secale*, *Plantago lanceolata*-type, *Artemisia*, *Urtica*, Cannabaceae, Chenopodiaceae
CT2 *Picea-Fagus* zone	135.3-85.6	4765-1605 (2815 BC-345 AD)	Subboreal p.p., Subtalantic p.p.	Copper Age p.p., Bronze Age, Iron Age, Roman Time	AP 93% NAP 7%	*Picea*, *Fagus*, *Abies*, *Alnus*, *Quercus robur*-type, Poaceae, *Artemisia*
CT1 *Picea* zone	239.9-135.3	7660-4765 (5710-2815 BC)	Atlantic p.p., Subboreal p.p.	Neolithic p.p., Copper Age p.p.	AP 90% NAP 10%	*Picea*, *Fagus*, *Alnus*, Poaceae

Chapter 16

The ombrotrophic character of the peat bog

The assessment of the trophic status of the natural archive under investigation constitutes a first important step towards a reliable palaeoenvironmental reconstruction. In particular, it is vital to ensure that exclusively atmospheric inputs are recorded. A number of properties can be observed and measured to ascertain the ombrotrophic character of a peatland, including geomorphic and botanical information obtained from visual inspection as well as the physical and chemical properties of peat, measured directly in the field and after the collection of the core (Shotyk, 1996; Givelet et al., 2004; Chambers et al., 2012).

A first visual inspection of the Coltrondo mire allowed us to evaluate the vegetation type, mainly dominated by *Sphagnum* mosses, *Eriophorum vaginatum*, *Calluna vulgaris* and *Vaccinium microcarpum*, typical of oligrotrophic environments (Pignatti, 1982).

The pore water extracted from peat samples from the first 100 cm of the core was used mainly to assess the trophic status of the mire, measuring the pH and determining Ca and Mg concentrations. The pH presents low values that range between 3.40 to 3.85, indicating oligotrophic conditions and acidic waters (Fig. 16.1a), typical of an ombrotrophic status. Indeed, as stated by Shotyk (1988), if the pore water of the first meter of the core were being influenced by groundwater, the acidity would be neutralized by the mineral matter with higher concentrations, and the pH would increase with depth.

The comparison of the Ca/Mg ratio of the pore water (Fig. 16.1b) to that of rain samples from Danta di Cadore (see Section 14.2), is a very useful tool to evaluate whether the bog is fed only by atmospheric depositions or also by surface runoff and groundwater. As explained in the Results, Section 14.2, in an ombrotrophic bog the Ca/Mg ratio of pore water presents lower or com-

parable values to the ones measured in the local rainwater, which represents the main source of nutrients in these types of peatlands. In a minerotrophic mire, influenced also by surface water and groundwater, the ratio in the pore water is usually much higher (Shotyk, 1996). As stated in Shotyk (1996), Ca is preferentially released over Mg during weathering processes, resulting in an higher additional input of Ca from non-atmospheric sources. In the Coltrondo peat bog the Ca/Mg ratio of the pore water in the first meter of the core is always below the 4.5 value calculated for the rainwater, suggesting an exclusive atmospheric input of Ca, i.e. an ombrotrophic environment.

The low values of bulk density and ash content along the core (mean values of 0.1 g cm^{-3} and 3.5% respectively) are in accordance with the values cited by Shotyk (1996) and MacKenzie et al. (1998) for ombrotrophic peatlands (Fig. 16.1c, d). While higher values of bulk density are related to slower peat accumulation, this is not the case of the ash content, whose peaks probably reflect a higher input of mineral matter from atmospheric sources. This is also confirmed by the high correlation between ash content and Ti (Pearson correlation coefficient = 0.92, $p<0.01$), suggesting that most inorganic content supplied to the bog came via atmospheric dust deposition (Martínez Cortizas et al., 2002; Kylander et al., 2005). Bulk density and ash content do not give precise information about a possible ombrotrophic/minerotrophic boundary, as they remain constant along the profile. They present a severe increase, ascribable to the transition between peat and peaty soil, in the last 10 cm of the core.

Other indicators for determining the trophic status in the deeper layers can also be evaluated. Ca and Sr may indicate groundwater influence through their dissolution and upward migration from the underlying bedrock (Shotyk et al., 2001; Kylander et al., 2005). Ca and Sr show a similar trend in the Coltrondo peat bog, with higher values in the superficial layers, due to biological activity. In the bottom layers, below 180 cm of depth, both Ca and Sr register a moderate increase, possibly suggesting the influence of groundwater (Fig. 16.1e, f).

The wide range of factors taken into account to evaluate the trophic status of the Coltrondo peat bog suggests ombrotrophic conditions down to ca. 180 cm. Below this depth the atmospheric dust input is integrated with the upward migration of chemical elements from the underlying bedrock, characterizing the chemical composition of the basal peat layers.

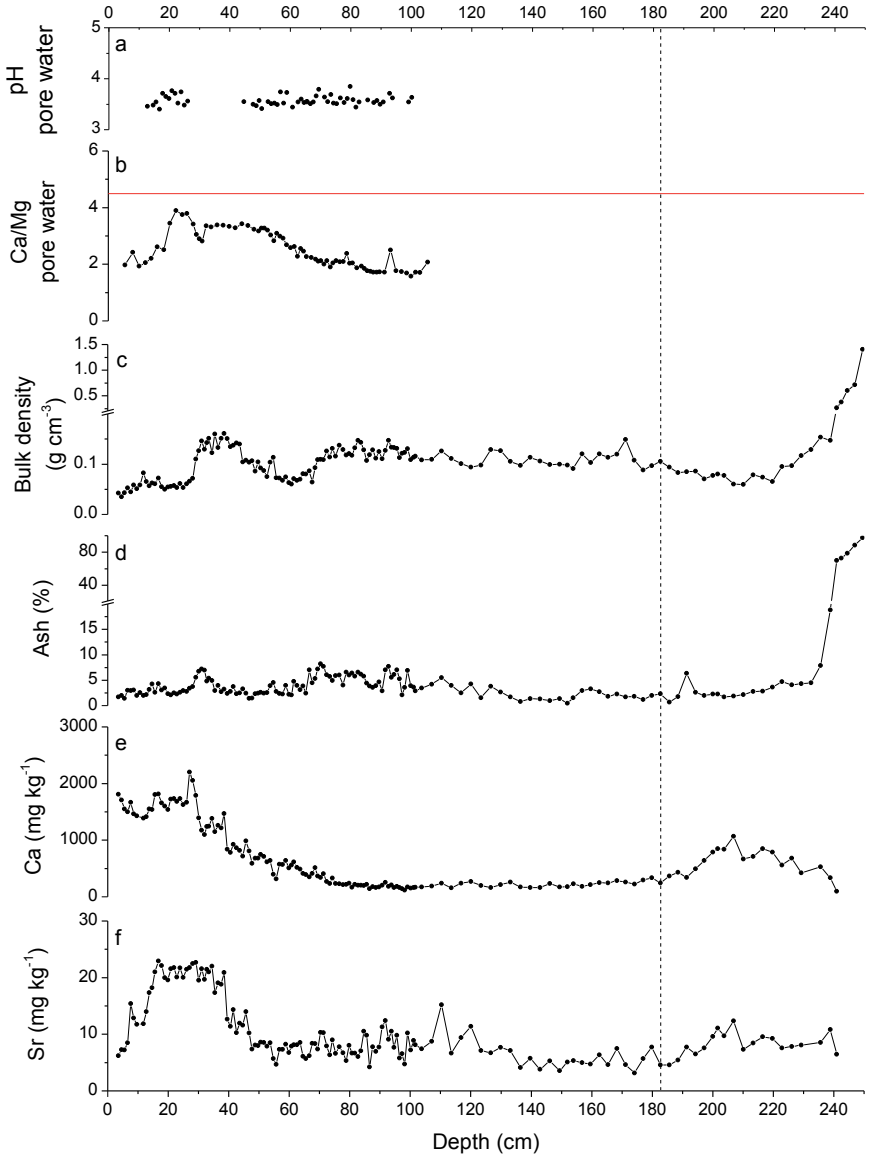

Figure 16.1: Indicators analysed to assess the trophic status of the peat bog. The red line in the graph of pore water Ca/Mg ratio (b) represents the value of the same ratio in rainwater (4.5). The vertical dashed line indicates the probable boundary between rain-fed peat and peat influenced by upward migration from the underlying mineral substrate.

Part IV

Holocene variability recorded by the Coltrondo peat bog

Chapter 17

The climatic and human history unravelled by the Coltrondo peat bog

The study of different proxies allowed the reconstruction of different aspects of the past history recorded by the peat bog: climatic events, vegetation history, land-use changes, anthropogenic disturbances mainly due to settlement, agriculture, pasture, mining and industrial activities.

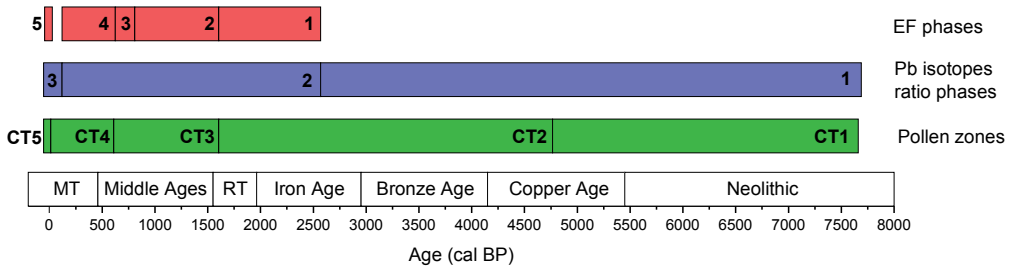

Figure 17.1: Different phases identified by the Pb, Zn, As, Ag, Cd and Cu enrichment factors (red), lead isotope ratios (blue) and pollen analysis (green) plotted on a time line in years cal BP. Archaeological periods (Festi et al., 2014) are shown, with RT = Roman Times and MT = Modern Time.

The analysis of physical, chemical and biological proxies along the Coltrondo peat bog core highlighted different phases (Fig 17.1). In particular, the enrichment factors of Pb, Zn, As, Ag, Cd and Cu allowed the individuation of 5 different phases for the last ca. 2500 years. The study of the $^{206}Pb/^{207}Pb$ ra-

tio distinguishes three different periods along all the core, while the changes in the vegetation individuate 5 local pollen assemblage zones (CTs).

The following discussion will gather the results obtained from the different proxies, with the aim to give an overall view on the climatic and human history registered in the core. After a first Section about the peat initiation, the discussion will be organized in other three Sections, following the three phases identified by the $^{206}Pb/^{207}Pb$ ratio: a first pre-anthropogenic phase, during which variations in the bog are mainly due to natural variability; a second phase during which humans start to impact on the environment, mainly through farming, grazing and mining activities; and a third and final phase characterized by a strong human impact related to the advent of industrialization.

To help infer past events, we performed correlations and ordinations of data for the three phases. For the linear correlations the following parameters were chosen:

- ash content as a proxy of mineral dust in the atmosphere. It is mainly related to erosional and weathering processes, and may give information about climate and/or human impact;
- PC2 axis scores of the PCA performed for chemical elements (see Section 14.1), as a proxy of the main lithogenic depositions.
- charcoal influx, as a proxy of natural and/or human-induced fires. For this analysis the three size-classes are summed together;
- climax trees, as representative of the main vegetation of the area. Variations in the percentage of this vegetation assemblage may be linked to climate and/or human impact;
- indicators of settlements, cultural and pasture activities, as well as coprophilous fungi, all proxy of human presence and human activities; in the first phase, non-arboreal pollen (NAP) was chosen instead of human indicators. NAP may give information about the openness of the area and therefore about possible climatic variations;
- Pb enrichment factor, as representative of trace metal depositions, as proxy of human impact on the environment.

17.1 The peat initiation

Peat bogs develop in areas where precipitation exceeds evapotranspiration and surface runoff, and they can form either by terrestrialization or paludification. Terrestrialization is the process by which a shallow lake is slowly infilled with accumulated organic and inorganic matter, while in paludification the peat forms directly over a mineral substrate, with the absence of a previous limnic phase. Differently from terrestrialization, which naturally occurs over time in any suitable water-collecting basin, paludification generally needs a shift in hydrological conditions, linked to a change in external factors, such as climate (Charman, 2002).

A first visual inspection of the peat core, the LOI measurements and the pollen record all suggest that the peatland followed a process of paludification. The measured organic matter shows a transition from the mineral substrate to peaty soil and peat, registering an increase from 2.5% at the bottom of the core (ca. 7900 cal BP, 250 cm) up to values of 81% around 7600 cal BP (239.9 cm), corresponding to the level of the first pollen sample analysed. The first pollen samples are characterized by the occurrence of *Sphagnum* species. These mosses play a crucial role in the autogenic development of the bog because of their ability to acidify the environment and isolate the mire from the effects of groundwater (Clymo, 1983). Moreover, the vegetation of these first peat stages, characterized by a sparse *Picea* forest with local *Alnus viridis* and by the presence of light-demanding taxa, such as Poaceae and Rosaceae, suggests a cool and humid climatic spell that may have triggered the peat initiation process.

Lower temperatures, higher rates of precipitation and higher superficial runoff may have driven a shift in local hydrological conditions, producing a water-logging of the mineral substrate, characterized by strong water retention and enhanced impermeability (see Section 4.1). As a consequence, the decay rate was reduced significantly below that of production, leading to the formation of peaty soil first, and then peat (Charman, 2002; Rydin et al., 2013).

17.2 Environmental and climatic signals in pre-anthropogenic times (7800 – 2500 cal BP)

The first phase analysed covers the depth interval 239.9 – 101.6 cm (ca. 7800 – 2500 cal BP). During this phase, Pb isotope ratios have a range of

1.193 – 1.209, close to the ones registered for the Earth's crust (Kramers and Tolstikhin, 1997), possibly suggesting no human interference in the area. This possibility is also suggested by pollen analysis, which shows a very moderate human signal during the Bronze Age (ca. 4150 – 2950 cal BP), most likely due to long-distance transport and not related to local disturbances.

Table 17.1 presents the Pearson's coefficients between physical, biological and chemical proxies. Ash content presents a highly significant correlation with the second component of the PCA of chemical elements (0.78, $p<0.01$). As previously discussed in Section 14.1, the second axis of geochemical PCA mainly explains lithogenic elements, that are highly correlated with the ash content. NAP mainly explains the behaviour of light-demanding taxa and it shows a highly significant negative correlation with climax trees (-0.82, $p<0.01$) as expected. Micro-charcoal influx does not show any significant correlation in this phase.

A likely explanation for these results is the evolution of the vegetation, strongly related to climatic conditions. Under favourable conditions, a dense spruce forest thrives in the area, to the detriment of light-demanding taxa. Conversely, during a regressive phase, the lowering of the timberline and shorter growing seasons result in a thinning of the forest, allowing the growth of other plants in the area and facilitating the arrival of pollen grains via long-distance transport. Moreover, the amount of dust in the atmosphere (mainly registered by the ash content and lithogenic elements in the Coltrondo peat bog) is related to erosional and weathering processes, which are more prominent during severe climatic conditions, also because a lower vegetation canopy protects the ground, possibly resulting in an enhanced erosion of the soil.

Table 17.1: Pearson correlation coefficients between physical, chemical and biological proxies for the interval 7800 – 2500 cal BP. * = significant correlation with $p<0.05$, ** = highly significant correlation with $p<0.01$. Charcoal influx = sum of the three size-classes influxes. NAP = Non Arboreal Pollen.

	Ash	PC2 chem.	Charcoal influx	Climax trees	NAP
Ash	1	0.78**	0.11	-0.54*	0.65**
PC2 chem.	**0.78****	1	0.43	-0.52*	0.42
Charcoal influx	0.11	0.43	1	-0.04	-0.23
Climax trees	**- 0.54***	**-0.52***	-0.04	1	-0.82**
NAP	**0.65****	0.42	-0.23	**-0.82****	1

17.2.1 7800 – 5000 cal BP

In its early stages, the mire was surrounded by a *Picea* forest with local *Alnus viridis* growing in the vicinity. Nevertheless, the presence of light-demanding taxa, such as Poaceae and Rosaceae, suggest a sparse forest until ca. 7200 cal BP (CT1, Fig. 15.1 and 15.2).

The peat initiation and the observed local vegetation seem to be related to climate, reflecting a cool and humid climatic spell in the Eastern Alps, possibly the so-called Frosnitz deterioration (Patzelt, 1977). Arboreal pollen decreases, probably due to either a depression of the timberline and/or a reduction in pollen production caused by shorter/colder growing season (Kofler et al., 2005), while grasses (Poaceae) and other herbs (Rosaceae) increase, indicating a thinning of the spruce forest, as evidenced also by the PCA in Figure 17.2. The growth of wetland plants (Cyperaceae) and mosses (*Sphagnum* spp.) on the bog also indicates wetter conditions.

This Frosnitz event is registered also at the nearby site of Lake Sant'Anna, with a decrease of the *Picea* forest and an increase in Poaceae and other light-demanding species (Kral, 1986a). This regressive phase lasted between ca. 7200 and 6800 cal BP and is also registered in other palynological works on the Alps, such as the analysis carried out in South-Tyrol (Natzer Plateau and Villanderer Alm) by Seiwald (1980), in the Ötz valley and Kauner valley in Austria (Eastern Alps), respectively at Krummgampen and Brunnboden bogs (cold phase Brunnboden D; Kofler et al., 2005) and at Lago Basso, near the Splügen pass (cold period SPL-7, Wick and Tinner (1997), CE-4, Haas et al. (1998)). The advance of the Gepatschferner Glacier (Nicolussi and Patzelt, 2000b) in the Eastern Alps and the lake level fluctuations studied by Magny (2013) in the Central Alps, on the Swiss Plateau (cold phase CE-4, Haas et al., 1998) are also coeval with this climatic oscillation (Fig. 17.3). During this time total solar irradiation (TSI) was the lowest of the Holocene (Steinhilber et al., 2009).

From ca. 7200 cal BP onward, the *Picea* forest expanded and became denser (see Fig. 17.2) in the lower subalpine belt (ca. 1700 - 2000 m a.s.l), where the bog is located, while at lower altitudes, in the montane zone (ca. 800 - 1700 m a.s.l.), spruce is mixed with *Fagus* and *Abies*. *Pinus cembra* is present at higher altitudes. The occurrence of pollen of *Quercus robur*-type, *Tilia*, *Ulmus*, *Ostrya*-type, *Acer* and *Fraxinus* spp. suggest the presence of thermophilous deciduous trees at the valley bottom (Padola valley).

Other sites in the Eastern and Central Alps register the development of dense forests (Seiwald, 1980; Kral, 1986a; Oeggl and Wahlmüller, 1994; Wick and Tinner, 1997; Stumböck, 2000; Burga and Egloff, 2001; Pini, 2002; Heiss et al., 2005). The treeline is high and reaches its maximum elevation for the

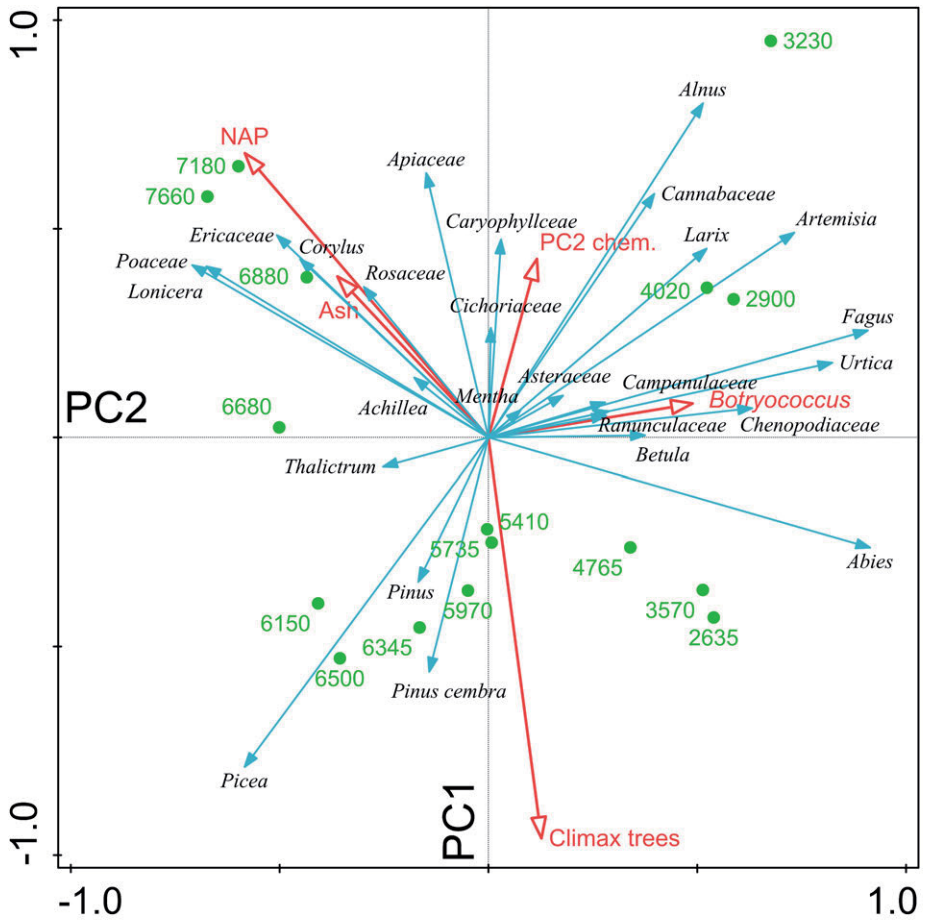

Figure 17.2: PCA of pollen taxa for the interval 7800 – 2500 cal BP. The first axis PC1 informs about the openness of the vegetation, while the second axis PC2 is more related to the moisture conditions. Red arrows are supplementary variables that help in the interpretation of the graph.

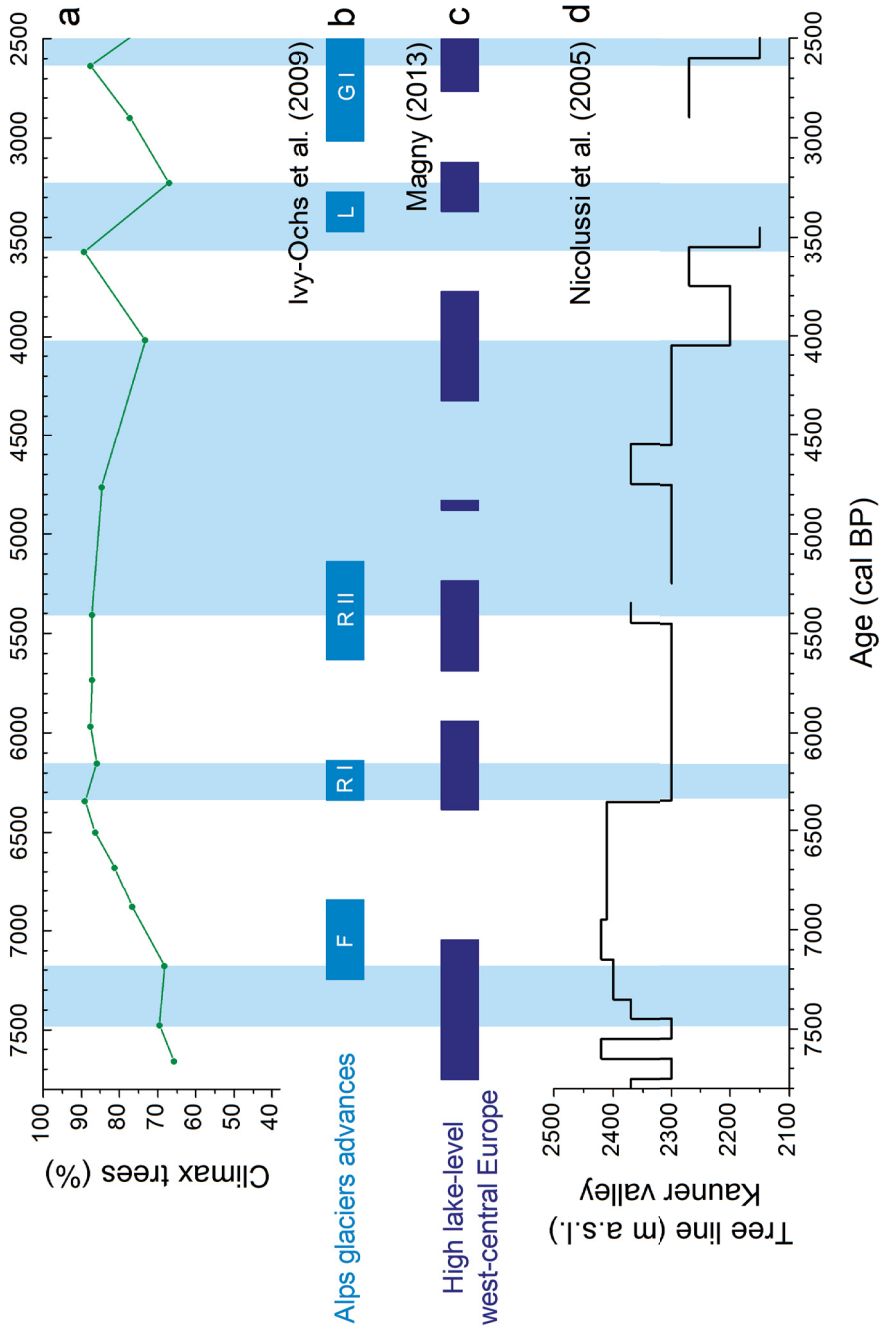

Figure 17.3: Comparison of (a) the Coltrondo peat bog climax community with other palaeoclimate records: (b) main Alpine glacier advances during Frosnitz (F), Rotmoos I and II (RI and RII), Löbben (L) and Göschener I (GI) cold oscillations (Ivy-Ochs et al., 2009); (c) lake-level high stands in Western-Central Europe (Magny, 2013); (d) tree line variability in Kauner Valley, Eastern Alps (Nicolussi et al., 2005). Light blue rectangles indicate colder phases registered in the pollen diagram.

Holocene (Oeggl and Wahlmüller, 1994; Wick and Tinner, 1997; Nicolussi et al., 2005), as depicted in Figure 17.3 for the Eastern Alps. The increase in the percentages of Coltrondo arboreal pollen is related to the Holocene Thermal Optimum (ca. 11,000 - 5000 cal BP, Renssen et al., 2009), a period of time characterized by higher summer temperatures in the Northern Hemisphere (Wanner et al., 2011). During this time, however, the climate is not stable. Several climatic changes occurred, such as the previously mentioned Frosnitz event, causing the temporary retreat of the timberline and impacting on the vegetation. The expansion of *Fagus* in the montane zone, around 6200 cal BP, followed by *Alnus viridis* and an increase in grasses (Poaceae) at the Coltrondo site, suggest a wetter and colder climate, leading to a more open landscape. This is observed also by a simultaneous opening of the local spruce forest. There is a second *Fagus* expansion at the end of the Atlantic period, accompanied by the expansion of *Abies*, reflecting the establishment of a spruce, beech and fir forest ca. 5400 cal BP (the end of the lpaz CT1). *Picea* population decreases while a more open vegetation is present, as testified by a higher biodiversity and abundance of herbaceous taxa (mainly *Artemisia*, Cannabaceae, *Plantago lanceolata*-type, *Urtica*, Chenopodiaceae, Apiaceae, Asteraceae, Cichorioidae, Ranunculaceae, Rosaceae).

The expansion of more oceanic species and the reduction of the spruce forest, possibly due to a lowering of the timberline or shorter growing seasons, register a climatic regressive phase, more humid and cooler. These two successive climatic variations are concomitant with two cooling events, Rotmoos I and Rotmoos II, observed for the first time by Bortenschlager (1970) in the pollen record of Rotmoos mire from the Ötztal Alps (Austria). Other pieces of palynological evidence for these cold events are encountered in Seiwald (1980) (Natzer Plateau and Villanderer Alm, Eastern Alps), Burga and Egloff (2001) (Astalm and Penser Joch, Eastern Alps), Kofler et al. (2005) (Ötzvalley, Eastern Alps), Wick and Tinner (1997) (SPL-9, Splügen Pass, Central Alps).

During the Rotmoos I oscillation (6300 – 6100 cal BP), the Eastern Alpine glaciers advanced, as recorded by Nicolussi and Patzelt (2000a) for the Pasterze Glacier, the largest glacier in Austria, and by Nicolussi and Patzelt (2000b) for the Gepatschferner Glacier (Fig. 17.3). A reduction in the treeline altitude is shown for the Kauner Valley (Kofler et al., 2005; Nicolussi et al., 2005) and the Ötzvalley (cold phase Brunnboden E, Kofler et al., 2005) in the Eastern Alps. Higher lake levels are also registered by Magny (2013) in the Central Alps, and the same event is registered as a cold period CE-5 by Haas et al. (1998). This regressive phase is coeval with the so-called Piora I oscillation first recorded in the Swiss Alps by Zoller (1960).

Rotmoos II oscillation (5600 – 5100 cal BP) (Bortenschlager, 1970; Patzelt,

1977) is a severe climate deterioration affecting the Alps (Baroni and Orombelli, 1996; Wick and Tinner, 1997; Haas et al., 1998; Nicolussi and Patzelt, 2000b) but also globally widespread. This regressive phase is recorded by different archives and proxies in several localities in the Northern Hemisphere (e.g., Lamb, 1977; Bradbury et al., 1993; O'Brien et al., 1995; Svendsen and Mangerud, 1997; Mayewski et al., 1997; Hughes et al., 2000; Payette et al., 2002; Schmidt et al., 2002; Tinner and Theurillat, 2003; Blaauw et al., 2004; Haas and Magny, 2004; Magny et al., 2006; Magny, 2013; Solomina et al., 2015) and in the Southern Hemisphere (e.g., Hjort et al., 1997; Heusser, 1998; Steig et al., 1998; Porter, 2000; Lamy et al., 2002; Thompson et al., 2002; Noon et al., 2003; Solomina et al., 2015).

17.2.2 5000 – 2500 cal BP

From ca. 5400 cal BP the *Picea* forest starts decreasing. The significant presence of *Botryococcus* in the bog suggests moister climatic conditions, also indicated by the high abundance of *Alnus* and the composition of the forest in the montane zone, with *Fagus* and *Abies* steadily present, competing with *Picea* (Fig. 15.1 and 15.2); this higher humidity is evidenced also by the PCA (Fig. 17.2).

These changes occurring in the arboreal vegetation may be ascribed to the onset of the Neoglacial period (ca. 5000 cal BP). The Neoglaciation was dominated by decreasing summer temperatures in the Northern Hemisphere due to decreasing insolation during the boreal summer, mainly triggered by changes in orbital forcings (Kofler et al., 2005; Renssen et al., 2006; Wanner et al., 2011; Solomina et al., 2015).

The pollen record presents low percentages of human-related taxa, such as *Artemisia*, Cannabaceae, Chenopodiaceae, *Urtica* and *Plantago lanceolata*-type possibly suggesting a first sign of anthropogenic interference since the beginning of the Bronze Age at ca. 4000 cal BP (CT2, Fig. 15.1 and 15.2). Nevertheless, the extremely low percentages of human impact indicators and micro-charcoal influx values at that time, and the absence of archaeological evidence in the area (Collodo, 1988), leads to interpret the human signal as a more regional one.

Some major openings of the *Picea* forest are visible in the pollen diagram, the one already mentioned starting from ca. 5400 cal BP to ca. 4000 cal BP and another one between ca. 3600 and 3200 cal BP (a third one between 2600 - 2000 cal BP will be discussed in the next Section).

The first reduction of *Picea* is coeval with the increase of *Alnus*, Cyperaceae and *Botryococcus*, all taxa suggesting wetter conditions. The lowest percentages of *Picea* are registered at ca. 4000 cal BP. Next to the Coltrondo

peat bog, at the Braies lake (Schneider et al., 2010), a humid and cooler phase is also registered between 4250 and 3950 cal BP. Kral (1991) also mentions a decrease in *Picea* between the known Rotmoos and Löbben oscillations (see later on in this Section) at the Wiser-Werfen site. Such a decrease may be related to the same cooler conditions registered at the Coltrondo peat bog. In the Alpine region this phase is also recorded by the lowering of the timberline as observed by Nicolussi et al. (2005) at the Kauner valley and the level fluctuation of Swiss lakes, between 4150 and 3950 cal BP (Magny, 2013) (Fig. 17.3).

The cooler and moister climatic conditions registered in the Coltrondo site may be partly related to the so-called 4.2 event (Bond event 3, Bond et al., 2001), a widespread climatic deterioration proposed by Wanner et al. (2011) and Walker et al. (2012) as the boundary between the Middle and Late Holocene.

The second opening (3600 - 3200 cal BP) in the spruce forest registered at the Coltrondo peat bog is also coeval with the expansion of *Alnus* and, since human presence and its impact on the vegetation were probably very moderate at that time, it may also signal a regressive phase that caused the lowering of the timberline or shorter cold/wet growing seasons. Other palynological works suggest a cooler and humid phase during this period of time, as evidenced by Schneider et al. (2010) at Lake Braies (cooler conditions between 3450–2900 cal BP); Seiwald (1980) registers this colder phase at the Malschötscher Hotter site; Schmidt et al. (2007) records cooler and moister conditions at the Oberer Landschitzsee (Niedere Tauern, Austria); and Haas et al. (1998) individuated as cold phase CE-7. Moreover, a lowering of the timberline is registered at the Kauner valley (Nicolussi et al., 2005).

This phase is possibly related to the Löbben oscillation (Patzelt, 1977), also testified in the Alps by the advance of numerous glaciers (Ivy-Ochs et al., 2009) and by higher lake levels (Holzhauser et al., 2005; Magny, 2013) (17.3). Cooler and moister conditions are widespread in the Northern Hemisphere during this period of time (e.g., Mayewski et al., 1997; Bond et al., 2001; Boettger et al., 2003; Hallett et al., 2003; Hammarlund et al., 2003; Zolitschka et al., 2003; Magny, 2004; Sadori et al., 2004; Lloyd et al., 2007; Mokeddem et al., 2007; Shakesby et al., 2007; Magny et al., 2009; Solomina et al., 2015), while in the Southern Hemisphere cooler and drier conditions are registered (e.g., Finkel et al., 2003; Noon et al., 2003; Vincens et al., 2003; Glasser et al., 2004; Haberle and David, 2004; Masson-Delmotte et al., 2004; Prasad et al., 2007).

17.3 Human fingerprint and climate events in the pre-industrial age (2500 cal BP – AD 1830)

The second phase (101.6 – 38.5 cm) is characterized by the settlement of humans in the area and consequently by anthropogenic disturbances due to agricultural, pasture and mining activities, all of which prospered during the Middle Ages, as testified by the pollen analysis, by the decreasing trend of $^{206}Pb/^{207}Pb$ ratio, approaching the values registered for ore deposits in the Eastern Alps, and by historical documentation.

Climate also influences the vegetation but may be masked by human signals. This often results in the difficulty to disentangle between the two signals when both are registered in the peat bog archive.

Table 17.2 presents the Pearson's coefficients obtained by correlating physical, chemical and biological proxies for this interval. With respect to the previous interval of time, due to the human impact on the area, settlement, cultural, pasture and mining indicators are added to the analysis.

Pollen indicators of human presence are all highly positively correlated and present a highly negative correlation with climax trees, as expected. Coprophilous fungi (*Sporormiella*, *Sordaria*, *Podospora* and *Cercophora*) are significantly correlated with pasture indicators (0.43, $p<0.05$), while micro-charcoal particles are correlated only with cultural indicators (0.57, $p<0.01$), possibly implying human-driven fires aimed at clearing the area for farming activities. The negative correlation of Pb EF with ash (-0.49, $p<0.05$) and lithogenic elements (-0.71, $p<0.01$) suggests a different origin for lead, mainly deriving from mining activities, while atmospheric dust probably has a more natural origin, unrelated to human activities.

17.3.1 Iron Age and Roman Times

Around 2400 cal BP, during the Iron Age, clear evidence of stable human settlements in the area is still missing. However, such settlements are possibly suggested by higher micro-charcoal influx values, a general slight increase in Poaceae and human-related taxa (*Artemisia*, Cannabaceae, *Urtica*, Chenopodiaceae, *Plantago lanceolata*-type) and the occurrence of *Juniperus*-type, known to be related to human activity (Behre, 1981) (CT2, Fig. 15.1 and 15.2). Evidence for human activity is first indicated in the pollen record, but the PCA described in Figure 17.4 suggests a very low human impact. The reduction in the *Picea* forest between ca. 2600 to 2000 cal

Table 17.2: Pearson correlation coefficients between physical, chemical and biological proxies for the interval 2500 cal BP – AD 1831. * = significant correlation with $p<0.05$, ** = highly significant correlation with $p<0.01$. Charcoal influx = sum of the three size-classes influxes.

	Ash	PC2 chem	Charc. influx	Climax trees	Sett. ind.	Cult. ind.	Past. ind.	Copr. fungi	Pb EF
Ash	1	0.63**	0.00	-0.47*	0.38	0.13	-0.01	-0.22	-0.49*
PC2 chem	**0.63****	1	0.28	-0.39	0.27	0.10	-0.13	-0.09	-0.71**
Charcoal influx	0.00	0.28	1	-0.43*	-0.07	0.57**	0.17	0.04	-0.13
Climax trees	**-0.47***	-0.39	**-0.43***	1	-0.57**	-0.68**	-0.49*	-0.27	0.07
Settlement indicators	0.38	0.27	-0.07	**-0.57****	1	0.51*	0.59**	0.20	-0.13
Cultural indicators	0.13	0.10	**0.57****	**-0.68****	**0.51***	1	0.89**	0.32	0.11
Pasture indicators	-0.01	-0.13	0.17	**-0.49***	**0.59****	**0.89****	1	0.43*	0.21
Coprophilous fungi	-0.22	-0.09	0.04	-0.27	0.20	0.32	**0.43***	1	0.07
Pb EF	**-0.49***	**-0.71****	-0.13	0.07	-0.13	0.11	0.21	0.07	1

BP, accompanied by an expansion of *Alnus* and *Botryococcus*, may therefore be interpreted more likely to be climate driven, even if human disturbance cannot be entirely excluded.

This climatic spell is coeval with the Göschener I oscillation (Fig. 17.5), firstly evidenced in the pollen analysis by Zoller et al. (1966) in the Swiss Alps. This regressive phase is recorded in many regions of the Alps by pollen analysis (CE-8, Haas et al., 1998), by the advance of several glaciers (Holzhauser et al., 2005; Ivy-Ochs et al., 2009) as well as by fluctuations in the lake levels (Magny, 2013). A colder phase is also suggested also in other sites of the Northern Hemisphere, e.g., in the Netherlands around 2650 cal BP (van Geel et al., 1996) and in Greenland (O'Brien et al., 1995). The transition between Subboreal to Subatlantic is conventionally placed in this period of time, ca. 2500 cal BP, characterized by a cooling and increase of humidity in Northern Europe (Wanner et al., 2008). This change is registered by the vegetation also near to the Coltrondo site, for instance in the studies by Kral (1986b) at Lago di Sant'Anna, by Kral (1991) at the Rasner Möser mire and by Oeggl and Wahlmüller (1994) at the Hirschbichl site (see Table 4.1).

From ca. 2000 cal BP human presence becomes more evident, as testified by the onset of the cereals curve (Cerealia, followed by *Secale*), accompanied by the first occurrence of *Juglans*, followed by *Castanea*, both marking the beginning of the Roman period (Zoller, 1960). An expansion of *Larix* is also observed, possibly related to the creation of *Larix* meadows, a form of grazed forests common in the Central and Southern Alps (Gobet et al., 2003). Nevertheless, human pressure seems to be still quite low around the Coltrondo peat bog, according to PCA results (Fig. 17.4; see also Fig. 14.13).

Human impact is registered in the geochemical data which indicate a low signal of human activities, with the first decrease in the $^{206}Pb/^{207}Pb$ ratio towards more radiogenic values, and a slight increase of the lead enrichment factor, a possible signal of first mining activities (Fig. 17.4). During Roman times, lead mines were exploited all around Europe: this is testified by many palaeoenvironmental studies carried out mainly on lakes and peatlands, in Spain (Martínez Cortizas et al., 1997, 2002; Monna et al., 2004b; Kylander et al., 2005; Martínez Cortizas et al., 2013), in the British Isles (Le Roux et al., 2004; Mighall et al., 2009; Küttner et al., 2014; Mighall et al., 2014), in Switzerland (Shotyk, 1996; Shotyk et al., 1998), in France (Monna et al., 2004a) and in Sweden (Brännvall et al., 1997; Brännvall et al., 1999; Klaminder et al., 2003) (this list is not meant to be exhaustive).

In the Comelico area no archeological findings prove human presence and mines exploitation during the Roman period. Nevertheless, as reported by

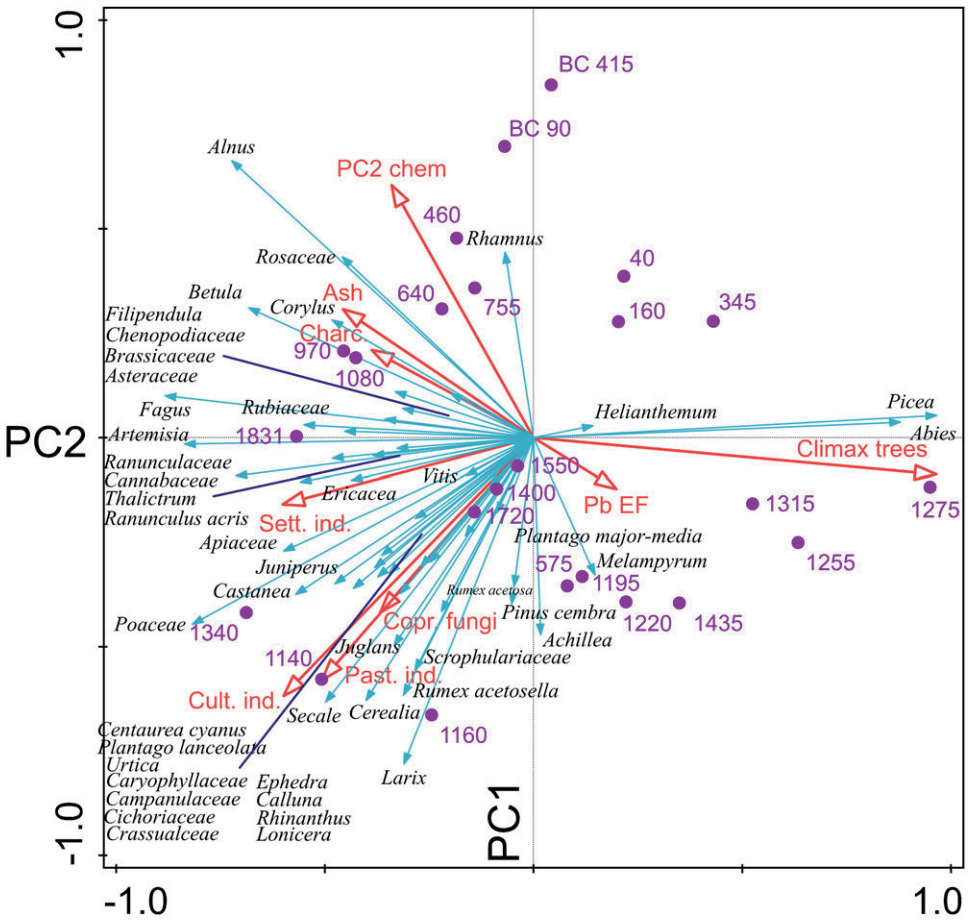

Figure 17.4: PCA of pollen taxa for the interval 2500 cal BP – AD 1831. The first axis PC1 informs us about the openness of the vegetation, while the second axis PC2 is more related to the human impact. Red arrows are supplementary variables that facilitate the interpretation of the graph. Samples are shown in ages BC/AD. Where not indicated the age is AD.

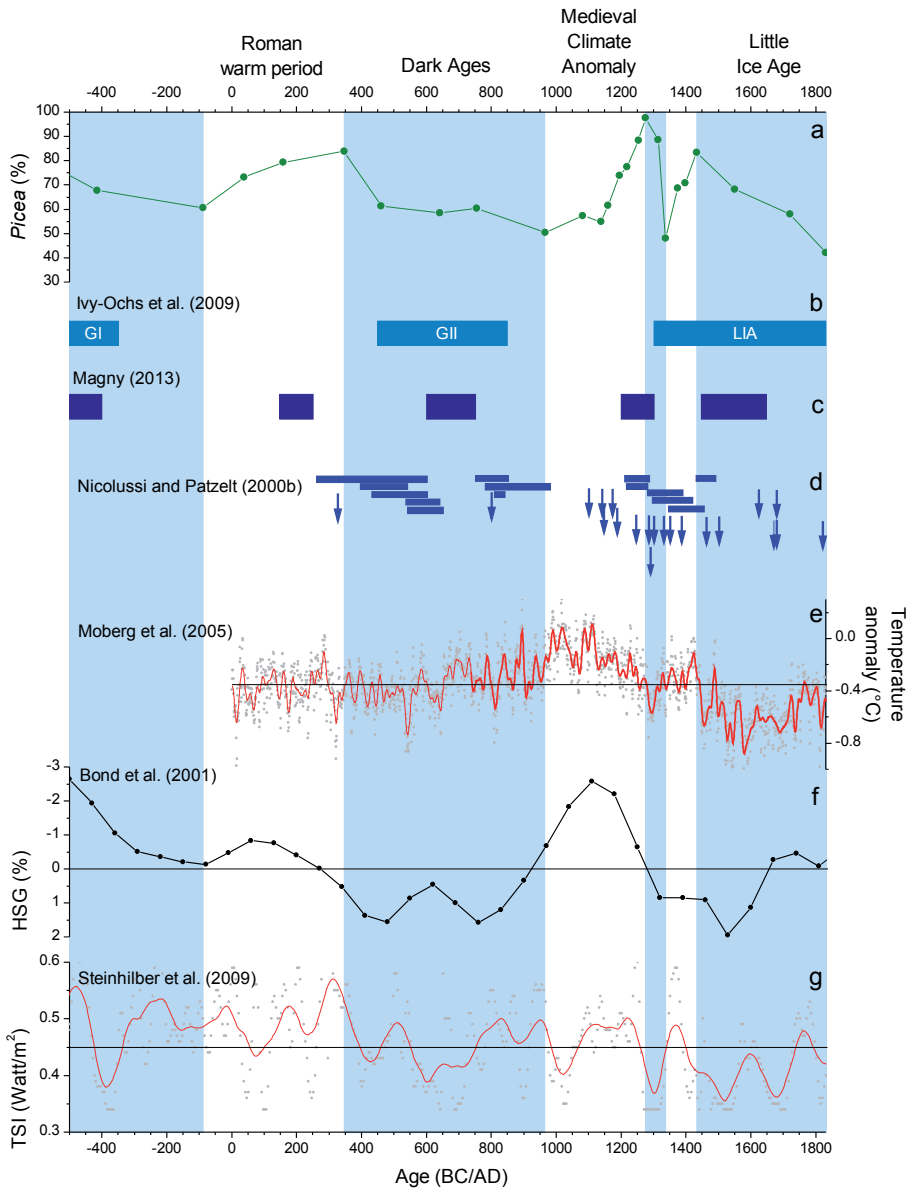

Figure 17.5: (a) The trend of *Picea*, chosen as representative of the climax community, is compared with climatic proxies: (b) main Alpine glacier advances during Göschener I and II (GI and GII) and Little Ice Age (LIA) cold oscillations (Ivy-Ochs et al., 2009); (c) lake-level high stands in Western-Central Europe (Magny, 2013), (d) advance of glaciers in the Eastern Alps (Pasterze and Gepatschferner glaciers, Nicolussi and Patzelt, 2000b), (e) temperature anomalies for the Northern Hemisphere (Moberg et al., 2005), (f) ice-rafted debris (hematite stained grains, %) (Bond et al., 2001) and (g) the total solar irradiance in Watt/m^2 (Steinhilber et al., 2009), climate forcing triggering climatic changes. Light blue rectangles indicate possible colder phases registered in the pollen diagram.

historical studies (Cucagna, 1961; De Lorenzo, 1999; Vergani, 2003), the presence of mining activities in the area during the Roman Empire is more than plausible. The main Pb-Zn deposits known to be exploited during the Middle Ages in the area are the Salafossa mine near Santo Stefano di Cadore, located 16 km from the Coltrondo bog, the *Argentiera* near Auronzo, 12 km, and the *Argentiera* in Valle Inferna, 36 km. These deposits, as well as other smaller ones (Cucagna, 1961), were likely exploited also in ancient times, and the atmospheric contamination due to mining and smelting may have been recorded in the peat bog.

Between BC 90 and AD 345, the pollen diagram registers an increase of the climax community vegetation, with a regeneration of the spruce forest, possibly implying an improvement of the climate (Fig. 17.5). The Roman period, which lasted between ca. BC 15 to AD 400 (the dating varies regionally), is indeed characterized by high total solar irradiance (TSI, Steinhilber et al., 2009) and generally by warmer climatic conditions in Europe and in the Northern Hemisphere, as testified by a low ice drift in the North Atlantic (low percentage of ice-rafted debris, Bond et al., 2001) and by the absence of glacial advances in the Alpine region (Nicolussi and Patzelt, 2000b). Geochemical proxies studied in Austrian Alpine lakes (Schmidt et al., 2007) also support the idea of a warmer phase during this period of time.

17.3.2 Middle Ages and Modern Times

During the Middle Ages, the spruce forest mixed with beech and fir still dominated the high montane belt, with a considerable presence of *Fagus* between ca. AD 350 (the end of the Roman Times) and AD 900, accompanied by a severe reduction in the *Picea* population. The vegetation was more open during that time, as testified by a significant presence of grasses (Poaceae) and other herbaceous taxa (Apiaceae, Asteraceae, Campanulaceae, Cichorioaceae, Ranunculaceae, Rosaceae, Rubiaceae and Scrophulariaceae) (CT3 Fig. 15.1 and 15.2).

Higher human pressure on the valley and possibly near the peat bog is also evident (Fig. 17.6): there is the regular occurrence of *Secale* and other cereals (Cerealia), the expansion of *Castanea* and *Juglans*, which are cultivated for their edibles fruits. *Olea europea* and *Vitis* also occur, constituting an extra-regional pollen component. The fertile soils in the valley were probably dedicated to cultivation, whereas the higher altitudes surrounding the mire were used as pasture, as also suggested by the increase of *Larix* (*Larix* meadows), herbaceous taxa growing in meadows (*Artemisia*, Cannabaceae, *Urtica*, Chenopodiaceae, *Plantago lanceolata*-type) and the presence of coprophilous fungi (*Sporormiella*; van Geel et al., 2003). The sporadic occurrence of *Cen-*

taurea cyanus might indicate the attempt to cultivate cereals (*Secale*) also in the surrounding area of the bog (Kofler and Oeggl, 2010). The increase in bryophyte and pterydophyte spores (*Dryopteris*, *Pteridium*, *Selaginella selaginoides* and *Botrychium*) also suggest an anthropogenic disturbance.

In addition to pasture and agriculture, important for the subsistence of the population of these severe mountain environments, as evidenced by the presence of written rules for the proper management of these activities (*laudi*; see Section 4.4.1), an important resource for the Cadore area were the ore-deposits. Such deposits mainly consisted of iron, copper, lead and zinc. A first sign of mining exploitation is possibly registered by the increase in the lead enrichment factor and by the decrease of $^{206}Pb/^{207}Pb$ ratio in the bog during the Roman Times, as already mentioned. The subsequent decrease of the lead enrichment factor may suggest a period of inactivity concomitant with the invasions of Nordic populations. This trend is observable in many other peat bogs around Europe (e.g., Renberg et al., 1994; Martínez Cortizas et al., 1997; Shotyk et al., 1998; Brännvall et al., 1999).

From ca. AD 700, a new slight increase in the enrichment factor and a drop in the $^{206}Pb/^{207}Pb$ ratio suggest local mining exploitation (characteristic values of Belluno Province ores; Ros, 2008) well in accordance with the increasing human presence in the area, as inferred from the pollen data (Fig. 17.6). Between AD 900 and AD 1200, population increase and economic growth characterize Italy and Europe (Brännvall et al., 1999). This is reflected also in the Coltrondo peat bog (see Fig. 17.4), which registers an enhanced human impact, with the flourishing of agriculture, pasture and mining activities. Between the 11th and 12th centuries, according to Leidlmair et al. (2002), the Comelico area was inhabited at high altitudes, up to 1400 m a.s.l. The increase in lead, silver and copper enrichment factors (see Section 14.3, *Phase 3*) and the increase of the $^{206}Pb/^{207}Pb$ ratio towards the characteristic values of the Carnic Alps ores (Giunti, 2011) is ascribable to the prosperous metallurgic activities that expanded during this period of time in the Cadore area, as stated by De Lorenzo (1999) and Vergani (2003), and all around Europe (e.g., Brännvall et al., 1999; Breitenlechner et al., 2010; Mighall et al., 2014). An important example reported by Brännvall et al. (1999) is the mining site of the Harz region in Germany, a major producer of silver at the time.

The decreasing trend registered in the spruce forest during this whole period is mainly attributed to anthropogenic disturbance, nevertheless it may be partly driven by unfavourable climatic conditions that are registered also by other climatic proxies (Fig. 17.5). The period between AD 450 and AD 950, indeed, went through a colder and drier phase known as the Dark Ages Cold Period.

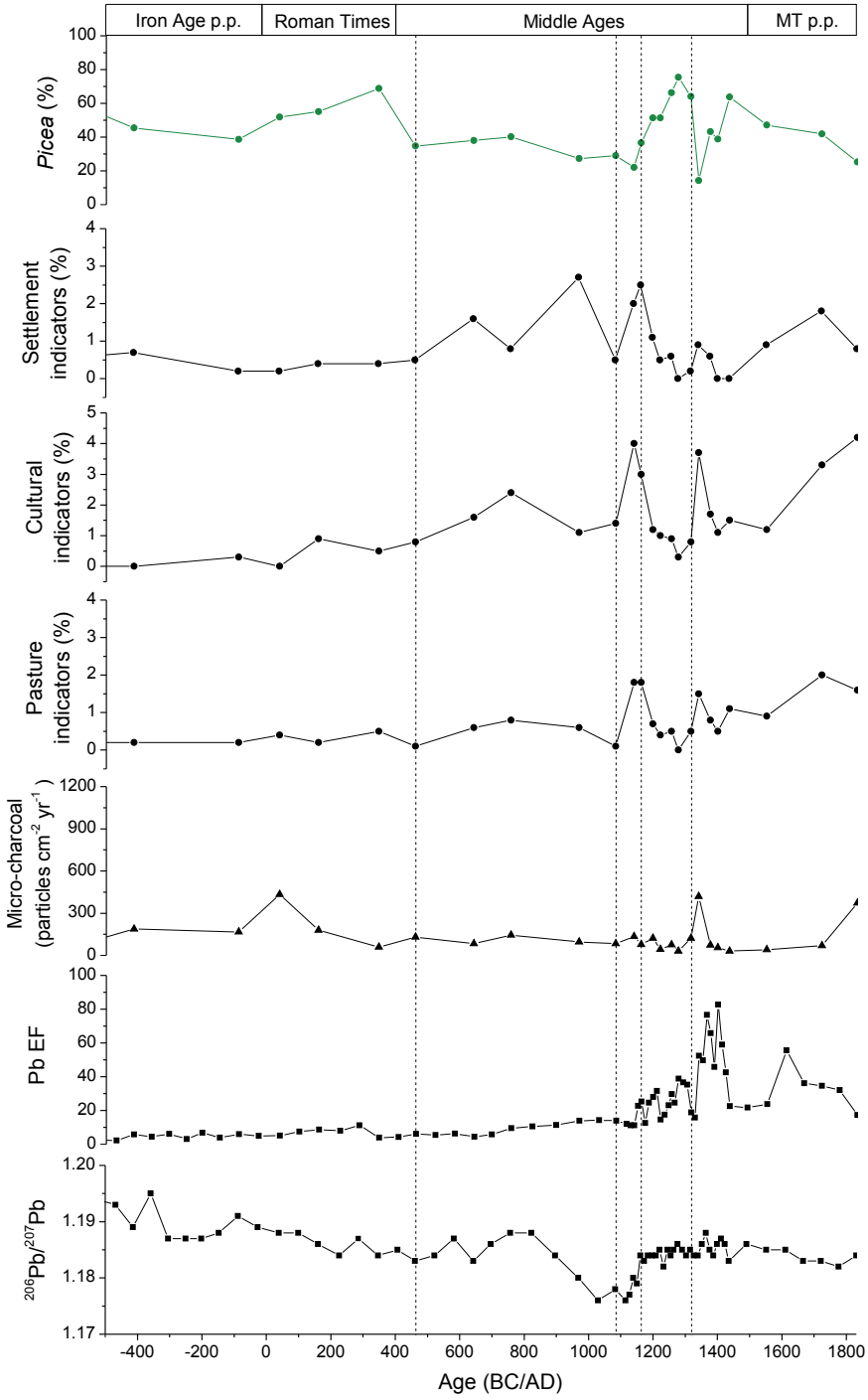

Figure 17.6: Biological and chemical data are compared for a more comprehensive interpretation. Dashed lines subdivide different phases of anthropogenic disturbance, according to the PCA of Fig. 17.4. Archeological period are shown.

From ca. AD 900 until about the end of the 13th century, a regeneration of the spruce forest is evident, mixed with *Abies* trees, possibly reflecting an amelioration of the climate. This is also supported by a higher sedimentation rate that suggests a higher productivity, probably due to favourable climatic conditions. This warmer phase is known in European literature as the Medieval Climate Anomaly, a period characterized by a La Nina-like situation in the Pacific Ocean and by positive modes of the North Atlantic Oscillation (Trouet et al., 2009). This phase lasted between ca. AD 900 and 1300 (Holzhauser et al., 2005; Kress et al., 2014). When the *Picea* forest thrives and reaches its maximum percentages (ca. AD 1270), human indicators almost disappear from the pollen record, suggesting a densely forested area.

Between AD 1275 and 1340, the peat bog registers a sharp decrease in the percentage of the climax community vegetation, from ca. 98% down to 48%. This is coeval with a micro-charcoal peak in the influx values and an increase in grasses and other herbaceous and human-related taxa (Fig. 17.6). The severe decrease of *Picea* is likely human-driven and associated with the clearance of cultivable areas as well as with timber commercialization, which from the 14th century started to have a role in mountain economy (Leidlmair et al., 2002). One cannot however completely exclude the contribution of colder and wetter conditions, recorded by other proxies in the Alps (e.g., the advances of glaciers; Nicolussi and Patzelt, 2000b) and in the Northern Hemisphere (Bond et al., 2001; Moberg et al., 2005) for this period of time (Fig. 17.5).

A recovery of the *Picea* population is registered 1340 to AD 1450 (CT4, Fig. 15.1 and 15.2). During this time a spruce forest, mixed with *Fagus* and *Abies*, thrives in the montane zone. *Larix* meadows develop and human activity is recorded in the pollen diagram by indicators of settlement and of cultural and pasture activities, and by the presence of bryophyte and pterydophyte spores (*Dryopteris*, *Pteridium*, *Selaginella selaginoides* and *Botrychium*. Moreover, enrichment factors suggest a high human pressure, reaching the highest values of the Middles Ages, probably in relation to the prosperous mining activities in the Cadore area – the three *Argentiera* of Valle Inferna, Auronzo and Salafossa are active, even if only intermittently, in these centuries (Vergani, 2003) – and all over Europe (Brännvall et al., 1999; Vergani, 2003). The subsequent decrease, taking into account radiocarbon uncertainties, may be registering the general decrease in mining activities throughout Europe and also in the Cadore area (Vergani, 2003) that followed the discovery of America and the consequent exploitation and importation of American metal resources. There is a new peak in the 17th century, followed by a decrease that may be ascribed to the abandonment of several mining

sites with the decline of the Republic of Venice.

The opening in the forest recorded between AD 1450 to ca. AD 1830, accompanied by the decrease of *Abies*, *Larix* and *Fagus* may be related to human activity and to the well-known economic importance of timber for the Republic of Venice between the 16th and 18th century, and also afterwards. Nevertheless, this decrease in the climax community vegetation, concomitant with a drop in the sedimentation rate, is synchronous with the well-documented and LIA, characterized by a lowering of the total solar irradiance (Steinhilber et al., 2009), a higher percentage of ice-drifted debris (Bond et al., 2001), advances of the Alpine glacier (Ivy-Ochs et al., 2009) and lower temperatures for the Northern Hemisphere (Moberg et al., 2005) (Fig. 17.5). It is not possible to disentangle between human and climate signal, both of which structured the vegetation in the area at that time. The severe reduction in the climax trees may be therefore interpreted as a combination of the two: a climatic regressive phase and the anthropogenic disturbance.

17.4 The strong human impact during the industrial time: the last 180 years

This last interval covers ca. the last 180 years, a period of time mainly characterized by technological development and the industrial revolution. This is clearly evidenced by the $^{206}Pb/^{207}Pb$ ratio (Fig. 17.7), which registers a severe drop reaching minimum values in the 1970s and 1980s. Pollen also testifies the economic boom of these last decades, registering a general abandonment of agricultural and pasture activities in mountain areas.

Table 17.3 shows the correlations between the physical, biological and chemical parameters listed at the beginning of this Chapter: ash content, PC2 axis scores of the PCA performed for chemical data, micro-charcoal influx, pollen indicators for settlement, agriculture and pasture, Pb enrichment factor. The ash content is positively correlated with the chemical PC2 (0.85, $p<0.01$) and it shows positive correlation also with micro-charcoal influx (0.57, $p<0.01$), cultural and pasture indicators (0.57, $p<0.05$) and coprophilous fungi (0.69, $p<0.01$). The possible explanation is that the more intense exploitation of the area by humans (human-driven fires, agriculture and pasture activities) is reflected in a more exposure of the soil to erosional and weathering processes. The increase of the lead enrichment factor is positively correlated with climax trees (0.59, $p<0.05$), probably registering the general abandonment of the mountain area and the regeneration of the forest, synchronous with the economic boom and with enhanced atmospheric

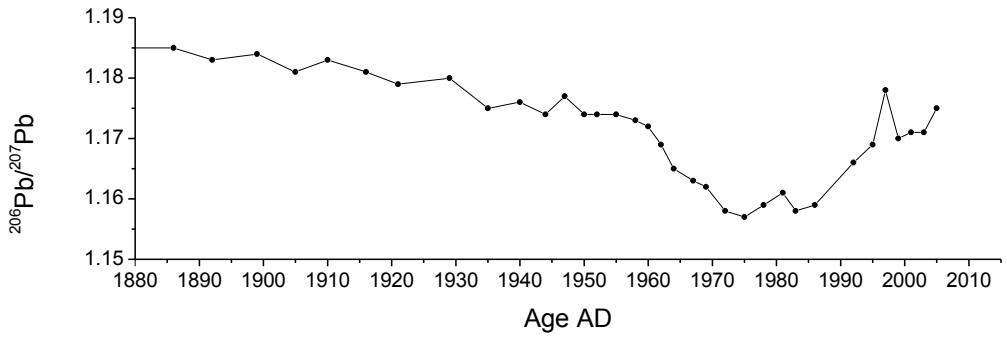

Figure 17.7: The advent of industrialization is recorded in the peat bog through the lowering of the $^{206}Pb/^{207}Pb$ ratio. The first decrease in $^{206}Pb/^{207}Pb$ values at the end of the 1880s is mainly ascribable to the increased exploitation of mining sites and metallurgic activities. The steep decrease in $^{206}Pb/^{207}Pb$ ratio registered around AD 1955 is due to the introduction of other sources of lead, such as leaded gasoline. The phasing out of leaded gasoline is overwhelmingly responsible for the recent increase in $^{206}Pb/^{207}Pb$ ratio.

lead pollution, not only on a local scale, but also on a regional one.

From ca. AD 1850 the *Picea* forest start regenerating, with the coeval severe reduction of *Fagus*. The vegetation is still open, as testified by the increase of light-demanding taxa such as Ericaceae, *Calluna vulgaris* and Poaceae (CT4, Fig. 15.1 and 15.2). In this period of time, the highest human impact on the vegetation is registered in the pollen record: higher abundance of Cannabaceae and *Urtica* indicative for settlement, higher occurrence of *Castanea*, *Juglans*, and cereals (Cerealia and *Secale*) indicative of cultivation. Pasture activity is also visible, as recorded mainly by *Plantago lanceolata*-type, *Plantago major-media*-type, *Rumex acetosella* and by coprophilous fungi (*Sporormiella*, *Sordaria*, *Podospora* and *Cercophora*; van Geel et al., 2003). Furthermore, an increment of micro-charcoal influx values is visible, documenting an enhanced fire activity probably deriving from human intervention. The PCA presented in Fig. 17.9 also provide evidence of more sizable human impact. This is in agreement with the population trend registered for the Comelico area (Fig. 17.8) and with the historical documentation of high-altitude cultivation (up to 1400 m a.s.l.) (Leidlmair et al., 2002) until the first decades of the 20th century. The increase in mineral matter registered in the bog between 1831 and 1930 (31.0 to 38.5 cm) may be related to changes in the landscape, mainly due to agriculture and pasture activities (Tolonen, 1984). The enrichment factor of lead and other elements (As, Ag, Cd, Cu) shows low values for this interval of time, probably, as already mentioned in the Section 14.4, due to the high values of titanium,

Table 17.3: Pearson correlation coefficients between physical, chemical and biological proxies for the interval 1831 – 2005. * = significant correlation with $p<0.05$, ** = highly significant correlation with $p<0.01$. Charcoal influx = sum of the three size-classes influxes.

	Ash	PC2 chem	Charc. influx	Climax trees	Sett. ind.	Cult. ind.	Past. ind.	Copr. fungi	Pb EF
Ash	1	0.85**	0.77**	-0.35	0.50	0.57*	0.64*	0.69**	-0.18
PC2 chem	**0.85****	1	0.64*	-0.32	0.44	0.54*	0.59*	0.66*	-0.02
Charcoal influx	**0.77****	**0.64***	1	-0.32	0.55*	0.68**	0.47	0.92**	-0.16
Climax trees	-0.35	-0.32	-0.32	1	-0.89**	-0.75**	-0.70**	-0.52	0.59*
Settlement indicators	0.50	0.44	**0.55***	**-0.89****	1	0.84**	0.76**	0.72**	-0.62*
Cultural indicators	**0.57***	**0.54***	**0.68****	**-0.75****	**0.84****	1	0.77**	0.84**	-0.37
Pasture indicators	**0.64***	**0.59***	0.47	**-0.70****	**0.76****	**0.77****	1	0.57*	-0.18
Coprophilous fungi	**0.69****	**0.66***	**0.92****	-0.52	**0.72****	**0.84****	**0.57***	1	-0.27
Pb EF	-0.18	-0.02	-0.16	**0.59***	**-0.62***	-0.37	-0.18	-0.27	1

which mask any trace of human-induced metal atmospheric pollution. In the peat bog of Danta di Cadore, studied by Poto (2013), an enrichment in Pb, Ag and Cd related to the *Argentiera* of Auronzo and Salafossa mine is registered at this time. The site was exploited between the end of 19th and the beginning of 20th century (De Lorenzo, 1999).

Figure 17.8: Comelico Superiore population. More detailed information is available from the second half of the XIX century.

Between AD 1935 and AD 2005 (CT5), the vegetation of the peat bog registered a significant thickening of the spruce forest, mixed mainly with *Larix* and some *Pinus cembra*, with a concomitant general decrease of light-demanding and human-related herbaceous taxa. The peat bog was characterized by the thriving of *Calluna vulgaris* and by a very high sedimentation rate. This latter feature is likely related to the ongoing climatic warming and therefore to more suitable climatic conditions for the growth of *Sphagnum* mosses.

The general trend of the vegetation mainly reflects the gradual abandonment of the area by humans (Fig. 17.8). As stated by Leidlmair et al. (2002), after the second World War there was a short demographic expansion, stopped with the economic upturn which caused the abandonment of agriculture and pasture activities (Table 17.4) and the migration towards bigger centres to work in the industry sector.

The advent of industrialization is recorded in the peat bog through higher enrichment factors of all the elements considered between AD 1930 and AD 1986 (see PCA in Fig. 17.9), and the lowering of the $^{206}Pb/^{207}Pb$ ratio (Fig. 17.7). The first decrease in $^{206}Pb/^{207}Pb$ values is mainly ascribable to

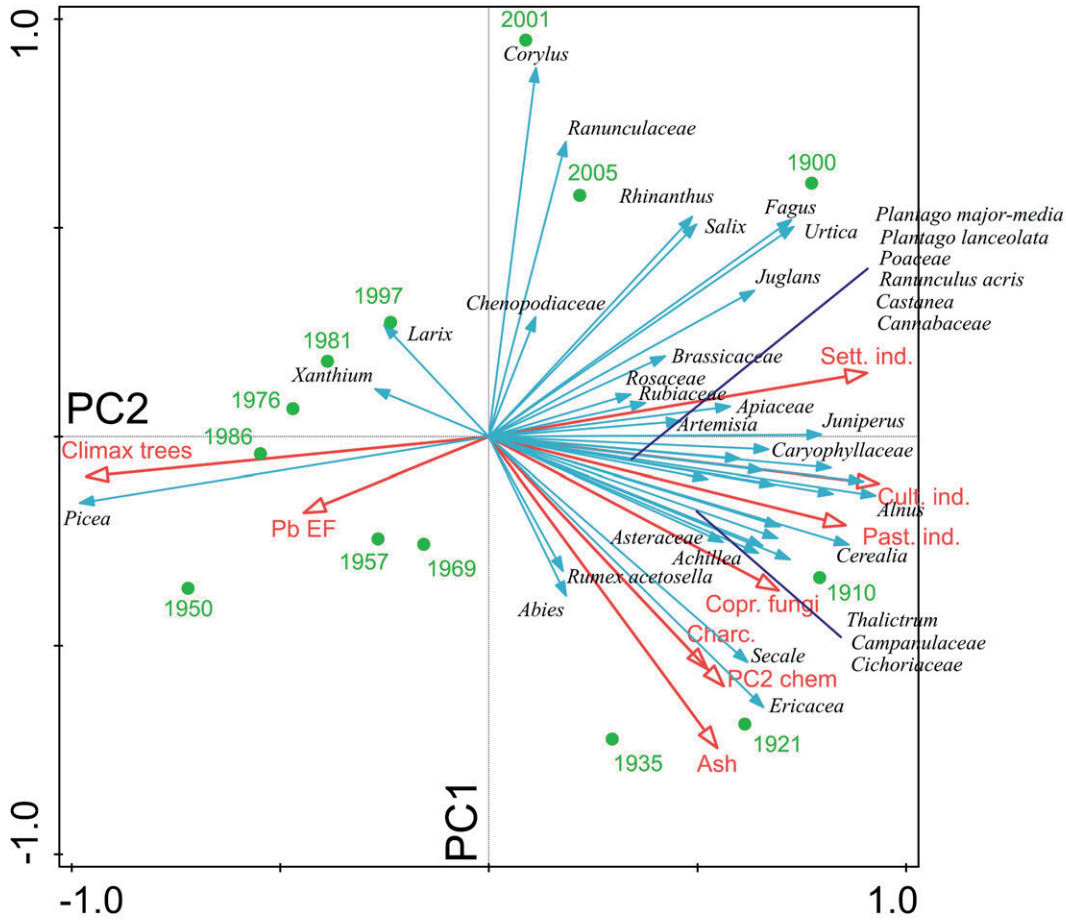

Figure 17.9: PCA of pollen taxa for the interval AD 1831 – 2005. The first axis PC1 informs us about the openness of the vegetation, while the second axis PC2 is more related to the human impact. Red arrows are supplementary variables that facilitate the interpretation of the graph.

Table 17.4: Comelico Superiore statistical data about agricultural and pasture activities and the number of houses present vs. inhabited ones in the second half of the XX century (Leidlmair et al., 2002).

	1951	**1961**	**1970**	**1988**	**1999**
Agricultural companies	1058	748	688	20	20
Agricultural area (ha)		7642.05	3135.26	477.06	253.61
Cattle companies			189	20	20
Houses/Inhabited houses	1007/157		1096/214	1094/479	1082/869

the increased exploitation of mining sites and metallurgic activities, and the beginning of coal combustion (Komárek et al., 2008), which characterized the onset of industrialization at the beginning of the 20th century in Europe.

Afterwards, the steep decrease in $^{206}Pb/^{207}Pb$ ratio registered around AD 1955 is due to the introduction of other sources of lead. Leaded gasoline was introduced in Europe around AD 1945 and in Italy in AD 1955 (Bono et al., 1995; Shotyk et al., 1998; Bindler et al., 2004; Farmer et al., 2005; Kylander et al., 2005), impacting severely on the atmosphere and the environment. The banning of leaded gasoline is overwhelmingly responsible for the recent increase in $^{206}Pb/^{207}Pb$ ratio to less radiogenic values (Farmer et al., 2005). In Italy the phasing out of leaded gasoline started in the 1970s (D.E. 70/220/CE), with consecutive reductions of lead concentration in gasoline from 1974 onward. The most important decreases date back to the 1980s (Bono et al., 1995). The leaded gasoline was completely banned in Italy only in 2002, after receiving the European D.E. 98/70/CE.

Regarding mining activities, the Salafossa mining site was active during the second half of the 20th century for the extraction zinc and, to a lesser extent, lead. Zinc mineral processing accounted for 1/3 of the Italian production. The mine was definitively closed in AD 1985 (De Lorenzo, 1999). The general abandonment of mining activities in the Cadore area in the last decades also contributed to the recent increase of $^{206}Pb/^{207}Pb$ ratio.

Nowadays, the Comelico area is mainly devoted to industrial activities, mainly in the optical sector, and to mountain tourism. Not far from the peat bog, a mountain hut is open during summer to accommodate tourists who are trekking in the Dolomitic area. The presence in the last peat samples of Cannabaceae, *Plantago lanceolata*-type, *Urtica*, *Artemisia*, Chenopodiaceae is in agreement with the modern vegetation of the area, related to human presence, mainly for tourism.

Part V

Conclusions and future perspectives

Chapter 18

Conclusions

The Coltrondo core encompasses the Middle and Late Holocene, since ca. 7900 cal BP. The analysis of physical, chemical and biological parameters allows us to unravel the environmental and climatic history of the Comelico area, as well as the anthropogenic impact since the first human settlements in the area.

The objectives and questions raised at the beginning of the dissertation (see Section 3) were investigated and discussed throughout the thesis.

The first fundamental step was to ascertain the validity of the peat bog as an archive of palaeoclimatic and palaeoenvironmental information. An ideal climatic archive is fed solely via atmospheric deposition, with no influence from groundwater and/or superficial runoff. The multi-proxy approach, with the analysis of botanical, physical and chemical parameters, permitted to assess the ombrotrophy of the peat bog along the profile, with the influx of groundwater and the upward migration of ions from the underlying bedrock only below 180 cm of depth.

The identification of the ideal environmental archive must be associated to an adequate chronology in order to contextualise the interpretation of the data in a accurate chronological framework. The age-depth model obtained combining ^{210}Pb and ^{14}C dating techniques allowed us to create a reliable and robust chronology for the Coltrondo peat bog core that covers ca. 7900 cal BP. All the elements supplied in the last ca. 6300 cal BP of peat accumulation derive exclusively from atmospheric inputs and may be interpreted to infer the climatic and human history of the area.

The reconstruction of the main climatic oscillations of the Holocene was one of the main objectives of this thesis. The study of the Coltrondo peat bog allowed us to reconstruct the main climatic phases of the Middle and Late Holocene, registering both regional and more global climatic events. Given

the scarcity and fragmentation of records investigated in the Eastern sector of the Italian Alps, this study adds important information on the past climate variability of the area. Several cold events were registered by the peatland: the first took place at ca. 7200 cal BP, triggering the beginning of the peat bog; a second one at ca. 6200 cal BP; and another between ca. 5400 cal BP and 4000 cal BP, marking the transition between the Holocene Thermal Optimum and the Neoglaciation. A new cold phase was registered between 3600 and 3200 cal BP, related to a global climatic shift, with cooler and moister conditions in the Northern Hemisphere and cooler and drier conditions in the Southern Hemisphere. From ca. 2500 cal BP, human activities started impacting on the vegetation, making it difficult to disentangle between climatic and human signals, both of which structured the vegetation. Human activities modified the landscape and vegetation of the area due to forest clearing, the introduction of new taxa related to agriculture and pasture, the use of wood in mines and metallurgic activities (for tunnel construction and metal processing), as well as the commercialization of timber, leading to the selective exploitation of different trees (mainly *Picea* and *Fagus*). All these activities were probably regulated since ancient times in the Comelico area, as documented by written rules, the *laudi*, which highlight the importance of pasture and mountain resources and their proper management for the subsistence of the inhabitants of these harsh mountain environments. Known climatic phases, such as the Roman Warm Period (BC 90 – AD 345), the Dark Ages cold period (AD 450 – 950), the Medieval Climate Anomaly (AD 900 – AD 1275), the Little Ice Age (AD 1450 – 1830) and the current global warming, are registered by variations in the percentages of the climax trees and in the accumulation rate. However, modifications in the vegetation do not allow to clearly divide the amplitude of Holocene climate natural variability from human-related changes.

Another important objective of this thesis was to improve the rather scarce knowledge about human history in the Comelico area. Indeed, there are no historical data about human settlements in the area. Historians speculate that the area started being inhabited around the 6th century, during the Lombard domination. Human activities, mainly agriculture, pasture and mining, are not documented until the 11th – 12th century. The documentation for the Middle Ages remains fragmentary until the Republic of Venice in AD 1420. In this light, this study adds valuable information and new insights into the human presence in the area. The vegetation started registering the first evidence of human presence already during the Bronze Age (ca. 4000 cal BP). However, the very low percentages of human impact indicators and micro-charcoal particles lead to interpret this first human signal as a regional

rather than a local phenomenon. Around 2400 cal BP, during the Iron Age, the slight increase of human-related taxa is possibly related to a first appearance of humans in the Comelico area. The Roman period is marked by the onset of cereals and the first occurrence of *Juglans* and *Castanea* (ca. 2000 cal BP). Human disturbance started to become more evident, although it remained low. In this period of time, the peat bog started registering also atmospheric metal deposition (mainly lead) and a lowering of the $^{206}Pb/^{207}Pb$ ratio towards more radiogenic values that are possibly signals of the first mining activities in the area. Higher human impacts started to be registered from the 6th century, in accordance with the hypothesis of a definitive settlement of humans in the Comelico area during this period of time. During the Middle Ages, agriculture and pasture were important activities for the local population, as testified by the increase in culture and pasture pollen indicators. Mining activities also prospered at that time in the Cadore area, as well as in the rest of Europe, as suggested by the enhanced atmospheric metal depositions of lead, silver and copper and to $^{206}Pb/^{207}Pb$ ratio values approaching those registered for the Carnic Alps ores. In Modern Times, the highest impact on the vegetation is registered in the second half of the 19th century, in accordance with the population trend of that time. The onset of industrialization in the 20th century is recorded in the peat bog through higher enrichment factors of all the elements considered and through the lowering of the $^{206}Pb/^{207}Pb$ ratio. This also mark the introduction of leaded gasoline in the 1950s. In the last decades, the decrease of human disturbance registered by both vegetation and atmospheric metal deposition marks the gradual and general abandonment of the mountain areas that followed the economic upturn after the Second World War, the abandonment of mining activities in the area and, on a broader scale, technological improvements and the greater attention paid to industrial air pollution with the establishment of emissions limits and the banning of leaded gasoline.

The study of the Coltrondo peat bog, supported by a robust chronological framework, allowed us to detect the main climatic oscillations before human settlements in the area. Afterwards, human pressure on the environment makes it difficult to clearly divide the amplitude of Holocene climate natural variability from human-related changes. This work may be considered as a first fundamental step for the study of this area, adding valuable information about the climate and human history of Eastern Italian Alps, a strategic sector that needs further investigations.

Chapter 19

Future perspectives

The study of the Coltrondo peat bog revealed its high quality as a palaeoclimatic and palaeoenvironmental archive. The investigation of physical, chemical and biological proxies allowed us to unravel the climatic and human history of the area, adding valuable information about the Eastern section of the Italian Alps. This dissertation, however, should be considered as a basis for a future, in-depth investigation of climate variability in the Eastern Italian Alps during the Holocene. For a deep understanding of the climatic history recorded in the bog further investigations on the organic phase of peat will be performed, to gain more information about the main internal processes and mechanisms that may affect signals registered in the archive. Moreover, taking into consideration that physical, biological and chemical proxies studied are indirect indicators of climate variations, the next goal is therefore to find a direct palaeotemperature proxy in order to achieve a more accurate temperature reconstruction. We will focus our efforts on the study of two valuable proxies:

- the oxygen isotope composition of *Sphagnum* mosses cellulose. Cellulose is isotopically stable, even under conditions of partial decomposition and it is one of the most reliable and sensitive proxy for palaeotemperature reconstructions (Bilali and Patterson, 2012). There is a demonstrated and direct correlation between isotopic oxygen composition of cellulose and mean annual temperature (Kühl and Moschen, 2012; Bilali et al., 2013; Finsinger et al., 2013).

- the oxygen and hydrogen isotopic composition of *n*-alkanes in leaf waxes. They have been shown to track the source of water used during plant growth, and they are not influenced by diagenetic processes (Nichols et al., 2006). They are a valuable proxy to reconstruct changes

in the seasonality of precipitation and bog surface wetness (Nichols et al., 2009).

Such investigation is challenging, because the interpretation of the isotopic composition in peat in terms of environmental changes is complicated by several factors ranging from species-specific differences to the fractionation due to biosynthetic processes, the enrichment of isotope values due to evapotranspiration, and the signal preservation in decomposed peat (Tillman et al., 2010). Therefore, stable isotope records from peat sequences will be used and compared in a wider framework with other proxy data and other natural archives. In order to create a calibration dataset, data about temperatures recorded by meteorological stations will be recovered and precipitation will be collected and analysed. These data will be merged with the isotopic fingerprint of recent *Sphagnum* mosses collected in the bog and their interpretation will give us the chance to create a unique complete temperature series for the Cadore area.

Bibliography

Aaby, B. (1976). "Cyclic climatic variations in climate over the past 5,500 yr reflected in raised bogs". *Nature* 263, pp. 281–284.

Abraham, J. P., M. Baringer, N. L. Bindoff, T. Boyer, L. J. Cheng, J. A. Church, J. L. Conroy, C. M. Domingues, J. T. Fasullo, J. Gilson, G. Goni, S. A. Good, J. M. Gorman, V. Gouretski, M. Ishii, G. C. Johnson, S. Kizu, J. M. Lyman, A. M. Macdonald, W. J. Minkowycz, S. E. Moffitt, M. D. Palmer, A. R. Piola, F. Reseghetti, K. Schuckmann, K. E. Trenberth, I. Velicogna, and J. K. Willis (2013). "A review of global ocean temperature observations: Implications for ocean heat content estimates and climate change". *Reviews of Geophysics* 51(3), pp. 450–483.

Allan, M., G. Le Roux, N. Piotrowska, J. Beghin, E. Javaux, M. Court-Picon, N. Mattielli, S. Verheyden, and N. Fagel (2013a). "Mid- and late Holocene dust deposition in western Europe: the Misten peat bog (Hautes Fagnes – Belgium)". *Climate of the Past* 9(5), pp. 2285–2298.

Allan, M., G. L. Roux, F. D. Vleeschouwer, R. Bindler, M. Blaauw, N. Piotrowska, J. Sikorski, and N. Fagel (2013b). "High-resolution reconstruction of atmospheric deposition of trace metals and metalloids since AD 1400 recorded by ombrotrophic peat cores in Hautes-Fagnes, Belgium". *Environmental Pollution* 178, pp. 381–394.

Appleby, P. and F. Oldfield (1978). "The calculation of lead-210 dates assuming a constant rate of supply of unsupported 210Pb to the sediment". *CATENA* 5(1), pp. 1 –8.

Appleby, P., P. Nolan, D. Gifford, M. Godfrey, F. Oldfield, N. Anderson, and R. Battarbee (1986). "210Pb dating by low background gamma counting". English. *Hydrobiologia* 143(1), pp. 21–27.

Appleby, P., W. Shotyk, and A. Fankhauser (1997). "Lead-210 Age Dating of Three Peat Cores in the Jura Mountains, Switzerland". *Water, Air, and Soil Pollution* 100(3-4), pp. 223–231.

Arnold, J. R. and W. F. Libby (1949). "Age determinations by Radiocarbon Content: Checks with Samples of Known Age". *Science* 110 (2869), pp. 678–680.

Aubert, D., G. L. Roux, M. Krachler, A. Cheburkin, B. Kober, W. Shotyk, and P. Stille (2006). "Origin and fluxes of atmospheric REE entering an ombrotrophic peat bog in Black Forest (SW Germany): Evidence from snow, lichens and mosses". *Geochimica et Cosmochimica Acta* 70(11), pp. 2815–2826.

Auer, I., R. Böhm, A. Jurkovic, W. Lipa, A. Orlik, R. Potzmann, W. Schöner, M. Ungersböck, C. Matulla, K. Briffa, P. Jones, D. Efthymiadis, M. Brunetti, T. Nanni, M. Maugeri, L. Mercalli, O. Mestre, J.-M. Moisselin, M. Begert, G. Müller-Westermeier, V. Kveton, O. Bochnicek, P. Stastny, M. Lapin, S. Szalai, T. Szentimrey, T. Cegnar, M. Dolinar, M. Gajic-Capka, K. Zaninovic, Z. Majstorovic, and E. Nieplova (2007). "HISTALP—historical instrumental climatological surface time series of the Greater Alpine Region". *International Journal of Climatology* 27(1), pp. 17–46.

Barber, K. E. (1981). *Peat stratigraphy and climate change: a palaeoecological test of the theory of cyclic peat bog regeneration (Cumbria England).*

Barber, K., L. Dumayne-Peaty, P. Hughes, D. Mauquoy, and R. Scaife (1998). "Replicability and variability of the recent macrofossil and proxy-climate record from raised bogs: field stratigraphy and macrofossil data from Bolton Fell Moss and Walton Moss, Cumbria, England". *Journal of Quaternary Science* 13(6), pp. 515–528.

Baroni, C. and G. Orombelli (1996). "The Alpine "Iceman" and Holocene Climatic Change". *Quaternary Research* 46(1), pp. 78–83.

Baroni, C., G. Zanchetta, A. E. Fallick, and A. Longinelli (2006). "Mollusca stable isotope record of a core from Lake Frassino, northern Italy: hydrological and climatic changes during the last 14 ka". *The Holocene* 16(6), pp. 827–837.

Behre, K. E. (1981). "The interpretation of anthropogenic indicators in pollen diagrams". *Pollen et Spores* 23(2), pp. 225–245.

— ed. (1986). *Anthropogenic indicators in pollen diagrams*. Rotterdam: AA Balkema, p. 232.

Belokopytov, I. E. and V. V. Beresnevich (1955). "Giktorf's peat borers". *Torfânaâ promyslennost'* 8, pp. 9–10.

Berglund, B. E. (1987). *Handbook of Holocene palaeoecology and palaeohydrology*. John Wiley and Sons Inc., New York, NY.

Berglund, B. E. and M. Ralska-Jasiewiczowa (1987). "Pollen analysis and pollen diagrams". In: *Handbook of Holocene palaeoecology and palaeohydrology*. John Wiley and Sons Inc., New York, NY, pp. 455–484.

Beug, H.-J. (2004). *Leitfaden der Pollenbestimmung für Mitteleuropa und angrenzende Gebiete*. München: Pfeil.

Beyens, L. (1985). "On the Subboreal climate of the Belgian Campine as deduced from diatom and testate amoebae analysis". *Review of Palaeobotany and Palynology* 46(1), pp. 9–31.

Bilali, H. E. and R. T. Patterson (2012). "Influence of cellulose oxygen isotope variability in sub-fossil Sphagnum and plant macrofossil components on the reliability of paleoclimate records at the Mer Bleue Bog, Ottawa, Ontario, Canada". *Organic Geochemistry* 43, pp. 39–49.

Bilali, H. E., R. T. Patterson, and A. Prokoph (2013). "A Holocene paleoclimate reconstruction for eastern Canada based on δ^{18}O cellulose of *Sphagnum* mosses from Mer Bleue Bog". *The Holocene* 23(9), pp. 1260–1271.

Bindler, R., M. Klarqvist, J. Klaminder, and J. Förster (2004). "Does within-bog spatial variability of mercury and lead constrain reconstructions of absolute deposition rates from single peat records? The example of Store Mosse, Sweden". *Global Biogeochemical Cycles* 18(3).

Birks, H. J. B. and H. H. Birks (2004). *Quaternary Palaeoecology*. Blackburn Press.

Blaauw, M. (2010). "Methods and code for 'classical' age-modelling of radiocarbon sequences". *Quaternary Geochronology* 5(5), pp. 512–518.

Blaauw, M., B. Van Geel, and J. van der Plicht (2004). "Solar forcing of climatic change during the mid-Holocene: indications from raised bogs in The Netherlands". *The Holocene* 14(1), pp. 35–44.

Blytt, A. (1876). *Essay on the Immigration of the Norwegian Flora During Alternating Rainy and Dry Periods, by Axel Blytt*. A. Cammermeyer.

Boelter, D. H. (1969). "Physical properties of peats as related to degree of decomposition". *Soil Science Soc America-proc* 33(4), pp. 606–609.

Boettger, T., A. Hiller, and K. Kremenetski (2003). "Mid-Holocene warming in the northwest Kola Peninsula, Russia: northern pine-limit movement and stable isotope evidence". *The Holocene* 13(3), pp. 403–410.

Bond, G., B. Kromer, J. Beer, R. Muscheler, M. N. Evans, W. Showers, S. Hoffmann, R. Lotti-Bond, I. Hajdas, and G. Bonani (2001). "Persistent solar influence on North Atlantic climate during the Holocene". *Science* 294(5549), pp. 2130–2136.

Bono, R., C. Pignata, E. Scursatone, R. Rovere, P. Natale, and G. Gilli (1995). "Updating about reductions of air and blood lead concentrations in Turin, Italy, following reductions in the lead content of gasoline". *Environmental research* 70(1), pp. 30–34.

Booth, R. K. (2008). "Testate amoebae as proxies for mean annual water-table depth in *Sphagnum*-dominated peatlands of North America". *Journal of Quaternary Science* 23(1), pp. 43–57.

Borgatti, L., C. Ravazzi, M. Donegana, A. Corsini, M. Marchetti, and M. Soldati (2007). "A lacustrine record of early Holocene watershed events and vegetation history, Corvara in Badia, Dolomites (Italy)". *Journal of Quaternary Science* 22(2), pp. 173–189.

Bortenschlager, S. (1970). "Probleme und Ergebnisse der Untersuchung von Pollenspektren im Hochgebirge". *Mitteilungen der Ostalpen Gesellschaft für Vegetationskunde* 10, pp. 5–9.

Bradbury, J. P., W. E. Dean, and R. Y. Anderson (1993). "Holocene climatic and limnologic history of the north-central United States as recorded in the varved sediments of Elk Lake, Minnesota: a synthesis". *Geological Society of America Special Papers* 276, pp. 309–328.

Bradley, R. S. (1999). *Paleoclimatology: reconstructing climates of the Quaternary*. Vol. 68. Academic Press.

Breitenlechner, E., M. Hilber, J. Lutz, Y. Kathrein, A. Unterkircher, and K. Oeggl (2010). "The impact of mining activities on the environment reflected by pollen, charcoal and geochemical analyses". *Journal of Archaeological Science* 37(7), pp. 1458–1467.

Brigo, L., P. Dulski, P. Möller, H.-J. Schneider, and R. Wolter (1988). "Strata-bound mineralizations in the Carnic Alps/Italy". In: *Mineral deposits within the European Community*. Springer, pp. 485–498.

Brigo, L., G. Camana, F. Rodeghiero, and R. Potenza (2001). "Carbonate-hosted siliceous crust type mineralization of Carnic Alps (Italy-Austria)". *Ore Geology Reviews* 17(4), pp. 199–214.

Brown, D. H. and J. W. Bates (1990). "Bryophytes and nutrient cycling". *Botanical Journal of the Linnean Society* 104(1–3), pp. 129–147.

Brännvall, M.-L., R. Bindler, O. Emteryd, M. Nilsson, and I. Renberg (1997). "Stable isotope and concentration records of atmospheric lead pollution in peat and lake sediments in Sweden". *Water, Air, and Soil Pollution* 100(3-4), pp. 243–252.

Brännvall, M.-L., R. Bindler, I. Renberg, O. Emteryd, J. Bartnicki, and K. Billström (1999). "The Medieval Metal Industry Was the Cradle of Modern Large-Scale Atmospheric Lead Pollution in Northern Europe". *Environmental Science & Technology* 33(24), pp. 4391–4395.

Burga, C. A. and M. Egloff (2001). "Pollenanalytische Untersuchungen zur Vegetations-und Klimageschichte im Pustertal und Sarntal (Sudtirol, Italien)". *Berichte des naturwissenschaftlich-medizinischen Vereins in Innsbruck* 88, pp. 57–86.

Cairns, W. R. L. (2008). "The use of ICP-MS (inductively coupled plasma-mass spectrometry) in the field of chemistry and cultural heritage". In: *Chemistry and conservation Science*.

Carignan, J., G. Libourel, C. Cloquet, and L. Le Forestier (2005). "Lead isotopic composition of fly ash and flue gas residues from municipal solid waste combustors in France: implications for atmospheric lead source tracing". *Environmental Science & Technology* 39(7), pp. 2018–2024.

Casati, P., F. Jadoul, A. Nicora, M. Marinelli, N. Fantini Sestini, and E. Fois (1982). "Geologia della Valle dell'Ansiei e dei gruppi M. Popera-Tre Cime di Lavaredo (Dolomiti Orientali)". *Rivista italiana di paleontologia e stratigrafia* 87, pp. 371–510.

Caseldine, C. J., A. Baker, D. J. Charman, and D. Hendon (2000). "A comparative study of optical properties of NaOH peat extracts: implications for humification studies". *The Holocene* 10(5), pp. 649–658.

Cesco Frare, P. (2011). ""LE STRADE DELLE PECCORE". NOTE ETNOGRAFICHE E TOPONOMASTICHE IN MARGINE AGLI ANTICHI LAUDI DEL CENTENARO DI COMÈLICO INFERIORE". *Archivio Storico di Belluno Feltre e Cadore* 346, pp. 77–156.

Cesco Frare, P. and C. Mondini (2005). "Il mesolitico in provincia di Belluno – il quadro dei ritrovamenti. Quaderno n. 6". *Archivio Storico di Belluno Feltre e Cadore* 239, pp. 43–45.

Chambers, F. M. and D. J. Charman (2004). "Holocene environmental change: Contributions from the peatland archive". *The Holocene* 14, pp. 1–6.

Chambers, F. M., D. W. Beilman, and Z. Yu (2011). "Methods for determining peat humification and for quantifying peat bulk density, organic matter and carbon content for palaeostudies of climate and peatland carbon dynamics". *Mires and Peat* 7.

Chambers, F. M., D. Mauquoy, S. A. Brain, M. Blaauw, and J. R. Daniell (2007). "Globally synchronous climate change 2800 years ago: Proxy data from peat in South America". *Earth and Planetary Science Letters* 253(3–4), pp. 439–444.

Chambers, F. M., R. K. Booth, F. De Vleeschouwer, M. Lamentowicz, G. Le Roux, D. Mauquoy, J. E. Nichols, and B. van Geel (2012). "Development and refinement of proxy-climate indicators from peats". *Quaternary International* 268, pp. 21–33.

Charman, D. (2002). *Peatlands and Environmental Change*. John Wiley & Sons Ltd.

Ciani, G. (1862). *Storia del popolo cadorino*. Vol. 11. Forni.

Cloy, J. M., J. G. Farmer, M. C. Graham, and A. B. MacKenzie (2009). "Retention of As and Sb in ombrotrophic peat bogs: records of As, Sb, and Pb deposition at four Scottish sites". *Environmental Science & Technology* 43(6), pp. 1756–1762.

Clymo, R. S. (1984). "The limits to peat bog growth". *Philosophical Transactions of the Royal Society of London B: Biological Sciences* 303(1117), pp. 605–654.

Clymo, R. (1983). "Mires: Swamp, Bog, Fen and Moor, Ecosystems of the World, 4A". In: ed. by G. AJP. Elsevier Scientific Publishing Co. New York. Chap. Peat, pp. 159–224.

Coggins, A. M., S. G. Jennings, and R. Ebinghaus (2006). "Accumulation rates of the heavy metals lead, mercury and cadmium in ombrotrophic peatlands in the west of Ireland". *Atmospheric Environment* 40(2), pp. 260–278.

Collodo, S. (1988). "Il Cadore Medievale verso la formazione di un'identità di regione". In: *Il Dominio dei Caminesi tra Piave e Livenza. Atti del 1° Convegno*. Ed. by TIPSE. Circolo Vittoriese di Ricerche Storiche, pp. 23–50.

Cucagna, A. (1961). *Le industrie minerarie, metallurgiche e meccaniche del Cadore, Zoldano e Agordino durante i secoli passati: saggio di geografia storica*. Università degli Studi di Trieste, Facoltà di Economia e Commercio.

Dal Cin, R. (1972). "I conglomerati tardo-paleozoici post-ercinici delle Dolomiti". *Mitteilungen der Gesellschaft der Geologie und Bergbaustudenten in Österreich* 20, pp. 47–74.

Dal Ri, L. and S. Di Stefano (2005). *Littamum: una mansio nel Noricum*. Vol. 1462. British Archaeological Reports Ltd.

Damman, A. W. H. (1995). "Major mire vegetation units in relation to the concepts of ombrotrophy and minerotrophy: a worldwide perspective". *Gunneria* 70, pp. 23–34.

Damman, A. W. H. (1986). "Hydrology, development, and biogeochemistry of ombrogenous peat bogs with special reference to nutrient relocation in a western Newfoundland bog". *Canadian Journal of Botany* 64(2), pp. 384–394.

Davis, B. A. S., S. Brewer, A. C. Stevenson, and J. Guiot (2003). "The temperature of Europe during the Holocene reconstructed from pollen data". *Quaternary Science Reviews* 22(15–17), pp. 1701–1716.

Davis, R. B. and T. Webb (1975). "The contemporary distribution of pollen in eastern North America: a comparison with the vegetation". *Quaternary Research* 5(3), pp. 395–434.

De Jong, R., S. Björck, L. Björkman, and L. Clemmensen (2006). "Storminess variation during the last 6500 years as reconstructed from an ombrotrophic peat bog in Halland, southwest Sweden". *Journal of Quaternary Science* 21(8), pp. 905–919.

De Bon, A. (1938). "Rilievi di campagna". In: *La Via Claudia Augusta Altinate*. Reale Istituto Veneto di Science, Lettere ed Arti.

De Lorenzo, S. (1999). *Miniere e metalli in Cadore*. Edizioni Comitato Cadore.

De Vleeschouwer, F., F. M. Chambers, and G. T. Swindles (2011). "Coring and sub-sampling of peatlands for palaeonvironmental research". *Mires and Peat* 7.

De Vleeschouwer, F., L. Gérard, C. Goormaghtigh, N. Mattielli, G. Le Roux, and N. Fagel (2007). "Atmospheric lead and heavy metal pollution records from a Belgian peat bog spanning the last two millenia: human impact on a regional to global scale". *Science of the Total Environment* 377(2), pp. 282–295.

De Vleeschouwer, F., N. Piotrowska, J. Sikorski, J. Pawlyta, A. Cheburkin, G. Le Roux, M. Lamentowicz, N. Fagel, and D. Mauquoy (2009). "Multiproxy evidence of 'Little Ice Age' palaeoenvironmental changes in a peat bog from northern Poland". *The Holocene* 19(4), pp. 625–637.

Deevey, E. S. and R. F. Flint (1957). "Postglacial Hypsithermal Interval". *Science* 125(3240), pp. 182–184.

Delcourt, P. A., H. R. Delcourt, and T. Webb (1984). *Atlas of mapped distributions of dominance and modern pollen percentages for important tree taxa of eastern North America*. 14. American Association of Stratigraphic Palynologists Foundation.

Diolaiuti, G. A., D. Maragno, C. D'Agata, C. Smiraglia, and D. Bocchiola (2011). "Glacier retreat and climate change: Documenting the last 50 years of Alpine glacier history from area and geometry changes of Dosde Piazzi glaciers (Lombardy Alps, Italy)". *Progress in Physical Geography* 35(2), pp. 161–182.

Dreyer, A., C. Blodau, J. Turunen, and M. Radke (2005). "The spatial distribution of PAH depositions to peatlands of Eastern Canada". *Atmospheric Environment* 39, pp. 3725–3733.

Erdtman, G. (1960). "The acetolysis method. A revised description". *Svensk Botanisk Tidskrift* 54, pp. 561–569.

Erdtman, G. (1934). "Über die Verwendung von Essigsäureanhydrid bei Pollenuntersuchungen". *Svenska Botanica Tiddskrift* 28, pp. 354–361.

Fabbiani, G. (1992). *Breve storia del Cadore*. Magnifica Comunità di Cadore, p. 227.

Fægri, K. and J. Iversen (1989). *Textbook of pollen analysis*. Fourth Edition. John Wiley & Sons, Ltd.

Fægri, K., J. Iversen, P. E. Kaland, and K. Krzywinski (1993). *Bestimmungsschlüssel für die nordwesteuropäische Pollenflora*. Stuttgart, New York: Gustav Fischer Verlag Jena.

Fagel, N., M. Allan, G. L. Roux, N. Mattielli, N. Piotrowska, and J. Sikorski (2014). "Deciphering human–climate interactions in an ombrotrophic peat record: REE, Nd and Pb isotope signatures of dust supplies over the last 2500 years (Misten bog, Belgium)". *Geochimica et Cosmochimica Acta* 135, pp. 288–306.

Fairchild, I. J., A. Baker, A. Borsato, S. Frisia, R. W. Hinton, F. McDermott, and A. F. Tooth (2001). "Annual to sub-annual resolution of multiple trace-element trends in speleothems". *Journal of the Geological Society* 158, pp. 831–841.

Farmer, J. G., M. C. Graham, J. R. Bacon, S. M. Dunn, S. I. Vinogradoff, and A. B. MacKenzie (2005). "Isotopic characterisation of the historical lead deposition record at Glensaugh, an organic-rich, upland catchment in rural NE Scotland". *Science of the Total Environment* 346(1), pp. 121–137.

Festi, D. (2012). "Palynological reconstruction of the onset and development of alpine pasture in the Eastern Alps since the Neolithic". PhD thesis. Innsbruck: University of Innsbruck, p. 66.

Festi, D., A. Putzer, and K. Oeggl (2014). "Mid and late Holocene land-use changes in the Ötztal Alps, territory of the Neolithic Iceman "Ötzi"". *Quaternary International* 353. Environmental History of European High Mountains, pp. 17 –33.

Finkel, R. C., L. A. Owen, P. L. Barnard, and M. W. Caffee (2003). "Beryllium-10 dating of Mount Everest moraines indicates a strong monsoon influence and glacial synchroneity throughout the Himalaya". *Geology* 31(6), pp. 561–564.

Finsinger, W., K. Schoning, S. Hicks, A. Lücke, T. Goslar, F. Wagner-cremer, and H. Hyyppä (2013). "Climate change during the past 1000 years: a high-temporal-resolution multiproxy record from a mire in northern Finland". *Journal of Quaternary Science* 28(2), pp. 152–164.

Flament, P., M.-L. Bertho, K. Deboudt, A. Véron, and E. Puskaric (2002). "European isotopic signatures for lead in atmospheric aerosols: a source apportionment based upon $^{206}Pb/^{207}Pb$ ratios". *Science of the Total Environment* 296(1), pp. 35–57.

Frisia, S., A. Borsato, N. Preto, and F. McDermott (2003). "Late Holocene annual growth in three Alpine stalagmites records the influence of solar activity and the North Atlantic Oscillation on winter climate". *Earth and Planetary Science Letters* 216(3), pp. 411–424.

Fukumoto, Y., K. Kashima, A. Orkhonselenge, and U. Ganzorig (2012). "Holocene environmental changes in northern Mongolia inferred from diatom and pollen records of peat sediment". *Quaternary International* 254, pp. 83–91.

Giunti, I. (2011). "Geochemical and isotopic tracers in copper deposits and ancient artefacts: a database for provenance". PhD thesis. Padova: University of Padova, p. 161.

Givelet, N., G. Le Roux, A. Cheburkin, B. Chen, J. Frank, M. E. Goodsite, H. Kempter, M. Krachler, T. Noernberg, N. Rausch, S. Rheinberger, F. Roos-Barraclough, A. Sapkota, C. Scholz, and W. Shotyk (2004). "Suggested protocol for collecting, handling and preparing peat cores and peat samples for physical, chemical, mineralogical and isotopic analyses". *Journal of Environmental Monitoring* 6, pp. 481–492.

Glasser, N. F., S. Harrison, V. Winchester, and M. Aniya (2004). "Late Pleistocene and Holocene palaeoclimate and glacier fluctuations in Patagonia". *Global and planetary change* 43(1), pp. 79–101.

Gobet, E., W. Tinner, P. A. Hochuli, J. F. van Leeuwen, and B. Ammann (2003). "Middle to Late Holocene vegetation history of the Upper Engadine (Swiss Alps): the role of man and fire". *Vegetation History and Archaeobotany* 12(3), pp. 143–163.

Gobiet, A., S. Kotlarski, M. Beniston, G. Heinrich, J. Rajczak, and M. Stoffel (2014). "21st century climate change in the European Alps–A review". *Science of The Total Environment* 493, pp. 1138–1151.

Godwin, H. (1975). *The history of the British flora*. Cambridge University Press, London.

Gore, A. J. P. (1983). *Ecosystem of the World. Mires: Swamp, bog, fen and moor*. Elsevier.

Gorham, E., S. E. Bayley, and D. W. Schindler (1984). "Ecological effects of acid deposition upon peatlands: a neglected field in "acid-rain" research". *Canadian Journal of Fisheries and Aquatic Sciences* 41(8), pp. 1256–1268.

Grimm, E. C. (1987). "CONISS: a FORTRAN 77 program for stratigraphically constrained cluster analysis by the method of incremental sum of squares". *Computers & Geosciences* 13(1), pp. 13–35.

— (2011). *Tilia*. Illinois State Museum, Research and Collections Center. Version 1.7.16. Springfield, Illinois, USA.

Grousset, F. E., C. R. Quetel, B. Thomas, P. Buat-Menard, O. F. X. Donard, and A. Bucher (1994). "Transient Pb isotopic signatures in the western European atmosphere". *Environmental Science & Technology* 28(9), pp. 1605–1608.

Haas, J. N. and M. Magny (2004). "Die jungsteinzeitlichen Besiedlung von Arbon-Bleiche 3 im Rahmen der abrupten, globalen Klimaschwankungen vor 5600–5000 Jahren". *Die jungsteinzeitliche Seeufersiedlung Arbon-Bleiche* 3, pp. 41–49.

Haas, J. N., I. Richoz, W. Tinner, and L. Wick (1998). "Synchronous Holocene climatic oscillations recorded on the Swiss Plateau and at timberline in the Alps". *The Holocene* 8(3), pp. 301–309.

Haberle, S. G. and B. David (2004). "Climates of change: human dimensions of Holocene environmental change in low latitudes of the PEPII transect". *Quaternary International* 118–119, pp. 165–179.

Hallett, D. J., D. S. Lepofsky, R. W. Mathewes, and K. P. Lertzman (2003). "11 000 years of fire history and climate in the mountain hemlock rain forests of southwestern British Columbia based on sedimentary charcoal". *Canadian Journal of Forest Research* 33(2), pp. 292–312.

Hammarlund, D., S. Björck, B. Buchardt, C. Israelson, and C. T. Thomsen (2003). "Rapid hydrological changes during the Holocene revealed by stable isotope records of lacustrine carbonates from Lake Igelsj´on, southern Sweden". *Quaternary Science Reviews* 22(2–4), pp. 353–370.

Hansmann, W. and V. Köppel (2000). "Lead-isotopes as tracers of pollutants in soils". *Chemical Geology* 171(1), pp. 123–144.

Heiss, A. G., W. Kofler, and K. Oeggl (2005). "The Ulten Valley in South Tyrol, Italy: Vegetation and settlement history of the area, and macrofossil record from the Iron Age Cult Site of St. Walburg". *Palyno-Bulletin of the Institute of Botany, University of Innsbruck* 1, pp. 63–73.

Hendon, D., D. J. Charman, and M. Kent (2001). "Palaeohydrological records derived from testate amoebae analysis from peatlands in northern England: within-site variability, between-site comparability and palaeoclimatic implications". *The Holocene* 11(2), pp. 127–148.

Heusser, C. J. (1998). "Deglacial paleoclimate of the American sector of the Southern Ocean: Late Glacial–Holocene records from the latitude of Canal Beagle (55°S), Argentine Tierra del Fuego". *Palaeogeography, Palaeoclimatology, Palaeoecology* 141(3), pp. 277–301.

Hjort, C., Ó. Ingólfsson, P. Möller, and J. M. Lirio (1997). "Holocene glacial history and sea-level changes on James Ross Island, Antarctic Peninsula". *Journal of Quaternary Science* 12(4), pp. 259–273.

Holzhauser, H., M. Magny, and H. J. Zumbühl (2005). "Glacier and lake-level variations in west-central Europe over the last 3500 years". *The Holocene* 15(6), pp. 789–801.

Hopper, J. F. and H. B. Ross (1991). "Regional source discrimination of atmospheric aerosols in Europe using the isotopic composition of lead". *Tellus* 43(1), pp. 45–60.

Hughes, P. D. M. and K. E. Barber (2004). "Contrasting pathways to ombrotrophy in three raised bogs from Ireland and Cumbria, England". *The Holocene* 14(1), pp. 65–77.

Hughes, P. D. M., D. Mauquoy, K. E. Barber, and P. G. Langdon (2000). "Mire-development pathways and palaeoclimatic records from a full Holocene peat archive at Walton Moss, Cumbria, England". *The Holocene* 10(4), pp. 465–479.

Huntley, B. and H. J. B. Birks (1983). *An atlas of past and present pollen maps for Europe: 0-13000 years ago*. Cambridge: Cambridge University Press.

Huntley, B., I. C. Prentice, et al. (1993). "Holocene vegetation and climates of Europe". *Global climates since the last glacial maximum*, pp. 136–168.

Ingram, M. J., D. J. Underhill, and T. M. L. Wigley (1978). "Historical climatology". *Nature* 276(5686), pp. 329–334.

IPCC (2013). *Climate Change 2013: The Physical Science Basis. Contribution of Working Group I to the Fifth Assessment Report of the Intergovernmental Panel on Climate Change*. Ed. by T. Stocker, D. Qin, G.-K. Plattner, M. Tignor, S. K. Allen, J. Boschung, A. Nauels, Y. Xia, V. Bex, and P. M. Midgley. Cambridge University Press, Cambridge, United Kingdom and New York, NY, USA, p. 1535.

Ivy-Ochs, S., H. Kerschner, M. Maisch, M. Christl, P. W. Kubik, and C. Schlüchter (2009). "Latest Pleistocene and Holocene glacier variations in the European Alps". *Quaternary Science Reviews* 28(21–22). Holocene and Latest Pleistocene Alpine Glacier Fluctuations: A Global Perspective, pp. 2137–2149.

Kabata-Pendias, A. and B. Szteke (2015). *Trace Elements in Abiotic and Biotic Environments*. Crc Press.

Kempter, H. and B. Frenzel (1999). "The local nature of anthropogenic emission sources on the elemental content of nearby ombrotrophic peat bogs, Vulkaneifel, Germany". *Science of The Total Environment* 241(1–3), pp. 117–128.

Klaminder, J., I. Renberg, R. Bindler, and O. Emteryd (2003). "Isotopic trends and background fluxes of atmospheric lead in northern Europe: Analyses of three ombrotrophic bogs from south Sweden". *Global Biogeochemical Cycles* 17.

Kofler, W. and K. Oeggl (2010). "Pollenanalytische Untersuchungen zur Vegetations-, Klima- und Siedlungsgeschichte des Ultentales". In: *Alpine Brandopferplätze. Forschungen zur Denkmalpflege in Südtirol, Band IV*. Ed. by S. H., pp. 735–783.

Kofler, W., V. Krapf, W. Oberhuber, and S. Bortenschlager (2005). "Vegetation responses to the 8200 cal. BP cold event and to long-term climatic changes in the Eastern Alps: possible influence of solar activity and North Atlantic freshwater pulses". *The Holocene* 15(6), pp. 779–788.

Komárek, M., V. Ettler, V. Chrastný, and M. Mihaljevič (2008). "Lead isotopes in environmental sciences: a review". *Environment International* 34(4), pp. 562–577.

Korhola, A., J. Weckström, L. Holmström, and P. Erästö (2000). "A Quantitative Holocene Climatic Record from Diatoms in Northern Fennoscandia". *Quaternary Research* 54(2), pp. 284–294.

Krachler, M., C. Mohl, H. Emons, and W. Shotyk (2003a). "Atmospheric Deposistion of V, Cr, and Ni since the Late Glacial: Effects of Climatic Cycles, Human Impacts, and Comparison with Crustal Abundances". *Environmental Science & Technology* 37(12), pp. 2658–2667.

— (2003b). "Two thousand years of atmospheric rare earth element (REE) deposition as revealed by an ombrotrophic peat bog profile, Jura Mountains, Switzerland". *Journal of Environmental Monitoring* 5, pp. 111–121.

Kral, F. (1982). "Zur postglazialen Vegetationsgeschichte am Sudrand der Ostalpen. II. Pollenanalytische Untersuchungen im nordlichen Friaul". *Botanische Jahrbucher fur Systematik, Pflanzengeschichte und Pflanzengeographie* 103, pp. 343–370.

— (1983). "Ein Pollenprofil aus dem Wölflmoor bei Deutschnofen". In: *Der Schlern*. Vol. 57. Athesiadruck, pp. 733–739.

— (1986a). "Ein pollenanalytischer Beitrag zur Vegetationsgeschichte der Seiser Alm". In: *Der Schlern*. Vol. 60. Athesiadruck, pp. 31–36.

— (1986b). "Zur postglazialen Vegetationsgeschichte in den sudlichen Ostalpen. Pollenanalytische Untersuchungen im Comelico". *Botanische Jahrbucher fur Systematik, Pflanzengeschichte und Pflanzengeographie* 106(3), pp. 409–417.

— (1988). "Zur Wald-und Siedlungsgeschichte Osttirols: Pollenanalyse der Moore am Kartitscher Sattel". *Botanische Jahrbucher fur Systematik, Pflanzengeschichte und Pflanzengeographie* 75, pp. 61–67.

— (1991). "Zwei neue Pollenprofile aus Südtirol". In: *Der Schlern*. Vol. 65. Athesiadruck, pp. 504–515.

Kramers, J. D. and I. N. Tolstikhin (1997). "Two terrestrial lead isotope paradoxes, forward transport modelling, core formation and the history of the continental crust". *Chemical Geology* 139(1), pp. 75–110.

Kress, A., S. Hangartner, H. Bugmann, U. Büntgen, D. C. Frank, M. Leuenberger, R. T. Siegwolf, and M. Saurer (2014). "Swiss tree rings reveal warm and wet summers during medieval times". *Geophysical Research Letters* 41(5), pp. 1732–1737.

Kylander, M. E., J. Klaminder, R. Bindler, and D. J. Weiss (2010). "Natural lead isotope variations in the atmosphere". *Earth and Planetary Science Letters* 290(1), pp. 44–53.

Kylander, M., D. Weiss, A. M. Cortízas, B. Spiro, R. Garcia-Sanchez, and B. Coles (2005). "Refining the pre-industrial atmospheric Pb isotope evolution curve in Europe using an 8000 year old peat core from NW Spain". *Earth and Planetary Science Letters* 240(2), pp. 467–485.

Kühl, N. and R. Moschen (2012). "A combined pollen and δ^{18}O *Sphagnum* record of mid-Holocene climate variability from Dürres Maar (Eifel, Germany)". *The Holocene* 22(10), pp. 1075–1085.

Küttner, A., T. M. Mighall, F. D. Vleeschouwer, D. Mauquoy, A. M. Cortizas, I. D. L. Foster, and E. Krupp (2014). "A 3300-year atmospheric metal contamination record from Raeburn Flow raised bog, south west Scotland". *Journal of Archaeological Science* 44, pp. 1–11.

Lamb, H. H. (1977). *Climate: present, past and future*. Methuen & Company.

Lamy, F., C. Rühlemann, D. Hebbeln, and G. Wefer (2002). "High-and low-latitude climate control on the position of the southern Peru-Chile Current during the Holocene". *Paleoceanography* 17(2), pp. 16/1–16/10.

Laxon, S. W., K. A. Giles, A. L. Ridout, D. J. Wingham, R. Willatt, R. Cullen, R. Kwok, A. Schweiger, J. Zhang, C. Haas, S. Hendricks, R. Krishfield, N. Kurtz, S. Farrell, and M. Davidson (2013). "CryoSat-2 estimates of Arctic sea ice thickness and volume". *Geophysical Research Letters* 40(4), pp. 732–737.

Le Roux, G., D. Weiss, J. Grattan, N. Givelet, M. Krachler, A. Cheburkin, N. Rausch, B. Kober, and W. Shotyk (2004). "Identifying the sources and timing of ancient and medieval atmospheric lead pollution in England using a peat profile from Lindow bog, Manchester". *Journal of Environmental Monitoring* 6, pp. 502–510.

Le Roux, G., N. Fagel, F. De Vleeschouwer, M. Krachler, V. Debaille, P. Stille, N. Mattielli, W. O. Van Der Knaap, J. F. N. Van Leeuwen, and W. Shotyk (2012). "Volcano-and climate-driven changes in atmospheric dust sources and fluxes since the Late Glacial in Central Europe". *Geology* 40(4), pp. 335–338.

Leidlmair, A., H. D. Pohl, A. Draxl, A. Sacco, and E. Navarra (2002). *Comelico, Sappada, Gaital, Lesachtal: paesaggio, storia e cultura*. Ed. by E. Cason. Fondazione Giovanni Angelini.

Leistel, J. M., E. Marcoux, D Thiéblemont, C. Quesada, A. Sánchez, G. R. Almodóvar, E. Pascual, and R. Sáez (1997). "The volcanic-hosted massive sulphide deposits of the Iberian Pyrite Belt Review and preface to the Thematic Issue". *Mineralium Deposita* 33(1-2), pp. 2–30.

Livett, E. A., J. A. Lee, and J. H. Tallis (1979). "Lead, Zinc and Copper Analyses of British Blanket Peats". *Journal of Ecology* 67(3), pp. 865–891.

Lloyd, J. M., A. Kuijpers, A. Long, M. Moros, and L. A. Park (2007). "Foraminiferal reconstruction of mid-to late-Holocene ocean circulation and climate variability in Disko Bugt, West Greenland". *The Holocene* 17(8), pp. 1079–1091.

Lomas, K. (2003). "The mysterious deity of Lagole: ritual and writing in ancient Italy". *Archaeology International* 7, pp. 27–30.

Lowe, J. J., M. J. C. Walker, and S. C. Porter (2013). "Encyclopedia of quaternary science". In: Newnes. Chap. Understanding Quaternary Climatic Change.

MacKenzie, A. B., E. M. Logan, G. T. Cook, and I. D. Pulford (1998). "A historical record of atmospheric depositional fluxes of contaminants in west-central Scotland derived from an ombrotrophic peat core". *Science of the Total Environment* 222(3), pp. 157–166.

Magny, M. (2004). "Holocene climate variability as reflected by mid-European lake-level fluctuations and its probable impact on prehistoric human settlements". *Quaternary International* 113(1), pp. 65–79.

— (2013). "Orbital, ice-sheet, and possible solar forcing of Holocene lake-level fluctuations in west-central Europe: a comment on Bleicher". *The Holocene* 23(8), pp. 1202–1212.

Magny, M., U. R. S. Leuzinger, S. Bortenschlager, and J. N. Haas (2006). "Tripartite climate reversal in Central Europe 5600–5300 years ago". *Quaternary Research* 65(1), pp. 3–19.

Magny, M., D. Galop, P. Bellintani, M. Desmet, J. Didier, J. N. Haas, N. Martinelli, A. Pedrotti, R. Scandolari, A. Stock, et al. (2009). "Late-Holocene climatic variability south of the Alps as recorded by lake-level fluctuations at Lake Ledro, Trentino, Italy". *The Holocene* 19(4), pp. 575–589.

Mangini, A., C. Spötl, and P. Verdes (2005). "Reconstruction of temperature in the Central Alps during the past 2000 yr from a δ^{18}O stalagmite record". *Earth and Planetary Science Letters* 235(3), pp. 741–751.

Martínez Cortizas, A., X. Pontevedra-Pombal, J. C. Nóvoa Muñoz, and E. García-Rodeja (1997). "Four thousand years of atmospheric Pb, Cd and Zn deposition recorded by the ombrotrophic peat bog of Penido Vello (Northwestern Spain)". *Water, Air, and Soil Pollution* 100(3-4), pp. 387–403.

Martínez Cortizas, A., E. García-Rodeja, X. Pontevedra-Pombal, J. C. Nóvoa Muñoz, D. Weiss, and A. Cheburkin (2002). "Atmospheric Pb deposition in Spain during the last 4600 years recorded by two ombrotrophic peat bogs and implications for the use of peat as archive". *The Science of the Total Environmental* 292(1–2), pp. 33–44.

Martínez Cortizas, A., L. López-Merino, R. Bindler, T. Mighall, and M. Kylander (2013). "Atmospheric Pb pollution in N Iberia during the late Iron Age/Roman times reconstructed using the high-resolution record of La Molina mire (Asturias, Spain)". *Journal of Paleolimnology* 50(1), pp. 71–86.

Masson-Delmotte, V., B. Stenni, and J. Jouzel (2004). "Common millennial-scale variability of Antarctic and Southern Ocean temperatures during the past 5000 years reconstructed from the EPICA Dome C ice core". *The Holocene* 14(2), pp. 145–151.

Mauquoy, D., M. Blaauw, B. van Geel, A. Borromei, M. Quattrocchio, F. M. Chambers, and G. Possnert (2004). "Late Holocene climatic changes in Tierra del Fuego based on multiproxy analyses of peat deposits". *Quaternary Research* 61(2), pp. 148–158.

Mayewski, P. A., E. E. Rohling, J. C. Stager, W. Karlén, K. A. Maasch, L. D. Meeker, E. A. Meyerson, F. Gasse, S. van Kreveld, K. Holmgren, J. Lee-Thorp, G. Rosqvist, F. Rack, M. Staubwasser, R. R. Schneider, and E. J. Steig (2004). "Holocene climate variability". *Quaternary Research* 62(3), pp. 243–255.

Mayewski, P. A., L. D. Meeker, M. S. Twickler, S. Whitlow, Q. Yang, W. B. Lyons, and M. Prentice (1997). "Major Features and Forcing of High-atitude Northern Hemisphere Atmospheric Circulation using a 110,000-year-long Glaciochemical Series". *Journal of Geophysical Research* 102(C12), pp. 26345–26366.

Mighall, T. M., P. W. Abrahams, J. P. Grattan, D. Hayes, S. Timberlake, and S. Forsyth (2002). "Geochemical evidence for atmospheric pollution derived from prehistoric copper mining at Copa Hill, Cwmystwyth, mid-Wales, UK". *Science of The Total Environment* 292(1–2). Peat Bog Archives of Atmospheric Metal Deposition, pp. 69–80.

Mighall, T. M., S. Timberlake, I. D. L. Foster, E. Krupp, and S. Singh (2009). "Ancient copper and lead pollution records from a raised bog complex in Central Wales, UK". *Journal of Archaeological Science* 36(7), pp. 1504–1515.

Mighall, T., A. M. Cortizas, N. S. Sánchez, I. D. Foster, S. Singh, M. Bateman, and J. Pickin (2014). "Identifying evidence for past mining and metallurgy from a record of metal contamination preserved in an ombrotrophic mire near Leadhills, SW Scotland, UK". *The Holocene* 24, pp. 1–12.

Milanković, M. (1969). *Canon of insolation and the ice-age problem: (Kanon der Erdbestrahlung und seine Anwendung auf das Eiszeitenproblem) Belgrade, 1941.* Posebna izdanja. Israel Program for Scientific Translations;

[avialable from U.S. Dept. of Commerce, Clearinghouse for Federal Scientific and Technical Information, Springfield, Va.]

Miola, A. (2012). "Tools for Non-Pollen Palynomorphs (NPPs) analysis: A list of Quaternary NPP types and reference literature in English language (1972–2011)". *Review of Palaeobotany and Palynology* 186, pp. 142–161.

Moberg, A., D. M. Sonechkin, K. Holmgren, N. M. Datsenko, and W. Karlén (2005). "Highly variable Northern Hemisphere temperatures reconstructed from low- and hig-resolution proxy data". *Nature* 433, pp. 613–617.

Mokeddem, Z., A. Baltzer, M. Clet-Pellerin, A. V. Walter-Simonnet, R. Bates, Y. Balut, and C. Bonnot-Courtois (2007). "Fluctuations climatiques enregistrées depuis 20 000 ans dans le remplissage sédimentaire du loch Sunart (Nord-Ouest de l'Écosse)". *Comptes Rendus Geoscience* 339(2), pp. 150–160.

Monna, F., J. Lancelot, I. W. Croudace, A. B. Cundy, and J. T. Lewis (1997). "Lead isotopic composition of airborne material from France and the Southern UK implications for Pb pollution sources in urban areas". *Environmental Science & Technology* 31, pp. 2277–2286.

Monna, F., C. Petit, J.-P. Guillaumet, I. Jouffroy-Bapicot, C. Blanchot, J. Dominik, R. Losno, H. Richard, J. Lévêque, and C. Chateau (2004a). "History and Environmental Impact of Mining Activity in Celtic Aeduan Territory Recorded in a Peat Bog (Morvan, France)". *Environmental Science & Technology* 38(3), pp. 665–673.

Monna, F., J. Dominik, J.-L. Loizeau, M. Pardos, and P. Arpagaus (1999). "Origin and evolution of Pb in sediments of Lake Geneva (Switzerland-France). Establishing a stable Pb record". *Environmental Science & Technology* 33(17), pp. 2850–2857.

Monna, F., D. Galop, L. Carozza, M. Tual, A. Beyrie, F. Marembert, C. Chateau, J. Dominik, and F. E. Grousset (2004b). "Environmental impact of early Basque mining and smelting recorded in a high ash minerogenic peat deposit". *Science of the Total Environment* 327(1), pp. 197–214.

Moore, P. D., J. A. Webb, and M. E. Collinson (1991). *Pollen Analysis*. Second. Blackwell Scientific Publications.

Moreno, P. I. (2000). "Climate, Fire, and Vegetation between About 13,000 and 9200 14C yr B.P. in the Chilean Lake District". *Quaternary Research* 54(1), pp. 81–89.

Nesbitt, H. W. and G. Markovics (1997). "Weathering of granodioritic crust, long-term storage of elements in weathering profiles, and petrogenesis of siliciclatic sediments". *Geochemica et Cosmochimica Acta* 61(8), pp. 1653–1670.

Nichols, J. E., R. K. Booth, S. T. Jackson, E. G. Pendall, and Y. Huang (2006). "Paleohydrologic reconstruction based on *n*-alkane distributions in ombrotrophic peat". *Organic Geochemistry* 37(11), pp. 1505–1513.

Nichols, J. E., M. Walcott, R. Bradley, J. Pilcher, and Y. Huang (2009). "Quantitative assessment of precipitation seasonality and summer surface wetness using ombrotrophic sediments from an Arctic Norwegian peatland". *Quaternary Research* 72(3), pp. 443–451.

Nicolussi, K. and G. Patzelt (2000a). "Discovery of early Holocene wood and peat on the forefield of the Pasterze Glacier, Eastern Alps, Austria". *The Holocene* 10(2), pp. 191–199.

— (2000b). "Untersuchungen zur holozänen Gletscherentwicklung von Pasterze und Gepatschferner (Ostalpen). Mit 41 Abbildungen". *Zeitschrift fur Glet-scherkunde und Glazialgeologie* 36, pp. 1–87.

Nicolussi, K., M. Kaufmann, G. Patzelt, J. van der Plicht, and A. Thurner (2005). "Holocene tree-line variability in the Kauner Valley, Central Eastern Alps, indicated by dendrochronological analysis of living trees and subfossil logs". *Vegetation History and Archaeobotany* 14(3), pp. 221–234.

Nieminen, T. M., L. Ukonmaanaho, and W. Shotyk (2002). "Enrichment of Cu, Ni, Zn, Pb and As in an ombrotrophic peat bog near a Cu-Ni smelter in Southwest Finland". *Science of the Total Environment* 292(1), pp. 81–89.

Nilssen, E. and K.-D. Vorren (1991). "Peat humification and climate history". *Norsk geologisk tidsskrift* 71(3), pp. 215–217.

Nimis, P., P. Omenetto, I. Giunti, G. Artioli, and I. Angelini (2012). "Lead isotope systematics in hydrothermal sulphide deposits from the central-eastern Southalpine (northern Italy)". *European Journal of Mineralogy* 24(1), pp. 23–37.

Noon, P. E., M. J. Leng, and V. J. Jones (2003). "Oxygen-isotope ($\delta\,^{18}$O) evidence of Holocene hydrological changes at Signy Island, maritime Antarctica". *The Holocene* 13(2), pp. 251–263.

Novák, M. and P. Pacherova (2008). "Mobility of trace metals in pore waters of two Central European peat bogs". *Science of The Total Environment* 394(2–3), pp. 331–337.

Novák, M., S. Emmanuel, M. A. Vile, Y. Erel, A. Véron, T. Pačes, R. K. Wieder, M. Vaneček, M. Štepánová, E. Brízová, et al. (2003). "Origin of lead in eight Central European peat bogs determined from isotope ratios, strengths, and operation times of regional pollution sources". *Environmental Science & Technology* 37(3), pp. 437–445.

Novak, M., L. Zemanova, P. Voldrichova, M. Stepanova, M. Adamova, P. Pacherova, A. Komarek, M. Krachler, and E. Prechova (2011). "Exper-

imental Evidence for Mobility/Immobility of Metals in Peat". *Environmental Science & Technology* 45(17), pp. 7180–7187.

O'Brien, S. R., P. A. Mayewski, L. D. Meeker, D. A. Meese, M. S. Twickler, and S. I. Whitlow (1995). "Complexity of Holocene Climate as Reconstructed from a Greenland Ice Core". *Science* 270(5244), pp. 1962–1964.

Oeggl, K. and N. Wahlmüller (1994). "Holozäne Vegetationsentwicklung an der Waldgrenze der Ostalpen: Die Plancklacke (2140 m)/Sankt Jakob im Defreggen, Osttirol". *Dissertationes Botanicae* 234, pp. 389–411.

Oeggl, K. (1994). "The palynological record of human impact on highland zone ecosystems". In: *Highland zone exploitation in Southern Europe*. Ed. by P Biagi and J Nandris, pp. 107–122.

Orombelli, G., C. Ravazzi, and M. B. Cita (2005). "Osservazioni sul significato dei termini LMG (UMG), Tardoglaciale e postglaciale in ambito globale, italiano e alpino". *Il Quaternario. Italian Journal of Quaternary Sciences* 18(2), pp. 147–155.

Osvald, K. H. (1923). *Die Vegetation des Hochmoores Komosse*. Vol. 1. Svenska vxtsociologiska sllskapet, pp. 1–436.

Padovan, E. (2014). *Scavi archeologici, i reperti del IV - V secolo*. Available on line.

Parkinson, C. L. and J. C. Comiso (2013). "On the 2012 record low Arctic sea ice cover: Combined impact of preconditioning and an August storm". *Geophysical Research Letters* 40(7), pp. 1356–1361.

Patzelt, G. (1977). "Erdwissenschaftliche Forschung 13". In: ed. by B. Frenzel. Chap. Dendrochronologie und postglaziale Klimaschwankungen in Europa, pp. 248–259.

Payette, S., M. Eronen, and J. J. P. Jasinski (2002). "The circumboreal tundra-taiga interface: Late Pleistocene and Holocene changes". *Ambio*, pp. 15–22.

Peyron, O., J. Guiot, R. Cheddadi, P. Tarasov, M. Reille, J.-L. de Beaulieu, S. Bottema, and V. Andrieu (1998). "Climatic Reconstruction in Europe for 18,000 YR B.P. from Pollen Data". *Quaternary Research* 49(2), pp. 183–196.

Pignatti, S. (1982). *Flora d'Italia*. Edagricole.

Pini, R. (2002). "A high-resolution Late-Glacial – Holocene pollen diagram from Pian di Gembro (Central Alps, Northern Italy)". *Vegetation History and Archaeobotany* 11(4), pp. 251–262.

Piotrowska, N., M. Blaauw, D. Mauquoy, and F. Chambers (2011). "Constructing deposition chronologies for peat deposit using radiocarbon dating". *Mires and Peat* 7.

Pontevedra-Pombal, X., T. M. Mighall, J. C. N. Muñoz, E. Peiteado-Varela, J. Rodríguez-Racedo, E. García-Rodeja, and A. Martínez-Cortizas (2013).

"Five thousand years of atmospheric Ni, Zn, As, and Cd deposition recorded in bogs from NW Iberia: prehistoric and historic anthropogenic contributions". *Journal of Archaeological Science* 40(1), pp. 764–777.

Porter, S. C. (2000). "Onset of neoglaciation in the Southern Hemisphere". *Journal of Quaternary Science* 15(4), pp. 395–408.

Poto, L. (2013). "Reconstruction of Holocene climate dynamics in the Dolomites from a peat bog core: the first multi-proxy study". PhD thesis. Venice: University Ca' Foscari of Venice, p. 176.

Poto, L., J. Gabrieli, S. J. Crowhurst, P. G. Appleby, P. Ferretti, N. Surian, G. Cozzi, C. Zaccone, C. Turetta, R. Pini, N. Kehrwald, and C. Barbante (2013). "The first continuous Late Glacial – Holocene peat bog multi-proxy record from the Dolomites (NE Italian Alps)". *Quaternary International* 306, pp. 71–79.

Pozzan, A. (2012). "Confini, comunità e conflitti nel Cadore del XVI secolo". PhD thesis. Padova: Università degli Studi di Padova, p. 402.

Prasad, V., B. Phartiyal, and A. Sharma (2007). "Evidence of enhanced winter precipitation and the prevalence of a cool and dry climate during the mid to late Holocene in mainland Gujarat, India". *The Holocene* 17(7), pp. 889–896.

Punt, W., ed. (1976). *The Northwest European Pollen Flora, I.* Amsterdam: Elsevier Scientific Publishing Company.

Punt, W. and G. C. S. Clarke (1980). *The Northwest European Pollen Flora, II.* Amsterdam: Elsevier Scientific Publishing Company.

— (1981). *The Northwest European Pollen Flora, III.* Amsterdam: Elsevier Scientific Publishing Company.

— (1984). *The Northwest European Pollen Flora, IV.* Amsterdam: Elsevier.

Punt, W., S. Blackmore, and G. C. S. Clarke (1988). *The Northwest European Pollen Flora, V.* Amsterdam: Elsevier.

Rausch, N., L. Ukonmaanaho, T. M. Nieminen, M. Krachler, and W. Shotyk (2005). "Porewater evidence of metal (Cu, Ni, Co, Zn, Cd) mobilization in an acidic, ombrotrophic bog impacted by a smelter, Harjavalta, Finland and comparison with reference sites". *Environmental Science & Technology* 39(21), pp. 8207–8213.

Ravazzi, C. (2003). "An overview of the Quaternary continental straigraphic units based on biological and climatic events in Italy". *Il Quaternario. Italian Journal of Quaternary Sciences* 16(1Bis), pp. 11–18.

Reille, M. (1992). *Pollen et spores d'Europe et d'Afrique du Nord.* Laboratoire de Botanique Historique et Palynologie, Marseille.

Reimer, P., E. Bard, A. Bayliss, J. W. Beck, P. G. Blackwell, C. B. Ramsey, C. E. Buck, H. Cheng, R. L. Edwards, M. Friedrich, P. M. Grootes, T. P. Guilderson, H. Haflidason, I. Hajdas, C. Hatté, T. J. Heaton, D. L.

Hoffmann, A. G. Hogg, K. A. Hughen, K. F. Kaiser, B. Kromer, S. W. Manning, M. Niu, R. W. Reimer, D. A. Richards, E. M. Scott, J. R. Southon, R. A. Staff, C. S. M. Turney, and J. Van Der Plicht (2013). "Intcal13 and Marine13 radiocarbon age calibration curves 0-50,000 years cal BP". *Radiocarbon* 55(4), pp. 1869–1887.

Renberg, I., M. W. Persson, and O. Emteryd (1994). "Pre-industrial atmospheric lead contamination detected in Swedish lake sediments". *Nature* 368, pp. 323–326.

Renssen, H., H. Goosse, and R. Muscheler (2006). "Coupled climate model simulation of Holocene cooling events: oceanic feedback amplifies solar forcing". *Climate of the Past* 2(2), pp. 79–90.

Renssen, H., H. Seppä, O. Heiri, D. M. Roche, H. Goosse, and T. Fichefet (2009). "The spatial and temporal complexity of the Holocene thermal maximum". *Nature Geoscience* 2(6), pp. 411–414.

Robock, A. (2000). "Volcanic eruptions and climate". *Reviews of Geophysics* 38(2), pp. 191–219.

Ros, V. (2008). "Caratterizzazione isotopica e multielementare dei minerali per la valutazione delle aree sorgenti". MA thesis. University Ca' Foscari of Venice, p. 133.

Rothwell, J. J., K. G. Taylor, E. L. Ander, M. G. Evans, S. M. Daniels, and T. E. H. Allott (2009). "Arsenic retention and release in ombrotrophic peatlands". *Science of the Total Environment* 407(4), pp. 1405–1417.

Rothwell, J. J., K. G. Taylor, S. R. N. Chenery, A. B. Cundy, M. G. Evans, and T. E. H. Allott (2010). "Storage and behavior of As, Sb, Pb, and Cu in ombrotrophic peat bogs under contrasting water table conditions". *Environmental Science & Technology* 44(22), pp. 8497–8502.

Ruddiman, W. F. (2008). *Earth's Climate: Past and Future*. W. H. Freeman.

Rydin, H., J. K. Jeglum, and J. K. Jeglum (2013). *The biology of peatlands, 2e*. Oxford university press.

Sadori, L., C. Giraudi, P. Petitti, and A. Ramrath (2004). "Human impact at Lago di Mezzano (central Italy) during the Bronze Age: a multidisciplinary approach". *Quaternary International* 113(1), pp. 5–17.

Sapkota, A., A. K. Cheburkin, G. Bonani, and W. Shotyk (2007). "Six millennia of atmospheric dust deposition in southern South America (Isla Navarino, Chile)". *The Holocene* 17, pp. 561–572.

Schmidt, R., K. A. Koinig, R. Thompson, and C. Kamenik (2002). "A multi proxy core study of the last 7000 years of climate and alpine land-use impacts on an Austrian mountain lake (Unterer Landschitzsee, Niedere Tauern)". *Palaeogeography, Palaeoclimatology, Palaeoecology* 187(1), pp. 101–120.

Schmidt, R., C. Kamenik, and M. Roth (2007). "Siliceous algae-based seasonal temperature inference and indicator pollen tracking ca. 4,000 years of climate/land use dependency in the southern Austrian Alps". *Journal of Paleolimnology* 38(4), pp. 541–554.

Schneider, H., D. Höfer, R. Irmler, G. Daut, and R. Mäusbacher (2010). "Correlation between climate, man and debris flow events – A palynological approach". *Geomorphology* 120(1), pp. 48–55.

Schneider, S. H. and M. D. Mastrandrea (2013). "Paleoclimate relevance to global warming". In: *Encyclopedia of quaternary science*. Newnes.

Scholz, D., S. Frisia, A. Borsato, C. Spötl, J. Fohlmeister, M. Mudelsee, R. Miorandi, and A. Mangini (2012). "Holocene climate variability in northeastern Italy: potential influence of the NAO and solar activity recorded by speleothem data". *Climate of the Past* 8(4), pp. 1367–1383.

Schoning, K., D. J. Charman, and S. Wastegoard (2005). "Reconstructed water tables from two ombrotrophic mires in eastern central Sweden compared with instrumental meteorological data". *The Holocene* 15(1), pp. 111–118.

Seiwald, A. (1980). "Beitrage zur Vegetationsgeschichte Tirols IV: Natzer Plateau–Villanderer Alm". *Berichte des naturwissenschaftlich-medizini--schen Vereins in Innsbruck* 67, pp. 31–72.

Sernander, R. (1908). "On the evidences of Postglacial changes of climate furnished by the peat-mosses of Northern Europe". *Geologiska Föreningen i Stockholm Förhandlingar* 30, pp. 465–473.

Shakesby, R. A., J. G. Smith, J. A. Matthews, S. Winkler, P. Q. Dresser, J. Bakke, S.-O. Dahl, O. Lie, and A. Nesje (2007). "Reconstruction of Holocene glacier history from distal sources: glaciofluvial stream-bank mires and a glaciolacustrine sediment core near Sota Sæter, Breheimen, southern Norway". *The Holocene* 17(6), pp. 729–745.

Shotyk, W., D. Weiss, P. G. Appleby, A. K. Cheburkin, R. Frei, M. Gloor, J. D. Kramers, S. Reese, and W. O. Van Der Knaap (1998). "History of Atmospheric Lead Deposition Since 12,370 ^{14}C yr BP from a Peat Bog, Jura Mountains, Switzerland". *Science* 281, pp. 1635–1640.

Shotyk, W., D. Weiss, J. D. Kramers, R. Frei, A. K. Cheburkin, M. Gloor, and S. Reese (2001). "Geochemistry of the peat bog at Etang de la Gruere, Jura Mountains, Switzerland, and its record of atmospheric pb and lithogenic trace metals (Sc, Ti, Y, Zr, and REE) since 12,370 ^{14}C yr BP". *Geochimica et Cosmochimica Acta* 65, pp. 2337–2360.

Shotyk, W., M. E. Goodsite, F. Roos-Barraclough, R. Frei, J. Heinemeier, G. Asmund, C. Lohse, and T. S. Hansen (2003). "Anthropogenic contributions to atmospheric Hg, Pb and As accumulation recorded by peat

cores from southern Greenland and Denmark dated using the ^{14}C "bomb pulse curve"". *Geochimica et Cosmochimica Acta* 67(21), pp. 3991–4011.

Shotyk, W., M. E. Goodsite, F. Roos-Barraclough, N. Givelet, G. L. Roux, D. Weiss, A. K. Cheburkin, K. Knudsen, J. Heinemeier, W. O. van Der Knaap, S. A. Norton, and C. Lohse (2005). "Accumulation rates and predominant atmospheric sources of natural and anthropogenic Hg and Pb on the Faroe Islands". *Geochimica et Cosmochimica Acta* 69(1), pp. 1–17.

Shotyk, W. (1988). "Review of the inorganic geochemistry of peats and peatland waters". *Earth Science Reviews* 25(2), pp. 95–176.

— (1996). "Peat bog archives of atmospheric metal deposition: geochemical evaluation of peat profiles, natural variations in metal concentrations, and metal enrichment factors". *Environmental Reviews* 4(2), pp. 149–183.

Shotyk, W. and P. Steinmann (1994). "Pore-water indicators of rainwater-dominated versus groundwater-dominated peat bog profiles (Jura Mountains, Switzerland)". *Chemical Geology* 116(1–2), pp. 137–146.

Shotyk, W., M. Krachler, A. Martinez-Cortizas, A. K. Cheburkin, and H. Emons (2002). "A peat bog record of natural, pre-anthropogenic enrichments of trace elements in atmospheric aerosols since 12370 ^{14}C yr BP, and their variation with Holocene climate change". *Earth and Planetary Science Letters* 199(1-2), pp. 21–37.

Shotyk, W., H. Kempter, M. Krachler, and C. Zaccone (2015). "Stable (^{206}Pb, ^{207}Pb, ^{208}Pb) and radioactive (^{210}Pb) lead isotopes in 1 year of growth of *Sphagnum* moss from four ombrotrophic bogs in southern Germany: Geochemical significance and environmental implications". *Geochimica et Cosmochimica Acta* 163, pp. 101–125.

Singh, H. B. and M. Kanakidou (1993). "An investigation of the atmospheric sources and sinks of methyl bromide". *Geophysical Research Letters* 20, pp. 133–136.

Solomina, O. N., R. S. Bradley, D. A. Hodgson, S. Ivy-Ochs, V. Jomelli, A. N. Mackintosh, A. Nesje, L. A. Owen, H. Wanner, G. C. Wiles, and N. E. Young (2015). "Holocene glacier fluctuations". *Quaternary Science Reviews* 111, pp. 9–34.

Steig, E. J., C. P. Hart, J. W. C. White, W. L. Cunningham, M. D. Davis, and E. S. Saltzman (1998). "Change in climate, ocean and ice-sheet conditions in the Ross Embayment, Antarctica at 6 ka". *Annals of Glaciology* 27, pp. 305–310.

Steinhilber, F., J. Beer, and C. Fröhlich (2009). "Total solar irradiance during the Holocene". *Geophysical Research Letters* 36(19).

Steinmann, P. and W. Shotyk (1997). "Geochemistry, mineralogy, and geochemical mass balance on major elements in two peat bog profiles (Jura Mountains, Switzerland)". *Chemical Geology* 138(1–2), pp. 25–53.

Stockmarr, J. (1971). "Tablets with spores used in absolute pollen analysis". *Pollen et Spores* 13, pp. 615–621.

Strasburger, E., P. Pupillo, G. Caretta, and D. Lausi (1995). *Trattato di Botanica-parte generale. XXXIII Edizione.* Ed. by R. Delfino.

Stuiver, M., P. Reimer, E. Bard, J. Beck, G Burr, K. Hughen, B. Kromer, G. McCormac, J. van der Plicht, and M. Spurk (1998). "INTCAL98 radiocarbon age calibration, 24,000-0 cal BP." *Radiocarbon* 40(3), pp. 1041–1083.

Stumböck, M. (2000). "Natural Development and Anthropogenic Impacts on the Vegetation of the Passeiertal, South Tyrol, during the Late-Glacial and Holocene". *Acta Universitatis Carolinae, Supplementum* 35, pp. 99–110.

Surian, N. (1991). "Rilevamento geologico nei dintorni del Passo M. Croce di Comelico (Dolomiti Nord-Orientali)". MA thesis. Università degli Studi di Padova.

Svendsen, J. I. and J. Mangerud (1997). "Holocene glacial and climatic variations on Spitsbergen, Svalbard". *The Holocene* 7(1), pp. 45–57.

Swindles, G. T., G. Plunkett, and H. M. Roe (2007). "A delayed climatic response to solar forcing at 2800 cal. BP: multiproxy evidence from three Irish peatlands". *The Holocene* 17(2), pp. 177–182.

Taylor, R. (2000). *Inductively Coupled Plasma - Mass Spectrometry: practices and techniques*. San Diego, CA, USA: Academic Press.

Theurillat, J.-P. and A. Guisan (2001). "Potential Impact of Climate Change on Vegetation in the European Alps: A Review". *Climatic Change* 50(1–2), pp. 77–109.

Thompson, L. G., E. Mosley-Thompson, M. E. Davis, K. A. Henderson, H. H. Brecher, V. S. Zagorodnov, T. A. Mashiotta, P.-N. Lin, V. N. Mikhalenko, D. R. Hardy, and J. Beer (2002). "Kilimanjaro ice core records: evidence of Holocene climate change in tropical Africa". *Science* 298(5593), pp. 589–593.

Tillman, P. K., S. Holzkämper, P. Kuhry, A. B. K. Sannel, N. J. Loader, and I. Robertson (2010). "Stable carbon and oxygen isotopes in *Sphagnum fuscum* peat from subarctic Canada: Implications for palaeoclimate studies". *Chemical Geology* 270(1–4), pp. 216–226.

Tinner, W. and J.-P. Theurillat (2003). "Uppermost limit, extent, and fluctuations of the timberline and treeline ecocline in the Swiss Central Alps during the past 11,500 years". *Arctic, Antarctic, and Alpine Research* 35(2), pp. 158–169.

Tinner, W., M. Conedera, B. Ammann, and A. F. Lotter (2005). "Fire ecology north and south of the Alps since the last ice age". *The Holocene* 15(8), pp. 1214–1226.

Tolonen, K. (1984). "Interpretation of changes in the ash content of ombrotrophic peat layers". *Bulletin of the Geological Society of Finland* 56, pp. 207–219.

Trouet, V., J. Esper, N. E. Graham, A. Baker, J. D. Scourse, and D. C. Frank (2009). "Persistent Positive North Atlantic Oscillation Mode Dominated the Medieval Climate Anomaly". *Science* 324(5923), pp. 78–80.

Ukonmaanaho, L., T. M. Nieminen, N. Rausch, and W. Shotyk (2004). "Heavy Metal and Arsenic Profiles in Ombrogenous Peat Cores from Four Differently Loaded Areas in Finland". *Water, Air, and Soil Pollution* 158(1), pp. 277–294.

Van Geel, B., J. Buurman, and H. T. Waterbolk (1996). "Archaeological and palaeoecological indications of an abrupt climate change in The Netherlands, and evidence for climatological teleconnections around 2650 BP". *Journal of Quaternary Science* 11(6), pp. 451–460.

Van Geel, B., J. Buurman, O. Brinkkemper, J. Schelvis, A. Aptroot, G. van Reenen, and T. Hakbijl (2003). "Environmental reconstruction of a Roman Period settlement site in Uitgeest (The Netherlands), with special reference to coprophilous fungi". *Journal of Archaeological Science* 30(7), pp. 873–883.

Van Hoeve, M. L. and M. Hendrikse (1998). *A study of non-pollen objects in pollen slides. The Types as Described by Dr. Bas van Geel and Colleagues.* Utrecht.

Van Vuuren, D. P., J. Edmonds, M. Kainuma, K. Riahi, A. Thomson, K. Hibbard, G. C. Hurtt, T. Kram, V. Krey, J.-F. Lamarque, T. Masui, M. Meinshausen, N. Nakicenovic, S. J. Smith, and S. K. Rose (2011). "The representative concentration pathways: an overview". *Climatic Change* 109(1–2), pp. 5–31.

Van Geel, B. (1978). "A palaeoecological study of holocene peat bog sections in Germany and The Netherlands, based on the analysis of pollen, spores and macro- and microscopic remains of fungi, algae, cormophytes and animals". *Review of Palaeobotany and Palynology* 25, pp. 1–120.

Vergani, R. (2003). *Miniere e società nella montagna del passato: Alpi venete, secoli XIII-XIX.* Cierre.

Vincens, A., D. Williamson, F. Thevenon, M. Taieb, G. Buchet, M. Decobert, and N. Thouveny (2003). "Pollen-based vegetation changes in southern Tanzania during the last 4200 years: climate change and/or human impact". *Palaeogeography, Palaeoclimatology, Palaeoecology* 198(3–4), pp. 321–334.

Vinichuk, M., K. Johanson, H. Rydin, and K. Rosén (2010). "The distribution of ^{137}Cs, K, Rb and Cs in plants in a *Sphagnum*-dominated peatland in eastern central Sweden". *Journal of Environmental Radioactivity* 101(2), pp. 170–176.

Von Post, L. (1916). "Skogträdpollen i sydsvenska torvmosselagerföljder (Forest tree pollen in south Swedish peat bog deposits)". *Geologiska Föreningens i Stockholm Förhandlingar* 38, pp. 433–465.

Von Post, L. and R. Sernander (1910). *Guides des excursions en Suéde: Pflanzen-Physiognomische Studien auf Torfmooren in Närke. Excursion A7*. Norstedt.

Walker, M. J. C., M. Berkelhammer, S. Björck, L. C. Cwynar, D. A. Fisher, A. J. Long, J. J. Lowe, R. M. Newnham, S. O. Rasmussen, and H. Weiss (2012). "Formal subdivision of the Holocene Series/Epoch: a Discussion Paper by a Working Group of INTIMATE (Integration of ice-core, marine and terrestrial records) and the Subcommission on Quaternary Stratigraphy (International Commission on Stratigraphy)". *Journal of Quaternary Science* 27(7), pp. 649–659.

Walther, G.-R., E. Post, P. Convey, A. Menzel, C. Parmesan, T. J. C. Beebee, J.-M. Fromentin, O. Hoegh-Guldberg, and F. Bairlein (2002). "Ecological responses to recent climate change". *Nature* 416, pp. 389–395.

Wanner, H., J. Beer, J. Bütikofer, T. J. Crowley, U. Cubasch, J. Flückiger, H. Goosse, M. Grosjean, F. Joos, J. O. Kaplan, M. Küttel, S. A. Müller, I. C. Prentice, O. Solomina, T. F. Stocker, P. Tarasov, M. Wagner, and M. Widmann (2008). "Mid- to Late Holocene climate change: an overview". *Quaternary Science Reviews* 27(19–20), pp. 1791–1828.

Wanner, H., O. Solomina, M. Grosjean, S. P. Ritz, and M. Jetel (2011). "Structure and origin of Holocene cold events". *Quaternary Science Reviews* 30(21–22), pp. 3109–3123.

Wardenaar, E. C. P. (1987). "A new hand tool for cutting soil monoliths". *Canadian Journal of Soil Science* 67, pp. 405–407.

Warner, B. G., T. Asada, and N. P. Quinn (2007). "Seasonal influences on the ecology of testate amoebae (Protozoa) in a small *Sphagnum* peatland in Southern Ontario, Canada". *Microbial Ecology* 54(1), pp. 91–100.

Webb, T. and J. H. McAndrews (1976). "Corresponding patterns of contemporary pollen and vegetation in central North America". *Geological Society of America Memoirs* 145, pp. 267–300.

Webb, T., G. Y. Yeracaris, and P. Richard (1978). "Mapped patterns in sediment samples of modern pollen from southeastern Canada and northeastern United States". *Géographie physique et Quaternaire* 32(2), pp. 163–176.

Wedepohl, H. K. (1995). "The composition fo the continental crust". *Geochimica et Cosmochimica Acta* 59(7), pp. 1217–1232.

Weiss, D., W. Shotyk, J. Rieley, S. Page, M. Gloor, S. Reese, and A. Martinez-Cortizas (2002). "The geochemistry of major and selected trace elements in a forested peat bog, Kalimantan, SE Asia, and its implications for past atmospheric dust deposition". *Geochimica et Cosmochimica Acta* 66(13), pp. 2307–2323.

Whitlock, C., P. I. Moreno, and P. Bartlein (2007). "Climatic controls of Holocene fire patterns in southern South America". *Quaternary Research* 68(1), pp. 28–36.

Wick, L. and W. Tinner (1997). "Vegetation changes and timberline fluctuations in the Central Alps as indicators of Holocene climatic oscillations". *Arctic and Alpine Research*, pp. 445–458.

Yafa, C., J. G. Farmer, M. C. Graham, J. R. Bacon, C. Barbante, W. R. L. Cairns, R. Bindler, I. Renberg, A. Cheburkin, H. Emons, M. J. Handley, S. A. Norton, M. Krachler, W. Shotyk, X. D. Li, A. Martinez-Cortizas, I. D. Pulford, V. MacIver, J. Schweyer, E. Steinnes, T. E. Sjobakk, D. Weiss, A. Dolgopolova, and M. Kylander (2004). "Development of an ombrotrophic peat bog (low ash) reference material for the determination of elemental concentrations". *Journal of Environmental Monitoring* 6, pp. 493–501.

Zaccone, C., C. Cocozza, A. K. Cheburkin, W. Shotyk, and T. M. Miano (2007). "Enrichment and depletion of major and trace elements, and radionuclides in ombrotrophic raw peat and corresponding humic acids". *Geoderma* 141(3–4), pp. 235–246.

— (2008). "Distribution of As, Cr, Ni, Rb, Ti and Zr between peat and its humic fraction along an undisturbed ombrotrophic bog profile (NW Switzerland)". *Applied Geochemistry* 23(1), pp. 25–33.

Zaccone, C., V. D'Orazio, W. Shotyk, and T. Miano (2009a). "Chemical and spectroscopic investigation of porewater and aqueous extracts of corresponding peat samples throughout a bog core (Jura Mountains, Switzerland)". *Journal of Soils and Sediments* 9(5), pp. 443–456.

Zaccone, C., A. Gallipoli, C. Cocozza, M. Trevisan, and T. M. Miano (2009b). "Distribution patterns of selected PAHs in bulk peat and corresponding humic acids from a Swiss ombrotrophic bog profile". *Plant and Soil* 315, pp. 35–45.

Zaccone, C., T. M. Miano, and W. Shotyk (2012). "Interpreting the ash trend within ombrotrophic bog profiles: Atmospheric dust depositions vs. mineralization processes. The Etang de la Gruère case study". *Plant and Soil* 353, pp. 1–9.

Zanderigo Rosolo, G. (1982). *Appunti per la storia delle regole del Cadore nei secoli XIII-XIV*. Istituto bellunese di ricerche sociali e culturali, p. 366.

Zemp, M., W. Haeberli, S. Bajracharya, T. J. Chinn, A. G. Fountain, and et al.

Zennaro, P., N. Kehrwald, J. Marlon, W. F. Ruddiman, T. Brücher, C. Agostinelli, D. Dahl-Jensen, R. Zangrando, A. Gambaro, and C. Barbante (2015). "Europe on fire three thousand years ago: Arson or climate?" *Geophysical Research Letters* 42(12), pp. 5023–2033.

Zolitschka, B., K.-E. Behre, and J. Schneider (2003). "Human and climatic impact on the environment as derived from colluvial, fluvial and lacustrine archives – examples from the Bronze Age to the Migration period, Germany". *Quaternary Science Reviews* 22(1), pp. 81–100.

Zoller, H., C. Schindler, and H. Röthlisberger (1966). "Postglaziale Gletschstände und Klimaschwankungen im Gotthardmassiv und Vorderrheingebiet". *Verhandlungen der Naturforschungs Gesellschaft Basel* 77, pp. 97–164.

Zoller, H. (1960). "Pollenanalytische Untersuchungen zur Vegetationsgeschichte der insubrischen Schweiz". *Denkschriften der Schweizerischen Naturforschenden Gesellschaft* 83(2), pp. 45–156.

Estratto per riassunto della tesi di dottorato

L'estratto (max. 1000 battute) deve essere redatto sia in lingua italiana che in lingua inglese e nella lingua straniera eventualmente indicata dal Collegio dei docenti.

L'estratto va firmato e rilegato come ultimo foglio della tesi.

Studente: Michela Segnana matricola: 955996

Dottorato: Science and Management of Climate Change

Ciclo: XXVIII

Titolo della tesi:

Climatic variability and human impact during the Holocene from an Alpine peat bog

Abstract:

The Coltrondo peat bog located in the Eastern Italian Alps is the object of this research. A multi-proxy approach, that combines physical, chemical and biological analyses of peat samples, provides independent evidence about past climate changes and human activities, allowing us to obtain new insights into the variability that characterized the last 7900 years cal BP of the Dolomitic area. The pollen analysis combined with geochemical data (major and trace elements, rare earth elements and lead isotopes) allows the reconstruction of different aspects of the past history recorded by the bog. The main climatic oscillations were clearly registered before human settlements in the area; afterward, human pressure on the environment, mainly through agriculture, pasture, mining and, for the last century, industrial activities, makes it difficult to distinguish Holocene climate natural variability from human-related changes. This work is a fundamental step for the study of past climate changes in this area, adding valuable information about the history of this sector of the Alps, still scarcely investigated.

L'oggetto di questa ricerca è la torbiera di Coltrondo, situata nelle Alpi Italiane Orientali. Grazie ad un approccio multi-proxy, che combina analisi biologiche, fisiche, chimiche dei campioni di torba, sono state ottenute preziose informazioni sui cambiamenti climatici passati e sulle attività umane che hanno caratterizzato l'area Dolomitica negli ultimi 7900 anni. In particolare l'analisi pollinica e geochimica (elementi maggiori e in traccia, terre rare e isotopi del piombo) hanno permesso la ricostruzione di diversi aspetti della storia passata. Prima dell'insediamento umano nell'area, le principali oscillazioni climatiche sono state registrate chiaramente dalla torbiera. In seguito, l'impatto umano, principalmente dovuto ad attività agricole, di pascolo, minerarie e, nell'ultimo secolo, industriali, ha reso più difficile separare la variabilità naturale da quella legata alle attività umane. Questo lavoro ha un ruolo fondamentale per lo studio dei cambiamenti climatici di questa zona, aggiungendo preziose informazioni sulla storia delle Alpi Italiane Orientali, un settore strategico che necessita di ulteriori indagini.

Firma dello studente

Michela Segnana